THE FLOTATION OF HIGH TALC-CONTAINING ORE FROM THE GREAT DYKE OF ZIMBABWE

by

VELAPHI MOSES NASHWA

Submitted in partial fulfilment of the requirements for the

Masters of Science degree (Metallurgy)

in the Faculty of Engineering, Built Environment and Information Technology.
Pretoria University, South Africa.

September 2007

***….but those who hope in the LORD will renew their strength. They will soar on wings like eagles, they will run and not grow weary, they will walk and not be faint*.**

I dedicate this thesis to my lovely Mom and late Dad. I would like to thank them for their love, unwavering support and guidance through my dreams and endeavors.

Acknowledgement

The author is thankful to:

Mimosa mine, for supplying the two-ton ore sample that was used for experimental purposes as well as for the financial sponsorship provided by Mimosa mine in order to ensure the success of this project.

The project supervisors, Professor John Davidtz and Dr Thys (M.K.G.) Vermaak.

The Head of Department of Materials Science and Metallurgical Engineering, University of Pretoria, Professor Chris Pistorius.

Sarah Havenga, for her friendly, approachable personality and willingness to provide assistance with all the administrative work.

The author is also thankful to colleagues and everyone who made a contribution during experimental work on this thesis.

THE FLOTATION OF HIGH TALC-CONTAINING ORE FROM THE GREAT DYKE OF ZIMBABWE

by

VELAPHI MOSES NASHWA

Supervisors:

Doctor M. K. G. Vermaak

and

Professor J. C. Davidtz

Department of Materials Science and Metallurgical Engineering
University of Pretoria

Abstract

This project investigates the optimisation of platinum-group metals recovery at the Mimosa Mine in Zimbabwe. The first part of this research investigates how collector performance can be improved by using collector combinations (mixtures) of the standard sodium iso-butyl xanthate with a secondary collector. The synergistic effect of the sodium-iso-butyl-xanthate (SIBX) combined with trithiocarbonates (TTCs) or dithiophosphates (DTP) was investigated. The short chain and the long chain TTCs were investigated. These collector combinations were studied at various molar percent ratios. The SIBX:DTP combination was studied at a 1:1 mass ratio or molar ratio of 1:1.3.

Amongst all the collector combinations, it was established that the SIBX/DTP combination improved sulphur recoveries by 10% and subsequently the PGE+Au recovery by 10% compared to when the SIBX was used on its own. The C_4-TTC showed poor performance in the sulphur recovery; however an improvement in PGE + Au recovery was noticeable. There was generally no significant metallurgical improvement with respect to final grades and recoveries with C_{10} and C_{12}TTC

mixtures with SIBX. However, the 6.25 molar per cent substitution of SIBX by C_{12}TTC appeared to show some improvement on sulphur but not on PGM+Au recovery and grade. It was therefore concluded that the SIBX/DTP combination at 1:1 mass ratio (total moles of 0.64) showed a potential to improve the grades and recoveries of the Mimosa Mine.

The Mimosa ore is characterised by an unusually large amount of talc, which often causes problems during the flotation of the PGM minerals due to the fact that talc consumes high amount of reagents. Therefore the purpose of the second part of this thesis was to investigate the possibility of removing talc prior to the flotation process by de-sliming. Two cyclones (36.9 mm and 76.0 mm) were used for de-sliming the flotation feed. De-sliming the ore was able to reduce the depressant dosage up to 300 g/t as opposed to 500 g/t that is used at Mimosa Mine.

Keywords: *Froth flotation, platinum-group metals, talc, de-sliming, X-Ray diffraction, collector, trithiocarbonates, sodium isobutyl xanthate, dithiophoshate, hydro cyclones.*

TABLE OF CONTENTS Page

CHAPTER FOUR

MIXTURES OF SIBX WITH iC_4-DTP AND TTCs

CHAPTER FIVE

EXPERIMENTAL (PART II)

TALC DE-SLIMING

CHAPTER SEVEN

CONCLUSION AND RECOMENDATION

CHAPTER ONE

1.1. INTRODUCTION

Mimosa Mine is an underground mine jointly owned by Impala Platinum and Aquarius Platinum Limited of Australia. This mine is situated in the southern part of the Great Dyke in Zimbabwe on the Wedza Geological Complex, namely the South Hill Complex. Mining at Mimosa Mine extends to a depth of 200m with a well-defined ore-body (Implats, 2004). During the 2004 financial year the mine completed its expansion programme to reach an annual production level of 69 000 oz (Implats, 2004). Tonnes milled amounted to 1.33Mt in the year 2004 with expansion resulting in the production of 61 000 oz of platinum concentrate. The life span of this mine is 50 years with ore reserves of 29.8 Mt and mineral resources of 128.9 Mt in the Main Sulphide Zone (MSZ) (Implats, 2004). Recoveries at the mine's concentrators in the 2004 financial year were 79% (Implats, 2004). Although this was an improvement from the 76% recovery obtained in the past, it is still low compared to the recovery obtained from South Africa's Merensky ore, which is between 80 and 90% (Implats, 2004; Cramer, 2001 and Longwider, 2002).

The ore is mineralogically similar to that of Merensky reef in South Africa, but differs in that it contains high concentrations of talc. The lower recovery (of typically around 79%) is partly a result of the high concentrations of talc. Talc is naturally hydrophobic and therefore tends to float and report to the concentrate. During the experimental work done for this study, the author noticed that the presence of talc also changes the stability of the characteristics of the froth, resulting in difficulties in performing controlled flotation experiments. Therefore, in order to minimise the detrimental effect of floating talc that reports to the concentrate, depressant dosages of more than 500g/t are required. In addition, the adsorption of the collector by talc results in excessively high collector consumption, i.e. 530 g/t. With this high depressant dosage (500g/t), the BMS also tends to be depressed in the process.

The objective of this thesis is therefore twofold: firstly it aims to improve the collector reagent suit. The study aims to achieve this by testing the different blends of sodium

iso-butyl xanthate, trithiocarbonates and dithiophosphate. Secondly, it aims to lower the depressant consumption by first removing talc from the PGE ore using de-watering cyclones. The project process flowsheets shown in Figures 3.3 and 5.2 were developed for better coordination of the project. The process flowsheets effectively summarise the steps that were taken to achieve the objectives of the project. Pre-flotation of talc prior to flotation of PGMs was tested to compare the two methods and the process flowsheet for this is shown in Figure 5.6.

1.2. PROBLEM STATEMENT

There are two problems identified at the Mimosa Mine. They are:

(i) Low PGE recoveries (79% compared to the South African Merensky operation's recoveries of between 80% and 95% (Cramer, 2001)). This is due to loss of pyrrhotite to the tailings.

(ii) High concentration of talc resulting in high reagent consumption during flotation (Marais *et al*., 1992).

1.3. RESEACH OBJECTIVES

- Part I of this research is to test the combination of the TTC, DTC and DTP on recoveries and grades on the Mimosa ore.

- Part II of this research investigates the selective removal of talc from the PGM ore by de-slimming using hydro-cyclones. This method compares pre-floating of talc prior to flotation of the BMS.

CHAPTER TWO

LITERATURE REVIEW

2.1. BACKGROUND

2.1.1. Geological Aspects

The Great Dyke of Zimbabwe (see Figure 2.1) is the world's second largest platinum reserve after South Africa's Bushveld Igneous Complex (Oberthür, 1998a, 1998b, 1999, 2002; Prendergast, 1988, 1990). This 550 km long and 11 km maximum width layered intrusion (Prendergast, 1988; Oberthür, 2002a, 2002b), contains several hundred million tonnes of platinum-group element (PGE)-bearing potential ore with *in situ* unit dollar value comparable with those of the Bushveld Igneous Complex (Prendergast, 1988).

This geological feature is divided into two magma chambers: the North and South magma chambers. The magma chambers are further divided into subdivisions named the Musengezi and Hartley complexes and these are divided into the Dwarendale and Sebakwe sub-chamber and Selukwe and Wedza complex, respectively (Prendergast, 1988, 1990). The Great Dyke is generally said to be comprised of the lower ultramafic sequence (chromitite, dunites, pyroxenites and related cumulates) and an upper Mafic sequence consisting of plagioclase-rich rocks (mainly gabbros, norites gabbros-norites and olivine gabbros) (Prendergast, 1990; Oberthür, 2002a).

Mimosa Platinum Mine is situated on the Wedza Geological Complex on the southern part of the Great Dyke. The Wedza Complex hosts an estimated mineral deposit of 100 million tons of potential platinum ore (Prendergast, 1990). Mimosa Platinum is an important producer of platinum-group minerals (PGMs) on the Great Dyke. During the financial year 2004 the mine completed its expansion programme to reach an annual production level of 69 000 oz (Implats, 2004).

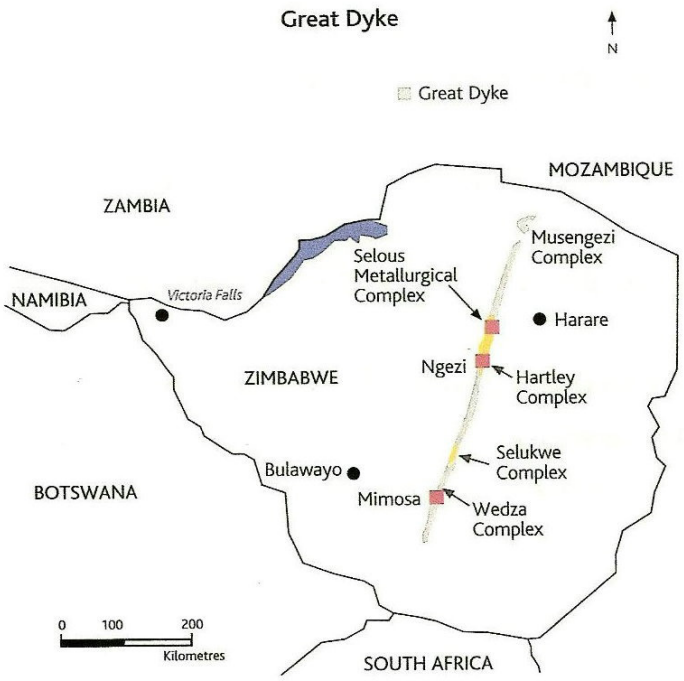

Figure 2.1: *Schematic indication of the Great Dyke in Zimbabwe (Implats, 2004).*

The PGM reserves of Mimosa Platinum can be divided into three geological blocks, namely the South Hill, North Hill and the Far South Hill. The South Hill and the North Hill are geologically similar: they consist of oxidised reserves (Oberthür, 1998a, 1998b, 1999, 2002). Oxidised reserves refer to the weathering of the pyroxinites to form secondary minerals such as talc and other iron aluminium, magnesium silicates, hydroxides and iron hydroxides (Oberthür, 1998a, 1998b, 1999, 2002), hence the oxidized reserves contain much higher levels of talc. A similar type of weathering has been observed at the shallow open cast mining reserves of the Merensky reef (Longwider, 2002). The following section discusses the South Hill Complex in more detail.

2.1.2. The South Hill Geological Complex

The South Hill geological complex strikes over a distance of 6km in a north-north-easterly direction at a width of approximately 4 km (Oberthür, 1998). The Mimosa Mine is a shallow underground mine that utilises wide-reef mining and the board-and-pillar mining methods (Aquarius, 2002). The maximum depth of this reserve is about

200 m and the reef dips at about 14 degrees (Aquarius, 2002; Implats, 2004). This makes it economically advantageous, considering the fact that some South African mines extract PGMs from depths of more than a kilometre. The shallow nature of this reserve contributes significantly to the economic advantage of Mimosa Mine. However the Great Dyke reef is known for its ill-defined platinum mineralisation zone, often resulting in extensive grade dilution (Oberthür, 1998a, 1998b, 1999, 2002). In addition to the shallow nature of the reef, the South Hill geological complex has a platinum mineralisation profile with a visible mid-point marker (Aquarius, 2002). The proven and probable reserves of this geological complex amount to some 51.7 million tons at a grade of 3.92g/t PGM +Au (Aquarius, 2002). The following section gives a detailed discussion of the Main Sulphide Zone.

2.1.3. The Main Sulphide Zone

Before any concentration technique can be applied to the ore, minerals must be liberated from the adjoining phases. In order to optimise the primary extraction processes, the mineralogy of the ore must be examined. This helps with determining aspects such as the fineness of the grind required to liberate the valuable minerals and flotation requirements for concentration.

The PGE, nickel (Ni) and copper (Cu) concentrations are restricted to the sulphide dissemination of the Main Sulphide Zone (MSZ) some meters below the ultramafic transition within the pyroxenitic rock (Oberthür, 1998a, 1998b, 1999, 2002; Prendergast, 1990)**.** The pyroxenitic rock usually consists of pyroxene minerals, which are single chain silicates of the composition $(SiO_3)_n$, held together by cations bound to the non-bridging oxygen atom (Wilson, 1994). The MSZ is described as a laterally continuous zone of disseminated sulphide mineralisation hosted within pyroxinite rock and is stratigraphically located a few meters below the contact between the margins and the axis of the Great Dyke (Oberthür, 1998a, 1998b, 1999, 2002).

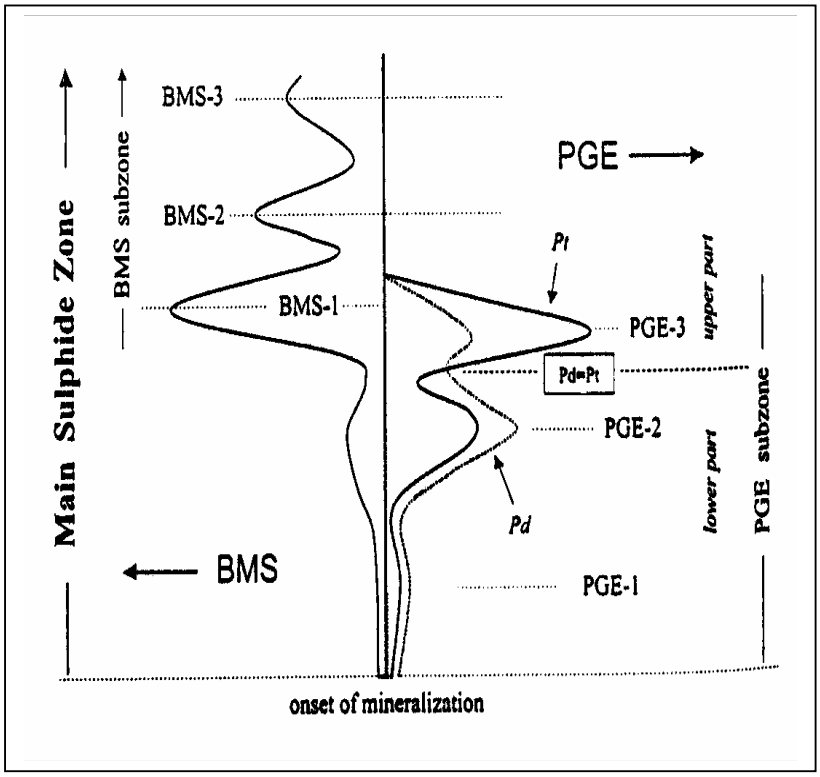

Figure 2.2: *An idealized vertical profile across the Main Sulphide Zone, which shows the vertical distribution of the base metal sulphur (BMS, Cu, Ni, S), Pt and Pd. This is mainly the Hartley mine based data,* (Oberthür *et al.*, 2002a, 2002c).

The MSZ is characterized by a typical vertical pattern of the base metal sulphides (BMS) and the PGE distribution (Figure 2.2). This pattern is characterized by a degree of decoupling and separation of the respective elements' distribution patterns and the peak concentration of the Pd from Pt and of all the PGE from the base metal (Oberthür, 2002a, 2002c). This may show a difference in the association of the two PGEs and might have an important consequence relating to the recoveries of the two elements. In some areas, particularly the Wedza Complex, the MSZ is 2-3m thick, therefore easily accessible for mining. Furthermore the MSZ is divided into two subdivisions, namely the lower PGE sub-zone, which is rich in Pt, Pd and other precious metals, and the upper sub-zone of BMS with very low precious metals (Oberthür, 2002a, and 2002c). The PGE sub-zone is further subdivided into two main portions that are defined on the basis of bulk Cu, Ni and Pd, Pt contents. The lower portion consists of Pd > Pt peak and the upper part consists of Pd < Pt peak, as can be seen in Figure 2.2 (Oberthür, 2002a). This means that the bulk base and precious

metal content increases upwards while the Pt/Pd ratios and Pt + Pd per unit sulphide increases downwards (Prendergast, 1990). This may be indicative of the difference in mineralogical association of the two PGE sub-zones, which will have important consequences relating to the recoveries of these two elements. The pyroxenite host rock consists of between 0.5 and 10 vol. % of the sulphides, namely pyrrhotite, pentlandite, chalcopyrite and very small percentages of the pyrite and it mainly occurs interstitially to cumulus orthopyroxene (Oberthür, 1999, 1998b). The following section investigates the mineralisation of the main sulphide zone.

2.1.4. Mineralisation of Mimosa Plant Feed

The Mimosa feed, as analysed by Penberthy (1999), is composed of complex silicate intergrowths of plagioclase, orthopyroxene, clinopyroxene, amphibole (antophyllite and possibly tremolite), talc, chlorite and quartz. Penberthy (1999) also gave the relative proportions of oxides, sulphides, and silicates (Table 2.1.)

Table 2.1: *Relative proportions (by mass) of oxides, sulphides and silicates (Penberthy, 1999).*

Phase	Feed Mass %	Tailings %
Oxides	0.3	0.2
Sulphides	1.5	0.7
Silicates	98.2	99.1

The base metal sulphide assemblage consists of pyrrhotite, pentlandite and chalcopyrite and is similar to that of the Merensky ore as reported by Cramer (2001) and Longwider (2002). However the 1.5% by mass of sulphides shown in Table 2.1 is lower than the Merensky's, which contains up to 3% sulphides (Longwider, 2002; Jones, 1999).

According to Marais (1992) the sulphides are coarse grained with some occurring as parallel tablets between flakes of micaceous minerals. The pyrrhotite consists of flame-like exsolutions of pentlandite (Penberthy, 1999; Prendergast, 1990). This is confirmed by Prendergast (1990), who also ascertained that pyrrhotite is the principal

base metal sulphide, which usually forms a core of composite grains. Pyrrhotite is, however, a slow floating base metal sulphide that is highly reactive and oxidises to form iron oxides or hydroxy-oxides at the surface (Sutherland, 1955) according to reaction 2.1 (Smart *et al*., 2003; Buckley and Woods, 1985; Heyes and Trahar, 1984).

$$Fe_{1-X}S(7-3x)H_2O = (1-x)Fe(OH)_3 + SO_4^{2-} + (11-3x)H^+ + (9+3x)e^- \qquad (2.1)$$

The high oxidation rate of the pyrrhotite has a negative impact on the flotation of this mineral as it makes it difficult to float.

The PGMs are contained in pyrrhotite or chalcopyrite and rarely in pentlandite, or they are located at the contacts, between the sulphides (BMS) or at the sulphide-silicate contacts, or within the silicates (Oberthür, 1999, Prendergast, 1990). These silicates mostly occur near the margins of the host grain (Oberthür, 1999; Prendergast, 1990)**.** According to Prendergast (1990) each PGM phase is associated without clear preference with pyrrhotite, pentlandite and chalcopyrite but the association with pyrite is very rare.

The grain size of the PGMs range from less than 5 to 50µm in general and may reach 373µm at their longest dimension (Oberthür, 1999). This implies that the grind or milling size has to be carefully examined in order to optimise the liberation of PGM grains. Analysis by Oberthür (1999) showed that the PGM suite was found to comprise of (Pt, Pd)-bismuthotellurides, mainly moncheite ($PtTe_2$), maslovite, merenskite ($PdTe_2$) and michenerite (PdBiTe), followed by sperrylite-$PtAs_2$, PGE-sulphurasenide, hollingworthite (RhAsS), platasite, irarsite and ruarsite (see Table 2.3). The (Pt, Pd) - sulphides (cooperite and braggite), laurite and electrum (Au-Ag alloy) are also reported by Prendergast (1990). Pentlandite is said to be most likely the major Pd-carrying mineral in the MSZ (Prendergast, 1990). The plant feed has been found to have average PGEs and gold concentrations as listed in Table 2.3 (Penberthy, 1999).

Table 2.2: *Proportions (by number of grains) of discrete PGM in pristine and oxidized MSZ ores. (Pt, Pd)(Bi, Te)* = (Pt, Pd)-bismuthtelluride. (Pt, Pd) S = cooperite and braggite. PGE-AsS$^+$ = PGE-sulphasenides. Proportions of (Pt, Pd)-oxides and –hydroxides in the oxidized MSZ could not be estimated (Oberthür, 2002b).*

Locality	**Sulphide MSZ**	**Oxide MSZ**
PGM (n) → **Type** ↓[%]	801	1293
(Pt, Pd)(Bi, Te)*	50.1	11.4
$PtAs_2$	19.0	57.2
(Pt, Pd) S	8.5	28.3
Pt and Pt-Fe alloys	2.4	3.1
PGE-AsS$^+$	11.9	-
Others	8.7	-

Table 2.3: *Typical precious metals analysis of Mimosa plant feed. (Penberthy, 1999).*

Element	**Concentration (ppm)**
Pt	1.75
Pd	1.41
Rh	0.17
Ir	0.08
Au	0.20

The average PGE concentrations given in Table 2.3 are lower than that of a typical South African plant feed which is between 4-10 g/t (Longwider, 2002). However this is compensated for by the low cost of mining (Longwider, 2002; Implats, 2004).

Apart from the other silica gangue minerals talc, which is a clay mineral, forms a greater part of the gangue of the Mimosa ore. As has already been mentioned in Section 2.1.1, talc is formed due to the weathering of the pyroxinites and forms a secondary mineral. Other iron, aluminium, magnesium silicates, hydroxides and iron

hydroxides are also formed (Oberthür, 1998a, 1998b, 1999, 2002). The following section investigates the properties of talc.

2.1.5. Talc and its Hydrophobic Nature

The mineralogical composition of an ore is important as regards the flotation reagents and flotation cell configuration used to effect a separation between the valuable and non-valuable (gangue) components of the ore. Besides choosing the correct collector for the application it is also important to establish if any of the gangue minerals will float and hence possibly necessitate the use of a depressant or the use of other means to separate the gangue material from the valuable minerals.

The Great Dyke consists of various clay minerals such as kaolinite, orthopyroxine, clinopyroxine, plagioclase, talc, calcite quartz, chlorite, amphibole and mica. Of all the clay minerals mentioned, talc has been described as the most problematic for the Mimosa platinum ore (Marais *et al.,* 1992; Penberthy, 1999). Table 2.4 details general information about the properties of talc.

Even though talc is also found in the South African Merensky ore, it occurs in lower percentages compared to the talc in the Mimosa ore. At high levels of talc, reagent consumption during flotation is up to six times the reagent consumption of the South African Merensky ore (Marais *et al.*, 1992). As a result the presence of this hydrous magnesium silicate clay mineral poses major difficulties in the PGM flotation circuits of Mimosa Mine.

Talc is a friable hydrous magnesium silicate with a chemical composition of the form $Mg_3Si_4O_{10}(OH)_2$ (McHardy and Salman, 1974; Berry *et al.,* 1983; Michot *et al.*, 1994; Wills, 1997) and its molecular structure is shown in Figure 2.3 (Khaisheh *et al.*, 2005). It is related to a stack of sheet-like structures of phyllosilicate ($Al_2Si_4O_{10}(OH)_2$). The crystalline structure of talc is a tri-octahedral 2:1 layer clay mineral and is characterized by three octahedral Mg positions per four Si positions that are similar to the discription given by Zbik (2002) and Nemecz (1981). Also known as soapstone or stealite (Wills, 1997), talc is a secondary mineral formed by alteration of olivine, pyroxene and amphibole along the faults in magnesium-rich

rocks (Berry *et al.*, 1983; Wills, 1997). It also occurs in schists, in association with actinolite (Berry *et al*., 1983; Wills, 1997).

Table 2.4: *Information on the general properties of talc. (http://webmineral.com/data/Talc.shtml)*

Physical Properties of Talc	
Density:	2.7 - 2.8, Average = 2.75
Fracture:	Uneven - Flat surfaces (not cleavage) fractured in an uneven pattern.
Hardness:	1 - Talc
Calculated Properties of Talc	
Electron Density:	$r_{electron}$=2.76 gm/cc
Radioactivity:	GRapi = 0 (Gamma Ray American Petroleum Institute Units) Talc is Not Radioactive
Chemical Formula:	$Mg_3Si_4O_{10}(OH)_2$ Molecular Weight = 379.27 gm
Composition	
Magnesium	Mg = 19.23 %, MgO = 31.88 %
Silicon	Si = 29.62 %, SiO_2 = 63.37 %
Hydrogen	H = 0.53 %, H_2O = 4.75 %
Oxygen	O = 50.62 %

According to Luzenac (2002) there are four main categories of talc, namely: magnesium carbonate derivative ore bodies, serpentinite derivative ore bodies, siliceous or silicon-aluminous rock derivative ore bodies and magnesium sedimentary deposit derivative ore bodies. The latter two are the most likely to be associated with the PGM ore. The following section investigates the hydrophobic nature of talc in more detail.

The hydrophobicity of talc has been thoroughly studied and it is a well-known fact that the breakage of talc, during grinding or milling for example, forms two surfaces (Jenkin *et al.*, 1997; Morris *et al.*, 2002). One surface results from the easy breaking of the Van der Waals bond of a surface from its neighbour (Moore and Reynolds, 1989), which forms a basal face that is hydrophobic, whilst the other arises due to

rapture of the ionic/covalent bonds within the layers and form edges that are hydrophilic in nature (Jenkin *et al*., 1997; Yehia *et al*., 1999 Morris *et al*., 2002;).

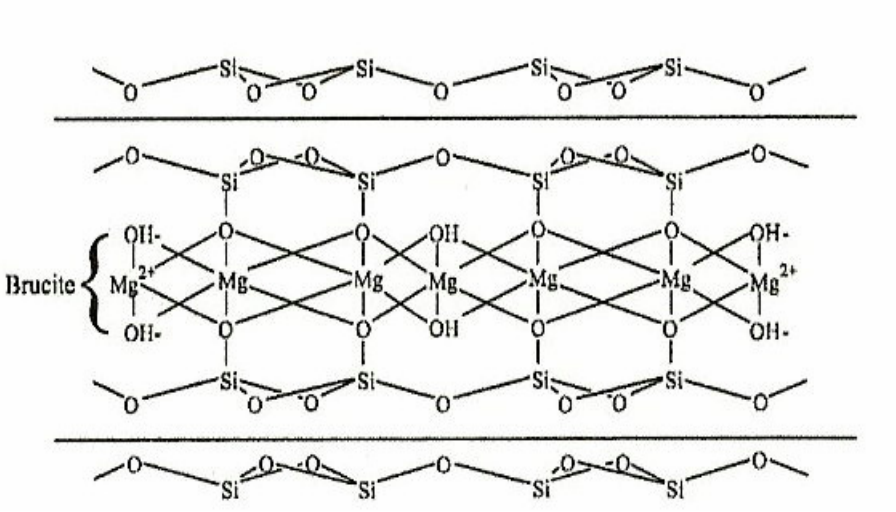

Figure 2.3: *Schematic diagram showing the molecular structure of talc (Khaisheh et al., 2005).*

From the chemistry point of view, the hydrophilic or ionic face would be in an unstable state immediately after the bond rapture and would seek to react with ions of the opposite charge in order to return to their stable state. Morris *et al.* (2002) point out that 90% of the talc surface consists of the hydrophobic surface. The reasons are due to the siloxane surface with the inert –Si-O-Si- links that are non-polar, hence hydrophobic. This clearly explains the natural floatability of talc and hence it is easily upgraded in the flotation concentrate. In the case of PGM concentrating plants like Mimosa the floatability is aggravated by the addition of reagents such as collectors and frothers. Yehia (1999) studied the natural flotation behaviour of talc by measuring the contact angle, floatation recovery and zeta potential. Polypropylene glycol was used as a frother to increase the talc flotation at relatively shorter times. From this study, it was shown that the highest natural floatability of talc was obtained at neutral pH and decreased to different degrees in both acidic and alkaline solutions. It was also shown that the flotation recovery of talc was higher in the presence of frother compared to the natural floatability.

A study conducted by Michot *et al.* (1994) suggests that the surface behaviour of talc is mainly controlled by the OH-groups of the octahedral layer, which points directly

towards the basal surfaces because of the perfect octahedral nature of talc. In this study, Michot *et al.* (1994) revealed that even though talc appears to be macroscopically hydrophobic in its natural form, it is microscopically very hydrophilic. This characteristic was observed when talc was out gassed at a medium temperature of between 100 and 400 ^{0}C. In another study, performed by Ulusoy and Yekeler (2004), it was discovered that the degree of hydrophobicity of talc (other minerals such as calcite, barite and quartz) increases with decreasing surface roughness. Considering the information given above, it is clear that under normal plant conditions a substantial amount of depressant is needed in order to depress talc. The disadvantage of high depressant concentration in the concentrator is the fact that valuable minerals also tend to be depressed. Section 2.2.8 discusses the depression of talc using polymer molecules in details.

2.2. MIMOSA OPERATIONS AND FLOTATION PRINCIPLES

2.2.1. Overview of the Metallurgical Process

The PGM beneficiation process usually consists of the following stages: comminution (which involves crushing and milling of the ore), froth flotation, drying, smelting, converting and refining. As with any other PGM operation, flotation at Mimosa Mine commences by comminution, which is used to increase the surface area of the ore and the liberation of the minerals for subsequent processing. The rocks are broken down during crushing and the crusher product is ground into powder with a desired size distribution in a mill. The author performed the size analysis of the Mimosa mill product and it was found to be 70% passing 75µm.

The bond index of the pristine ore from Mimosa Mine, as reported by Marais *et al.* (1992), is 19kWh/t at 106 microns limiting screen, which compares fairly well to 17-21kWh/t of the Merensky ore for 200 mesh limiting screen discussed by Cramer (2001). Figure 2.4 shows the original flow diagram of the Mimosa plant at the beginning of this investigation. The diagram indicates that a two stage milling circuit operating without an intermediate flotation step to remove the liberated sulphides was employed. Since talc is friable this milling configuration results in the over grinding of talc. Therefore more talc is liberated, resulting in high amounts of talc in the

flotation circuits. In the recently commissioned plant, the milling operation is interspaced with the flotation circuit and the configuration is called MF2 configuration. The MF2 configuration limits talc liberation with the sulphide. Since the purpose of milling is to liberate the valuable minerals, as soon as adequate liberation is achieved the ore is sent to the flotation circuit for concentration of the minerals. The concentrate is then transported by road to Mineral Processes in Rustenburg, South Africa in terms of the operations agreement with Impala Refining Services (IRS) (Implats, 2004). The focal point of this study will be the problems encountered during the flotation stage of the process shown in Figure 2.4 and how to address them. The following section will investigate the fundamentals of flotation, before the flotation practice at Mimosa Mine in more detail. The problems that led to this investigation are also highlighted.

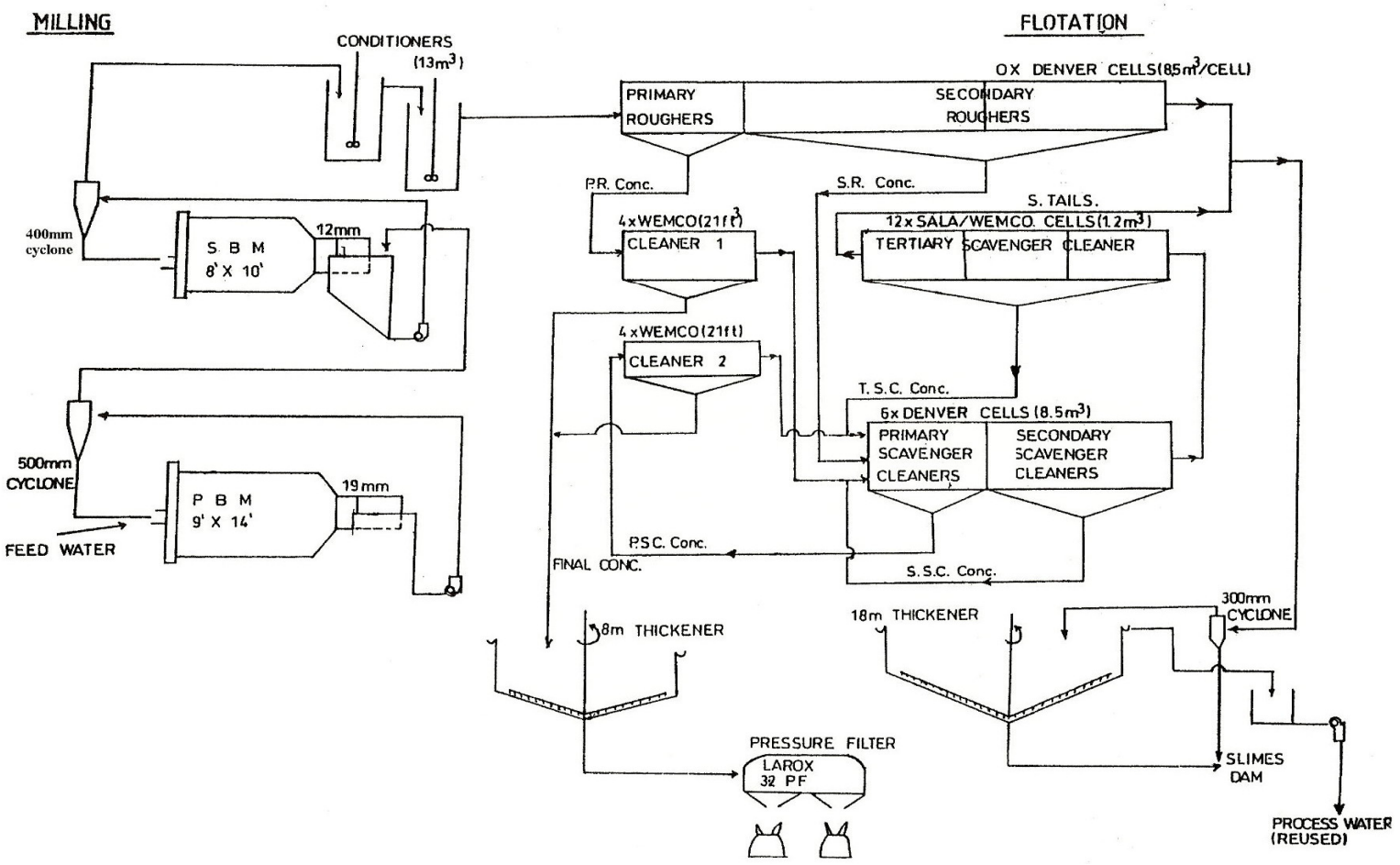

Figure 2.4: *Flow diagram of the original plant of Mimosa Mine.*

2.2.2. An Overview of the Flotation Principles

Before an investigation can be carried out under any subject, it is often very important that the basic principles underlying the subject are properly understood. Even though many factors can be looked at, flotation is central to this research. Hence this section gives a brief review of the principles underlying flotation.

Froth flotation is a process whereby valuable minerals are selectively separated from the invaluable material (gangue), based on the surface properties of the finely ground mineral particles. This mineral processing technology marks its origin around 1860 with William Hayenes' demonstration whereby he used oil avidity to separate minerals (Parekh, 1999). Flotation is achieved by selectively imparting hydrophobicity to the desired mineral particles and bubbling air bubbles through the slurry. The mineral is rendered hydrophobic by adding a surfactant or *collector chemical* to the slurry in a conditioning tank before the pulp is pumped into the flotation cell (Figure 2.5) where flotation takes place.

The particular collector chemical depends on the mineral that is being refined, for example, xanthate is widely used to extract base metals such as copper or PGM associated with the sulphides. The collector chemical is normally added together with other reagents such as *activators, depressants* and *frothers* and the role of these reagents is discussed later in this chapter.

As soon as chemical conditioning is achieved, flotation of the solid particles in the cell is initiated by the mechanical agitation of the slurry using the impeller and the induction of the air into the slurry (see Figure 2.5) in order to float the desired mineral. The air bubbles will then attach themselves to the particles and consequently levitate them to the water surface of the slurry, leaving the gangue material to sink to the bottom of the flotation cell. Dai *et al.* (1999) state that the particle-bubble attachment can be described by three independent sub-steps, i.e.: collision, attachment and stability. A detailed discussion of the three sub-steps is provided by Dai *et al.* (1999).

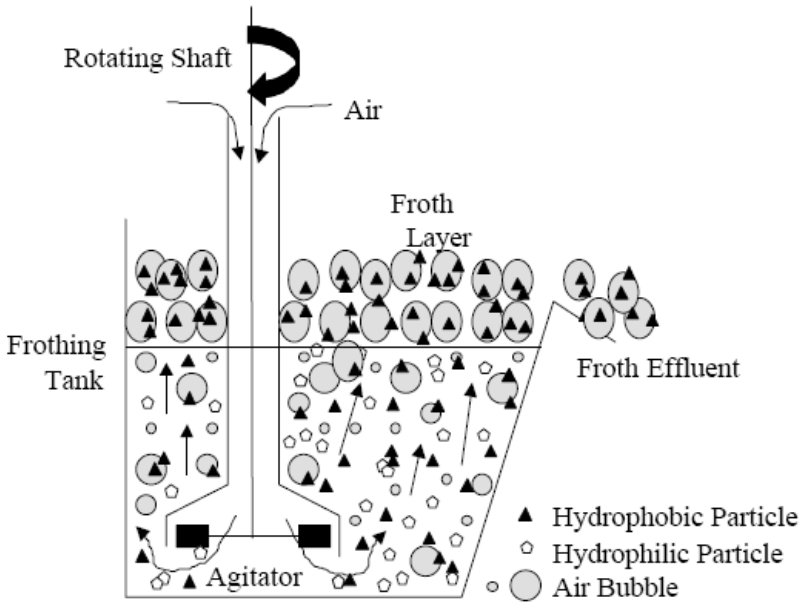

Figure 2.5: *Schematic representation of a flotation machine.*

Figure 2.6 shows a classical illustration of the three-phase contact between water and air bubble and the mineral particle surface. At equilibrium, the three interfacial free energies are related by the Young equation

$$\gamma_{ma} - \gamma_{mw} = \gamma_{wa} \cos\theta_c \qquad (2.2)$$

with γ_{ma}, γ_{mw} and $\boldsymbol{\gamma_{wa}}$ being the interfacial energies of the mineral-air, mineral-water and water-air respectively and θ_c is the contact angle (Kelly and Spottiswood, 1989).

For a bubble- mineral particle attachment to occur,

$$\gamma_{ma} - \gamma_{mw} < \gamma_{wa} \qquad (2.3)$$

And the change in free energy $\Delta\gamma$ associated with the creation of the mineral air interface is given by,

$$\Delta\gamma = \gamma_{ma} - (\gamma_{wa} + \gamma_{mw}) \qquad (2.4)$$

For flotation to occur the change in free energy $\Delta\gamma$ must be negative.

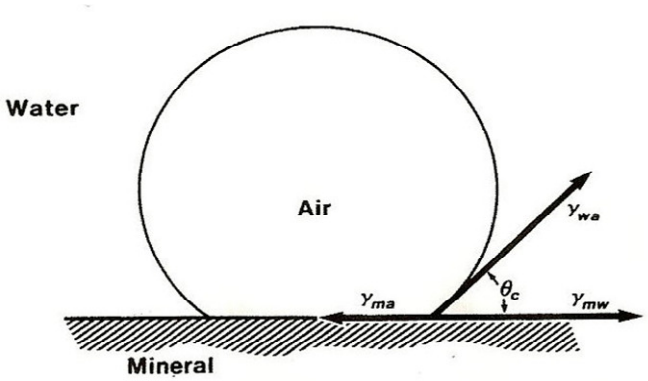

Figure 2.6: *An idealised illustration of the three-phase equilibrium contact between air, water and mineral surface. (Kelly and Spottiswood, 1989)*

The flotation process as a whole can be seen as dependent on three components, i.e.: *chemical component, equipment component* and *operation component* (Klimpel, 1984). The chemical component consists of the reagents, namely *collectors*, or *modifiers (depressants, activators and pH regulators)* and *frothers*. The equipment component encompasses the design of the flotation cell, agitation, air flow, cell bank configuration and cell bank control. The operation component encompasses factors such as the feed rate, the mineralogy, particle size distribution, pulp density and the temperature. In this study, the chemical component (collectors) and operational component (talc removal) will be investigated. The following section gives a general overview of the flotation chemistry, since it forms part of the chemical component of the study.

2.2.3. Flotation at the Mimosa Operation

Apart from the correct design of the flotation machines, the flotation and the product recovery efficiency is strongly dependant on the chemical conditioning. The principles of facial interaction between the mineral particles and the reagent molecules play a pivotal role for the selectivity of this method. A mineral could naturally possess hydrophobicity (for example, coal, talc, etc.) or it could be artificially imparted on the mineral particle by modifying its surface, as already

discussed in Section 2.2.2. Using a chemical suite or flotation reagent, the particle surface can be modified.

Other factors such as surface turbulence and instability, froth conditions retention or conditioning time, pH, temperature, particle size, weight fraction, flotation cell agitator speed, aeration rate, particle density, and the particle shape naturally affect the overall flotation plant performance. Crushing and milling and particle size distribution are but a small number of factors that would have to be considered in order to optimise the mineral recovery by flotation. The geology and mineralogy of the ore also form part of some of the major factors affecting the grades and recoveries.

In the case of the Mimosa ore, the major problem associated with the mineralogy is the high level of talc and some PGMs that are not associated with base metal sulphides. In a study conducted by Marais *et al.* (1992) it was shown that due to high talc levels, the use of chemical reagents is excessively high compared to their South African platinum mining counterparts mining the Merensky, which has a similar base metal sulphide suite.

Table 2.5: *The reagent suite of Mimosa plant compared to Merensky operations.*

		Mimosa	**Merensky**
Collector	SIBX	530 g/t	60g/t
Depressant	CMC Norilose	500 g/t	80g/t
Frother	Dow 200	48 g/t	60g/t
Activator	$CuSO_4$	0 g/t	70g/t

Table 2.5 summarises the reagent suite of the Mimosa Mine and it is compared to the typical Merensky operations. The excessive reagents addition is evident from this table. It is also worth noting that no activation by $CuSO_4$ is performed at Mimosa Mine.

Table 2.6: *Relative percentages of bases-metal sulphides in the feed and tailing samples reported in mass % (Penberthy, 1999).*

Phase	Feed %	Tailings %
Pyrrhotite $(Fe, Ni)_{1-x}S$	49	79
Pentlandite $(Ni, Fe, Co)_9S_8$	28	5
Chalcopyrite ($CuFeS_2$)	22	16
Pyrite (FeS_2)	<1	<1
Co-Fe- (Ni)-S	<1	<1

Table 2.6 shows that 79% of pyrrhotite and 16% of chalcopyrite is lost to the tailings. Pentlandite loss was 5% while less than 1% of pyrite and Co-Fe- (Ni)-S was lost to the tailings. Pentberthy (1999) discovered that copper and nickel losses occur in the form of locked chalcopyrite and pentlandite. The slow floating nature of pyrrhotite is due to its high oxidation rate and is highly likely to be the reason 79% is lost to the tailings. The floatability characteristic of the various BMSs generally has an impact on their recovery as well as on the associated PGE. Leja (1982) and Sutherland (1955) pointed out that the extensive superficial oxidation of sulphide minerals can generally be counteracted by sulphurdisation using a reasonable amount of sulphide species such as HS^- to convert the oxidized surfaces to normal sulphides. However, care must be taken because excessive amounts of the species can be detrimental to flotation (Leja, 1982). This phenomenon might have to be closely examined in another research.

2.2.4. Collector Adsorption

Collectors are bipolar molecules with one end being ionic and therefore hydrophilic in nature, while the opposite one is organic and therefore hydrophobic. Most of these collectors are weak acids, bases or salts (Wills, 1997). The ionic end selectively attaches itself onto the mineral surface by chemical adsorption or physical adsorption or all of the mechanisms.

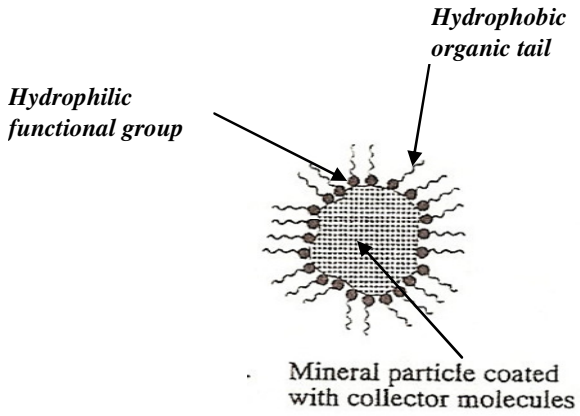

Figure 2.7: *Illustration of collector molecule on mineral particle surface.*

Once the collector is attached onto the particle surface (Figure 2.7.) with its hydrophilic functional group, the organic end orients perpendicular to the surface. As a result, a group of these collectors coat the particle's surface and hence impart hydrophobicity to the mineral particle surface, which is otherwise hydrophilic. Once the particle surface is hydrophobic, it will tend to move out of the water to the air, resulting in the bubble-particle attachment. As soon as the particle is attached to the particle it is then lifted to the slurry surface, leaving the hydrophilic gangue material to fall to the bottom of the flotation cell. The selected particles are then suspended on the slurry surface and kept there by a froth (this will be discussed later in Section 2.2.9). These mineral particles overflow with the froth from the slurry surface into the cell launder or collecting pan in the case of bench flotation.

Collectors can be classified according to the type of ion that is formed upon their dissociation in solution. They can be classified on the basis of composition and whether they exist as anionic, cationic or covalent species in solution (Fuerstenau, 1982; Kelly and Spottiswood, 1989; Wills, 1997). In this study, the anionic collectors will be investigated in detail, since they are widely preferred in the PGM processing industry.

The most widely used anionic collector is the sulphydryl type, where the polar functional group is comprised of bivalent sulphur (thiol compound). Xanthogenates,

technically known as xanthates and generically known as the dithiocarbonates (DTC), are examples of the bivalent sulphur compound. They are used for their high selectivity in the recovery of sulphide minerals. These compounds are prepared by reacting an alkali hydroxide (ROH), and alcohol (MOH) and carbon disulphide (CS_2) according to reaction 2.5 below:

$$ROH + CS_2 + MOH \rightarrow RO.CS_2M + H_2O \qquad (2.5)$$

The product structural ionic molecular model is illustrated in Figure 2.8. **R** represents the hydrocarbon group, which normally contains up to six carbon atoms and can be branched as well, while $\mathbf{M^+}$ represents a cation - usually potassium or sodium. Its role is to balance the negative charge, otherwise it plays no part in the reaction leading to the hydrophobicity of the mineral (Rao, 1971).

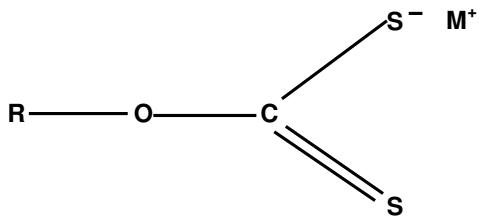

Figure 2.8: *Illustration of the structural molecular model of the xanthate anion.*

When a sulphide mineral that is conductive in nature is immersed in an aqueous solution, it develops a potential called the *rest potential*. At the surface of a sulphide, two independent electrochemical reactions occur. Dixanthogen can possibly form by anodic oxidation of adsorbed ion.

$$2X^- = X_2 + 2e^- \qquad (2.6)$$

Where X^- represents the xanthate ions and X_2 represents the dixanthogen.

The cathodic half reaction is the reduction of oxygen adsorbed at the surface and is as follows:

$$\frac{1}{2}O_{2(ads)} + H_2O + 2e^- = OH^- \qquad (2.7)$$

Electron transfer is through the sulphide mineral and the overall reaction is as follows:

$$2X + \frac{1}{2}O_{2(ads)} + H_2O = X_2 + OH^- \quad (2.8)$$

When the rest potential is less than the reversible potential for the xanthate oxidation, dixanthogen cannot form and the metal xanthate is the only possible adsorbed species.

Research conducted by Bozkurt *et al*. (1998a) on pyrrhotite/pentlandite interaction shows that dixanthogen is the main adsorption product on a mineral surface and its concentration was consistently higher on the pentlandite than on the pyrrhotite. Bozkurt *et al*. (1998) showed that for the two minerals sharing the same solution dixanthogen adsorption on pentlandite was increased compared to pentlandite alone.

Furthermore, Bozkurt's research (1998a) showed that the physical contact between the two minerals in suspension prompted the formation of dixanthogen on the pentlandite at the expense of depressing its formation on pyrrhotite. This phenomenon could be an additional reason why there is such a high loss of pyrrhotite and will require more attention in the future. The 5% loss of pentlandite could be attributed to the fact that some of the grains are locked in pyrrhotite as exsolution lamellae. Since the PGMs are contained in pyrrhotite and chalcopyrite and rarely in pentlandite (Prendergast, 1990; Pentberthy, 1999; Oberthür, 1998a, 1998b, 1999, 2002,), it means a method of preventing this high percentage loss of these minerals must be revisited. However, one significant point raised by Marais *et al.* (1992) is that the PGM sulphide mineralisation in the ore was found not to be closely associated. Hence, higher floatation recoveries do not result in higher PGM recoveries due to the poor nature of association between these minerals. Most of the observed PGMs occurred as liberated particles (Marais *et al.*, 1992). This clearly means that succeeding in floating the sulphides does not necessarily mean that the PGMs will be recovered. Mimosa ore also indicates losses due to PGMs enclosed in silicates, therefore finer grinding is required to improve the recovery. In addition, the low PGM recoveries could be due to the sulphide loss mainly in the form of pyrrhotite to the tailings, as indicated in Table 2.6. This shows that more innovative ideas in the processing of the Mimosa ore are required for optimum PGE recovery**.**

The following section discusses the trithiocarbonates achievements in improving grade and recoveries of various operations and research (Davidtz, 2002).

2.2.5. The Role of Trithiocarbonates

Since their inception around 1925, the xanthate collectors have been the workhorse of sulphide minerals flotation (Parekh, 1999). Their advantage is that they are inexpensive, easy to produce, available in solid form, totally soluble in water and they are very effective in the non-selective flotation of sulphide minerals (Klimpel, 1994). Their development over the years has led to the discovery of the trithiocarbonates and will also be referred to as TTCs in this study. What differentiates this type of collector species from the xanthates is that the oxygen atom in xanthates is replaced by a sulphur atom (Slabert, 1985). TTCs are generally synthesised by reacting mercaptan (R-SH) with carbon disulphide (CS_2) in the presence of potassium hydroxide (KOH) and according to reaction 2.9 in comparison to reaction 2.5:

$$R\text{-}SH + KOH + CS_2 \rightarrow R\text{-}S\text{–}CS_2K + H_2O \qquad (2.9)$$

According to Du Plessis (1999) there are basically two classes of TTCs, i.e. the ionic and the ester type. This means that a TTC structure can either be a normal straight chain or it can be branched. The ester type seems to perform better than the straight chain type. Some preliminary investigation conducted by Coetzer and Davidtz (1989) has shown that the ester type TTCs are very effective in bulk flotation of sulphides compared to the straight chain ionic TTC.

With oxygen possessing a higher electronegativity than sulphur, dithiocarbonate (DTC) treated mineral particles are expected to show a certain degree of polarity as to the TTCs such that surface hydration occurs in the former (Du Plessis, 1999). It is on this basis that TTCs have been reported to be stronger collectors than their DTC counterparts and can be used to lower dosages for near neutral pH slurries (Davidtz, 2002).

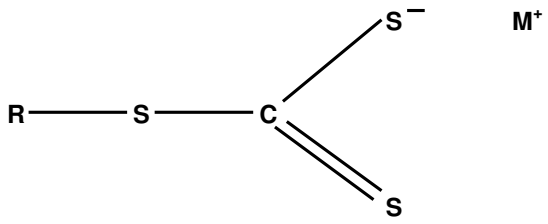

Figure 2.9: *The illustration of structural molecular model of the trithiocarbonate (TTC) anion.*

A study conducted by Slabert (1985) on the Merensky ore indicated that a 2% increase in the recovery of PGMs relative to the standards [mixture of sodium iso-butyl xanthate (SIBX) and dithiophosphate (DTP)] was achieved at Impala Platinum with isopropyl trithiocabonate (iC_3-TTC) collectors. According to Steyn (1996) short chain TTCs were discontinued from this operation due to the fact that they are unstable and therefore tend to produce an unpleasant odour. The chemical reaction that takes place during their decomposition is the reversal of reaction 2.9 and the unpleasant smell is due to the mercaptan that is formed during the decomposition (Davidtz, 2003).

Slabert (1985) also evaluated TTC against xanthates on copper sulphide ore from Phalaborwa Mining Company and found that the recovery rates and grades were consistently better than with xanthates. An investigation by Steyn (1996) also indicated that there was an improvement in the platinum-group mineral recovery of iron containing minerals like pentlandite and pyrrhotite. Therefore it would be expected that the TTCs would improve recovery of the sulphides during bulk flotation.

A study by conducted Van Rensburg (1987) on long chain TTC at high and low pH showed that they performed better compared to the short chain TTCs. The conclusion was that oxygen atom in collectors should be avoided, since they generally decreased the grades.

Makanza (2005) conducted an investigation on the flotation of auriferous pyrite using mixtures of TTCs and DTC.

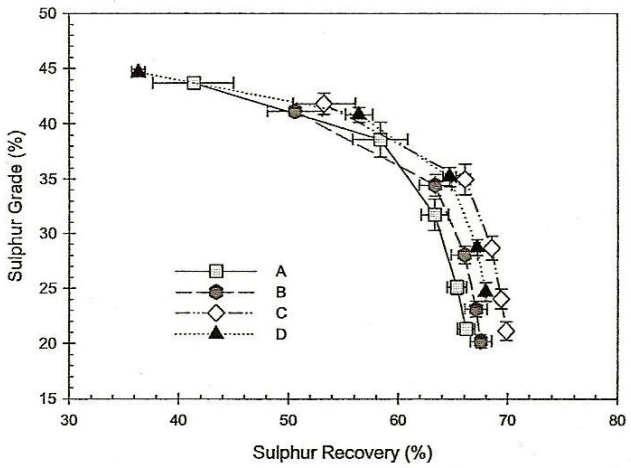

Figure 2.10: *Sulphur recovery-grade curves for [A] the standard, [B] 8 mole percent C_{12} TTC, diluted and aged for 24 hours, [C] 8 mole percent fresh C_{12} TTC and [D] 8 mole percent mercaptan (Makanza, 2005).*

Figure 2.10 shows the sulphur recovery-grade curve results obtained by Makanza (2005). The final recovery of sulphur in these graphs shows the best performance when 8 mole percent fresh C_{12}-TTC was used compared to the standard.

Figures 2.11 and 2.12 show the uranium and gold recovery-grade curves obtained by Makanza (2005) respectively. Based on these results, Makanza (2005) concluded that SIBX: C_{12} TTC mixture at 92%:8% performed better than the SIBX alone.

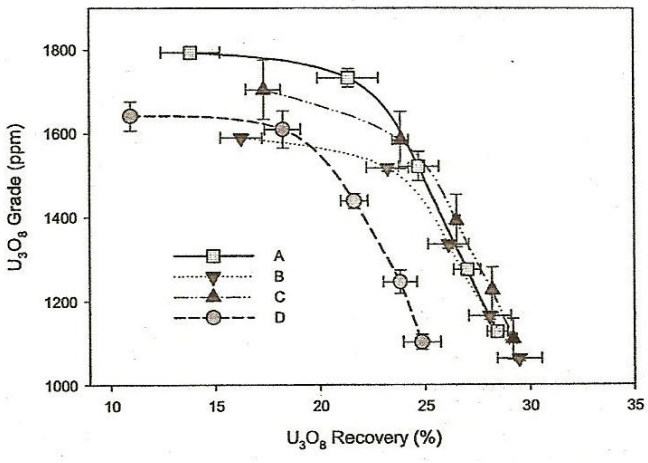

Figure 2.11: *Uranium recovery-grade curves for [A] the standard, [B] 8 mole percent C_{12} TTC, diluted and aged for 24 hours, [C] 8 mole percent*

fresh C_{12} TTC and [D] 8 mole percent C_{12} mercaptan (Makanza, 2005).

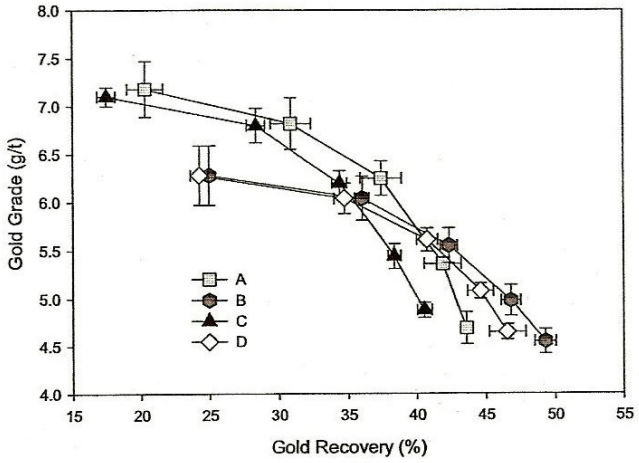

Figure 2.12: *Gold recovery-grade curves for [A] the standard, [B] 8 mole percent C_{12} TTC, diluted and aged for 24 hours, [C] 8 mole percent fresh C_{12} TTC and [D] 8 mole percent C_{12} mercaptan (Makanza, 2005).*

Figure 2.13 shows the grade-recovery curves obtained by Breytenbach *et al.* (2003) in a study of the synergistic effect between the dithiocarbonate (DTC), dithiophosphate and trithiocarbonates. It can be seen from Figure 2.13 that the highest grade-recovery curve was obtained with a 7.5 mole % TTC mixed with the standard collector of Implats. Breytenbach *et al.* (2003) discovered during their study that the mixture of the three collectors, namely TTC, DTC and DTP, significantly improved the overall flotation response by increasing the recovery and rate without negatively affecting the concentrate grade.

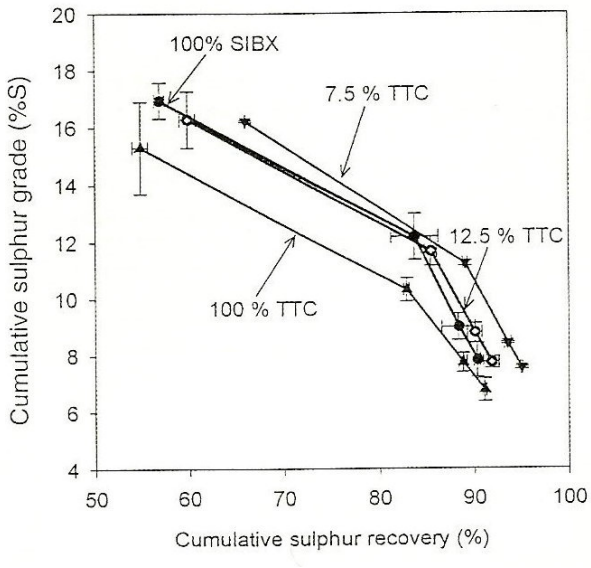

Figure 2.13: *Grade-recovery relationships of the selected mixtures of iso-butyl dithiocarbonate and n-C_{12}-triocarbonate and that of the pure species (Breytenbach et al., 2003).*

The interaction of the TTC with the sulphides (using pyrite) on more fundamental levels in comparison with the DTC has been studied by Du Plessis *et al*. (1999). In this study it was shown that TTC oxidizes easily compared to the DTC. Therefore the TTCs are expected to be more effective in sulphide mineral flotation. In a study by Du Plessis *et al.* (1999) on electrochemically controlled contact angle measurement at low potentials, low pH conditions (on the pyrite surface) revealed that a hydrophobic pyrite surface state can be created by the TTC even below the estimated standard potential for the TTC/$(TTC)_2$ couple. This suggests that in the case of TTC, dimmer formation is not responsible for imparting hydrophobicity to the pyrite surface.

It is therefore on the above mentioned basis that this research seeks to use the TTCs as the collectors to try and improve the grades and recoveries of PGMs of the Mimosa ore. This study investigates the flotation response of the short chain versus long chain TTCs and the synergism of these compounds with SIBX. The synergistic effect between SIBX and DTP is also investigated, since it is the preferred mixture in many of the Merensky operations of Impala and the following section gives a brief overview of the DTP.

2.2.6. The role of Dithiophosphates

A dithiophosphate (DTP) is a collector type of species used in flotation and it is synthesized by reacting phosphorus pentasulphide (PS_5), alcohols (MOH) and phenols (Ph) according to the following chemical reaction:

$$PS_5 + M^+OH^-Ph = (Ph)_2O_2PS_2M + H_2O \qquad (2.10)$$

The general chemical structure of the product (DTP) is as shown in Figure 2.14.

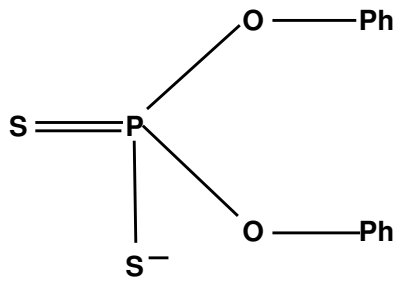

Figure 2.14: *Molecular structure of dithiophosphate collector*

DTPs are particularly insensitive to depressants and for this reason have found a wide application, especially in differential flotation of minerals. In the flotation of PGM ore of the Merensky reef, a xanthate collector is used by some operators as the primary collector in conjunction with a secondary collector such as DTP (Bradshaw, 2005a). Bradshaw (2005a) states that the use of DTP as a secondary collector has been shown to improve the collector effectiveness through both synergistic effect and froth stabilization. The synergistic effect of the DTP with dithiocarbamate in the flotation of arsenopyrite and pyrite was studied by O'Connor (1990) and the results showed that improved recoveries were obtained with a mixture of the two collectors rather than with the DTP alone. As part of this research exercise, the synergistic effect of the DTP with the SIBX will also be investigated on the Mimosa ore.

2.2.7. Activators

Modifiers are additional components that are commonly used in froth flotation and include the following: *activators, depressant*, *dispersants* and *pH regulators*. For the purpose of this study only the activators will discussed in this section. The depressants will be discussed briefly in the following section.

Activators are usually added to modify the mineral surface to enhance or increase the interaction of the collector with the particle surface, which is otherwise ineffective alone (Sutherland and Wark, 1955). One example of a widely used activator in the sulphide flotation is copper sulphate ($CuSO_4$). Other activators, such as Fe^{2+}, Pb^{2+} can also be used, depending on the mineral type. $CuSO_4$ is widely used in Merensky PGM flotation operations (Cramer, 2001).

In order to aid the flotation of pyrrhotite for example, $CuSO_4$ is usually added to the pulp. A study conducted by Bradshaw *et al.* (2005a) showed that the addition of $CuSO_4$ dramatically increased pyrrhotite flotation performance. These results confirmed results obtained by Wiese *et al*. (2005). Bradshaw *et al*. (2005a) state that the improvement in pyrrhotite flotation performance demonstrates that copper activation occurs at alkaline pHs, but the nature of the activation mechanism was not electrochemical and was likely to be chemical. The Cu^{2+} ions modify the surface of the pyrrhotite mineral and make it possible for the collector to easily attach itself to the activated surface. At the Mimosa Mine, $CuSO_4$ is not used at all as an activator. It is believed that $CuSO_4$ activates talc and makes it difficult to depress.

It is believed that pyrrhotite will adsorb xanthate in most cases and therefore it can be recovered without activation (Bryson, 2006). Copper is suspected of possibly activating gangue minerals at high pH values; but needs to be added in large dosages for this to occur (Bryson, 2006). Test work done by Wiese *et al*. (2005) on the Merensky ore indicated that the addition of DTP and copper sulphate led to the significant gangue activation, which is not reversed by the presence of a depressant. Another aspect relating to copper not being used at Mimosa Mine is that it reacts with the gangue depressants and therefore renders the depressant inactive (Bryson, 2006).

2.2.8. Depressants and Talc Depression

Depression of gangue is a well-known method employed by metallurgists during the flotation process. Depression could be defined as the opposite of activation; hence it implies reducing floatability of a mineral. The gangue is separated from the concentrate by using chemical species (polymers) known as depressants (see Figure 2.15). According to Ebbing (1993), a polymer is a chemical species with very high molecular weight that is made up from many repeating units of low molecular weight. These polymers, which could also be polysaccharides, are often used to selectively depress the gangue material while the valuable material is floated, thereby separating it from the gangue. This is achieved either by preventing the adsorption of collector onto the mineral surface or by co-adsorption of the depressant and collector molecules onto the surface (Klassen and Mokrousov, 1963). The quantity of depressant added is related to the quantity of gangue present in the ore, and if too much is added then depression of the valuable minerals such as the sulphides in the PGM ore and kerogen will occur (O'Connor *et al.,* 1984; O'Connor and Van Zyl, 1985).

Talc also acts as gangue material in the PGM operations and it reports to the concentrate due to its hydrophobic nature, as already discussed in Section 2.1.5.

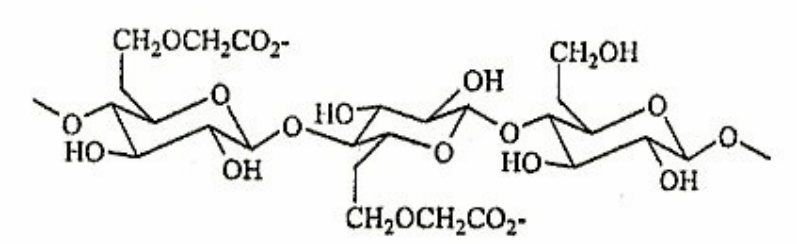

Figure 2.15: *Schematic diagram showing the molecular structure of carboxymethyl cellulose (Khaisheh et al., 2005).*

The upgrading of talc into the concentrate lowers the PGM grades and causes problems in the smelters due to the resulting high MgO content (Pugh, 1988a), forcing the smelter operators to impose penalties to the concentrators. It also causes the concentrate froth to be rigid and take time to break down. In the concentrating stage of a conventional mineral processing plant operation, talc is dealt with by depressing it together with other silicate gangue minerals. Various studies on the

depression of talc using different types of depressants have been conducted by various workers (Steenberg and Harris, 1984; Fuerstenau *et al.,* 1988; Pugh, 1988a; Pugh, 1988b; Tjus, 1989; Morris *et al.,* 2002; Zbik 2002; Khraisheh *et al.*, 2005).

The general understanding of the depression of talc is that the polymer adsorbs on the hydrophobic interaction of the hydrocarbon backbone at the talc face. The hydrophilic hydroxyl and carboxyl groups of polymers are therefore extended out from the talc surface, imparting some hydrophilic character to the talc particles and thereby depressing the gangue during flotation (Moris *et al.*, 2002). The interaction mechanism between the talc and polymer involves one or more of chemical, electrostatic, hydrogen and hydrophobic bond. Carboxymethylcellulose (CMC), guar gum, starch dextrin, polyphenols, etc, are examples of the depressants that are widely used in the mineral processing industry.

The adsorption mechanism of talc has been investigated and discussed by Steenberg and Harris (1989). They established that polymer adsorption occurs first in the basal plane and then on the talc edge. Steenberg and Harris (1989) showed that the low charged density of the basal plane enables the molecules to spread out on the uncharged surface, whereas they are densely packed on the hydrophilic-charged edges. They explained that the adsorption density of some polymers can be influenced by the specific inclusion of ion in the polymer layer, although the presence of these counter ions does not prevent adsorption. Hence the main adsorption mechanism must therefore involve hydrogen bonding of the large hydroxyl groups to the charged sites on the mineral surface. Steenberg and Harris (1989) concluded that the selectivity of the flotation process is created by the very much stronger specific interactions of the collectors, which displaces the weakly held polymers from the valuable mineral surface, leaving it in a hydrophobic state and available for flotation.

A study carried by Morris *et al.* (2002) indicated that the depression of talc increases with an increase in the adsorption density of polymers on the talc surface. In their study of polymer depressants at the talc-water interface, Morris *et al*. (2002) concluded that the solution conditions, such as ionic strength and pH, strongly influence the adsorption of the anionic polymers such as CMC and polyacrylamide (PAM-A) onto the talc surface. In this study Morris *et al*. (2002) showed that at acidic

pH or high ionic strength the adsorption density of the anionic polymer depressant increases, hence the talc depression is increased.

In contrast to the typical corboxymethylcellulose (CMC) concentration of 100g/t employed at the Merensky operation, a consumption of 500g/t (CMC) is used at Mimosa Mine (Marais *et al.*, 1992). The reason for this excessively high reagent dosage at Mimosa Mine is due to the fact that copious amounts of talc are liberated during milling and therefore a substantial amount of depressant is required to keep most of the talc from reporting to the concentrate. The hydrophobicity of talc is discussed in Section 2.1.5. The addition of high depressant concentrations may result in the depression of the base metal sulphides that are usually associated with the PGE. This could be one of the contributing factors for the 79% recovery at Mimosa. If the depressant strength could be lowered, this could release more base metal sulphides, consequently releasing more PGEs to the concentrate. The following section looks briefly at the frother and its role in the flotation of Mimosa ore.

2.2.9. Frothers

A frother is an important component of the flotation reagents that is used together with a collector in the flotation process. The addition of a frother has a two-fold purpose. Firstly, it allows for finer bubbles to be formed in the flotation pulp. The change in the bubble size is a function of the type and amount of frother used. Decreased bubble size implies the presence of more bubbles per unit volume of air, hence the likelihood of increased rates of flotation. Secondly, the frother allows for a suitable froth phase to form and correct frother usage will enhance flotation performance. The neutral frothers (i.e. frothers that do not specifically act as collectors) that are used in most flotation systems (Harris, 1982) are non-ionic compounds and consist of the monohydroxylated compounds of limited water solubility such as pine oil, cresylic acid and the aliphatic alcohols, the hydroxylated water-soluble frothers such as the polypropylene glycol ethers, and the alkoxy-substituted paraffin such as triethoxy butane.

According to Harris (1982), in general, the requirements of a good flotation frother are:

1) The stability of the froth formed must be such that a further degree of separation of valuable minerals from the non-floatable (entrained) material is obtained in the froth.
2) Once the froth containing the valuable mineral is removed it must break readily for any further treatment.
3) It must form a froth of sufficient volume and stability to act as a medium of separation at low concentration.
4) In the case of a neutral frother, it should have limited collecting tendencies.
5) It must possess a low sensitivity to changes in pH and dissolved salt concentration.
6) It must be readily dispersible in the aqueous solution.
7) It should be relatively cheap and abundant for large scale use.

Laskowski (2003) proposed a frother classification system based on Dynamic Foamability Index (DFI) and Critical Coalescence Concentration (CCC) measurements. This type of measurement would probably help in determining the effect of the frother to the Mimosa ore, since the froth formed on this tends to be rigid due to the presence of high levels of talc. The frother dosage at Mimosa Mine is given in Table 2.5 as 48g/t and is different from the normal 60g/t, which is the average for the Merensky operations. The reason for this amount of frother dosage is attributed to the fact that more talc will be floated should more frother be added to the slurry.

Yehia and Al-Wakeel (1999) studied natural flotation behaviour by measuring the contact angle, flotation recovery and zeta potential. Polypropylene glycol was used as a frother to increase the talc flotation at relatively shorter times. This study showed that the highest natural floatability of talc was obtained at neutral pH and decreased to different degrees in both acidic and alkaline solutions. It was also shown that the flotation recovery of talc was higher in the presence of frother compared to the natural floatability. Since frother forms one of the reagent suites, this is one of the reasons why it is so difficult to depress talc at Mimosa Mine. This phenomenon was used as the basis to remove talc by flotation prior to the flotation of the PGMs. In other words, the concentrating plant could be modified in such a way that talc is first floated prior to the concentration of the PGE+Au.

This study does not, however, look at this alternative in detail, as this could be an entire project on its own. In the following section (2.2.10) the removal of talc by hydro-cyclones prior to the flotation of sulphides is discussed.

2.3. TALC DE-SLIMING USING DE-WATERING CYCLONES

Over many years, the use of hydro-cyclones has become the accepted standard classifying (separation) method in the mineral processing industry. The reason for hydro-cyclones' popularity is based on the fact that they are relatively inexpensive, have a very high capacity, occupy a relatively small floor space and are easy to maintain.

A typical hydro-cyclone consists of a conical section, which is opened at its apex and is joined to a cylindrical section known as the barrel. The barrel is normally joined to a tangential feed inlet. The top of the inlet head is closed with a plate through which an axially mounted overflow pipe passes. This pipe is extended into the body of the cyclone by a short removable section known as the vortex finder, which prevents short-circuiting of feed directly into the overflow. An underflow discharger is fitted to the apex of the cyclone and is known as the spigot.

A hydro-cyclone separates the lighter particles from the heavier particles by speeding up the settling rate of the heavier or denser particles. This is achieved by introducing the feed through the tangential inlet under pressure, which imparts the swirling motion to the slurry. A low-pressure cylindrical zone is generated in the centre of the cyclone while the high-pressure zone is created towards the wall of the cyclone (see Figure 2.16). This is due to the drag force and the centrifugal force that develops and accelerates the settling rate of the particles, thereby separating the particles based on their size and density (Kelly, 1989; Wills, 1997). The lighter particles in the slurry tend to move to the low-pressure zone caused by the drag force and are carried upward to the overflow pipe while the denser particles move to the outer high-pressure zone due to centrifugal force and are carried to the underflow at the bottom of the cyclone. The performance of a cyclone is dependant on a number of factors such as the percentage of solids in the feed, feed pressure, cyclone configuration, etc.

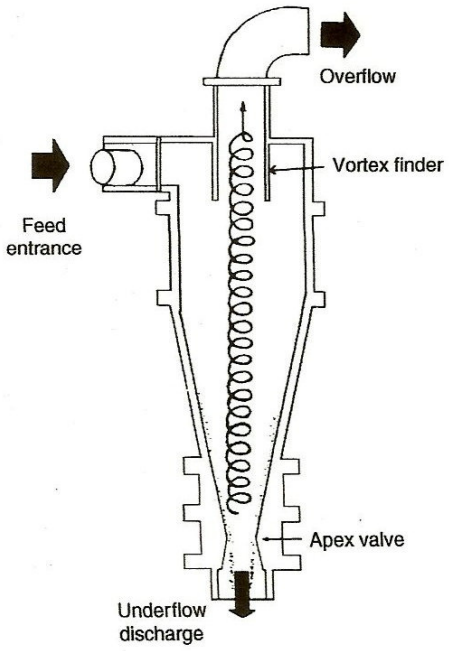

Figure 2.16: *Hydro-cyclone (Wills, 1997).*

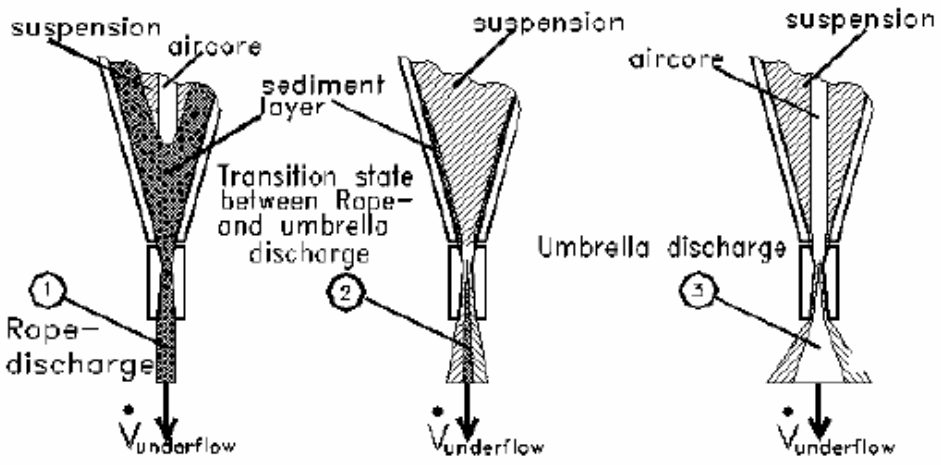

Figure 2.17: *The three different flow conditions in a hydro-cyclone (Neesse et al., 2003).*

The separation of the feed material into the overflow and underflow streams is dependent on three properties of the feed material, namely size distribution, density and shape. The maximum solids recovery of heavier particles in a hydro-cyclone depends on the form of the underflow discharge (Neesse *et al.*, 2003). When the discharge is similar to (1) in Figure 2.17, the discharge form is called rope discharge and the separation of the heavier particles from the lighter particles will not be

effective since the slurry will fall straight to the apex without undergoing any centrifugation. As a result the lighter material will report to the underflows without being classified. This happens when the feed pressure is too low. When the discharge is similar to (3) in Figure 2.17 then we have what is called the umbrella effect. This form happens when an air column is created in the middle of a cyclone and most of the denser particles report to the overflow by short-circuiting and the lighter particles will report to the underflow (Neesse *et al.*, 2003). When the discharge forms a balance between form (1) and form (3) then one obtains form (2). This occurs when a maximum solids recovery and high solid content in the underflow occurs and a near to perfect separation between denser particles and lighter particles takes place.

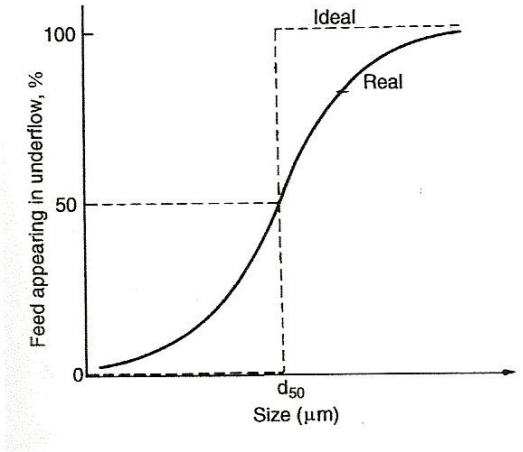

Figure 2.18: *Partition curve for a hydro-cyclone (Wills, 1997).*

The hydro-cyclone efficiency is represented by the so called performance or partition curve, which relates the weight fraction or percentage of each particle in the feed which reports to the apex or underflow to the particle size (Wills, 1997). Figure 2.18 shows an example of such a partition curve. The point labeled d_{50} on the partition curve is called the *cut-point* or the separation size of cyclone and it represents the point for which 50% of the particles in the feed report to the underflow. This means that the particles of size d_{50} have an equal chance of reporting to the underflow or overflow.

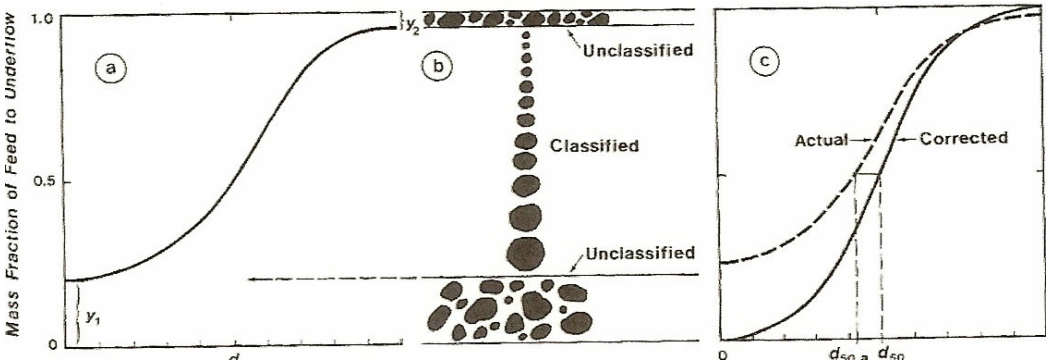

Figure 2.19: (a) *Characteristic form of a sedimentation classifier curve. (b) Relationship of the performance curve to particle classification. (c) The corrected performance curve (Kelly and Spottiswood, 1989).*

In practice the curve shown in Figure 2.18 is never achieved. Instead the real situation curve is shown in Figure 2.19 (a) and shown schematically in Figure 2.19 (b). Figure 2.19 (a) curve shows that a fraction of the finest particles report to the underflow where they are not supposed to, under ideal cyclone classifier and this fraction is represented as y_1 and y_2 is the imperfection due to feed material bypassing to the overflow (Kelly, 1989). According to Kelsall (1953) the unclassified feed solids to the underflow is directly proportional to the fraction of water in the cyclone feed that is recovered in the underflow product. This water is also known as α-water. Flintoff *et al*. (1987) state that from the hydrodynamic viewpoint this is sensible since one would expect fine particles to follow the water. Figure 2.19 (c) shows the actual curve and the corrected curve. The following mathematical equation is used to derive the corrected curve from the actual curve (Kelly and Spottiswood, 1989).

$$R_{(+)} = \frac{(R_{(+)a} - y_1)}{(1 - y_1 - y_2)} \tag{2.11}$$

Where, $R_{(+)}$ to equal to the corrected recovery to the underflow, $R_{(+)\,a}$ is the actual or uncorrected recovery to the underflow, y_1 is the fraction of the finest particles to the underflow, which is the same as the fraction of the feed water leaving through the underflow and y_2 is the imperfection due to feed material bypassing to the overflow. Generally, y_2 is negligible, although it may appear to exist when the particles have a range of densities (Kelly and Spottiswood, 1989). A detailed discussion on the theory

and other research work on the hydro-cyclones can be found elsewhere in this study (Kelsall, 1953; Plitt, 1971; Flintoff *et al.*, 1987; Kelly, 1989; Wills, 1997).

In this study, the removal of talc by de-sliming the milled Mimosa ore using de-watering hydro-cyclone is investigated. There are two fundamentals reasons why the removal of talc by de-sliming is envisaged for this study. Firstly, Table 2.4 shows that the density of talc ranges between 2.7 and 2.8 with an average of about 2.75. This makes it lighter compared to the base metal sulphides such as chalcopyrite (specific gravity = 4.1-4.3) pentlandite (specific gravity = 4.6-5.0), pyrrhotite (specific gravity = 4.6) and pyrite (specific gravity = 4.9-5.2). Secondly, as was already discussed in Section 2.1.5 of this study, talc is friable and therefore breaks easily into finer material during milling. It is therefore expected that the fine material of the Mimosa ore would consist of high concentrations of talc. It is postulated that talc can therefore be removed from the ore by de-sliming using de-watering cyclones. In order to minimize the amount of talc from the feed ore, the finer material (mostly talc in this instance) report to the overflow stream while the heavier material reports to the underflow stream.

As the second part of this study, de-sliming using de-watering cyclones was investigated. Based on the discussion given about the hydro-cyclones, the second part of this research investigates the possibilities of removing talc from the Mimosa ore using de-watering cyclones.

CHAPTER THREE

EXPERIMENTAL (PART I)

COLLECTOR OPTIMISATION

3.1. MATERIAL AND SAMPLE PREPARATION

3.1.1. Ore

The bulk PGM ore sample was received from Mimosa Mine as a crusher product weighing 800 kg (with particle top size 95% passing 9.5mm). This ore sample was hauled to South Africa contained in a one tonne bag that protected it from any kind of contamination. It was delivered at the Kumba Resources pilot plant in Pretoria West, where it was split by a rotating splitter into samples of 4kg each. After splitting the bulk sample into 4kg sub-samples it was transported to the Mineral Processing laboratory at the University of Pretoria where experiments were conducted. The specific gravity of the ore was determined and found to be 2.8 g/ml.

3.1.2. Crushing and Milling

Prior to flotation, the 4kg sample was crushed in a Massco cone crusher to reduce the particle size from 95.4% passing 9.5 mm to 96% passing 2.36 mm. Thereafter milling was carried out in a stainless steel bond mill measuring 300 mm in diameter and 300 mm in length. The rods used for milling were also made out of stainless steel and were in three sets according to different diameters. The three sets of rods consisted of 12.5 mm, 16.0 mm and 21.5 mm in diameter. The numbers of rods in each set were 31, 37 and 7 respectively with a total mass of 32.4 kg. The solids in the mill were kept at 60% (w/w) with the mill speed being 67 rpm throughout the experiments. A 3.3 kg representative portion of the 4kg sample was milled to 70% passing 75µm size in a laboratory scale stainless steel rod mill with the dimensions given in Table 3.1. The remaining portion of the sample was kept for head analysis (sulphur and PGE +Au).

Wet milling of the ore was performed at different time intervals to establish a milling curve in order to determine the time required for the correct size distribution. Figure 3.1 shows the milling curve for the bond mill that was used to mill the Mimosa ore. This curve was used to determine the time taken to reduce the ore from 96% passing 2.36mm to 70% passing 75µm. The aim of this exercise was to establish a particle size distribution similar to that of an industrial flotation plant.

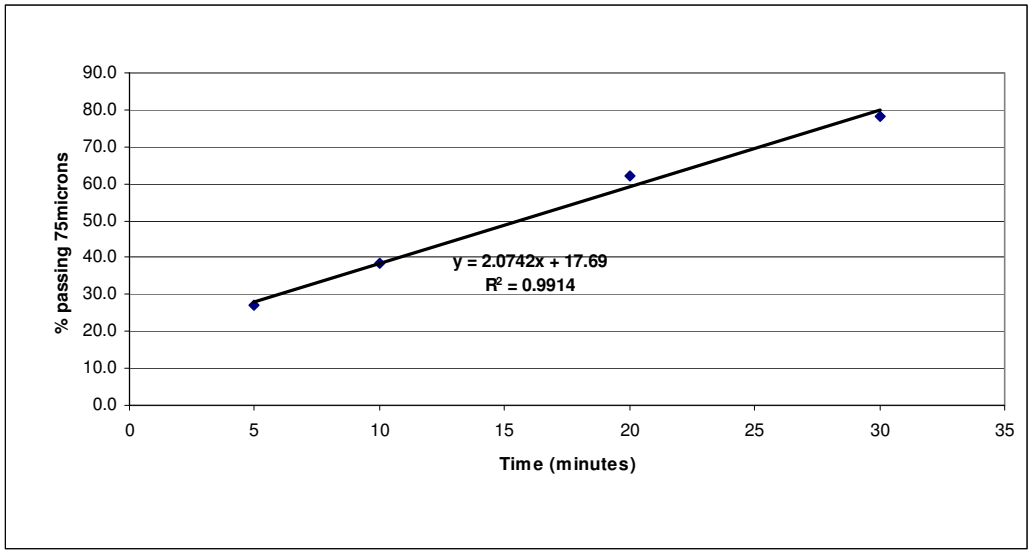

Figure 3.1: *The milling curve for the laboratory rod mill that was used to mill the Mimosa ore to 70% passing 75µm.*

The particle size distribution of the ore milled in the laboratory was compared with that obtained from the plant - depicted in Figure 3.2. The rods were used in the laboratory because they give a narrow size distribution that is close to that of the plant. The slight difference that is seen in the graph is due to the fact that the plant employs closed milling circuit with classification.

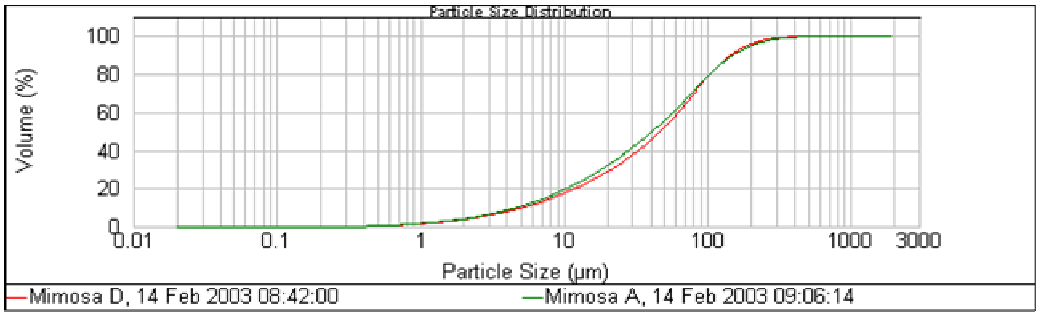

Figure 3.2: *The size distribution of the ore milled at Mimosa (Mimosa A) and the size distribution of the ore milled with the rod mill in the laboratory (Mimosa D).*

3.2. FLOTATION CELL USED DURING THE TEST WORK

The flotation machine used in this research was a D12 Denver flotation machine fitted to an 8-litre cell. The impeller speed was adjusted to 1600 rpm, with controlled air supply. A ten litre bucket was connected to an 8 litre cell via a rubber tubing of 10 mm diameter. The rubber tubing was fitted with an automatically controlled electronic valve. The electronic valve was connected to an automatic level control probe. The probe was attached to the flotation cell and it was in contact with the pulp as long as the pulp level was maintained. As soon as the pulp level dropped during the flotation experiment and the probe lost contact with the pulp, the valve opened and allowed water to flow from the bucket via the rubber tube and increase the pulp level to the set level. As a result, the pulp level was maintained. The froth level varied depending on the type of collector used. The aim was to keep the froth height at 30mm above the slurry level. The pulp pH was monitored using an Orion pH meter (model 420).

3.3. REAGENTS USED DURING THE FLOTATION TEST WORK

3.3.1. Collectors

Based on the literature survey discussions given in Chapter 2, five types of collectors were used during the flotation tests, either as pure or as mixtures in order to determine possible synergistic effects. Table 3.2 lists the collectors used. About 1kg of fresh SIBX together with a DTP was provided by SENMIN (South Africa). The SIBX solution was prepared by dissolving the yellow powder of SIBX to the correct concentration every day before the flotation experiment was carried out. The SIBX

was used as it is, without further purification. All the TTCs were synthesised in the laboratory using mercaptan, potassium hydroxide (KOH) and carbon disulphide (CS_2). Section 3.3.2 describes the procedure for synthesizing TTCs in the laboratory.

Table 3.1: *Types of collectors used during the flotation tests.*

Name	Abbreviation	Molecular structure	Molecular Weight (a.m.u.)	Molecular mass + water of crystallisation
Sodium iso-butyl xanthate	SIBX	$C_4H_9OCS_2Na$	172.2	208.2
Potassium n-butyl tri-thiocarbonates	C_4 TTC	$C_4H_9SCS_2K$	204.4	222.4
Potassium n-decyl tri-thiocarbonates	C_{10} TTC	$C_{10}H_{21}SCS_2K$	288.6	306.6
Potassium n-dodecyl tri-thiocarbonates	C_{12} TTC	$C_{12}H_{25}SCS_2K$	316.6	334.6
Sodium di-n-butyl dithiophosphate	DTP	$(C_4H_9)_2O_2PS_2Na$	264.3	266.0

Table 3.2 lists the abbreviations for the collectors and collector mixtures used during the flotation test. For the purpose of simplifying the discussion in the results and discussions section, the abbreviations are used in the graphs to represent the molar ratios as given in Table 3.2. Fresh stock solutions of the collectors shown in Table 3.2 were prepared daily.

3.3.2. Preparation of the TTCs

The TTCs were synthesized as a salt because of improved stability when compared to the liquid form. Although the TTC solutions are relatively stable at high pH, their half life is strongly dependant on pH (Davidtz, 2002). To avoid hydrolysis, potassium salts were prepared. The TTCs were prepared by first placing finely ground pellets of potassium hydroxide (KOH) in a flask which was placed in an ice bath (Drake *et al.*, 1993). Mercaptan (R-SH) solution (supplied by G.P. Chemicals, USA) was added in slight excess to the KOH. The reaction is strongly exothermic, the carbon disulphide (CS_2) was added dropwise, after which the reaction was allowed to proceed for 2 hours. The following is a general chemical reaction that takes place during the preparation of the TTCs.

$$R-SH+KOH+CS_2 \rightarrow R-S-CS_2K+H_2O \quad (3.1)$$

The yellow crystals were filtered and dried in a desiccator for 1-2 days. The desiccator was also used as a storage container. The TTC crystals were dissolved before the commencement of the flotation tests.

3.3.3. Dithiophosphates

Sodium di-n-butyl dithiophosphate was supplied as a pure liquid product by SENMIN (Pty) Ltd in Sasolburg (South Africa). This product was used as it is without any further purification. No other qualities were specified by the manufacturer.

3.3.4. Preparation of the Collector Mixtures

The different individual collectors were either used as pure collectors or as a mixture. The mixtures consisted of SIBX and TTC or DTP. The SIBX was used as a primary collector and the TTC and DTP were used as secondary collectors or co-collectors. Dosages were given in moles per ton of ore (mol/t). Except in Chapter 4 whose doses were given, in g/t. flotation data was reported in moles per ton (mol/t). Table 3.2 shows all the collectors and collector mixtures that were used. The first column of the table (from the left) states whether the collector was dosed in its pure form or as a mixture. The second column gives the acronym or short form of the collector or collector mixture. The third column shows the mole percent ratio of the collector components in the mixture. The last column (on the right) gives the total moles of the pure collector or collector mixture per ton of ore treated.

Table 3.2: *The table of collectors or collector mixtures, the molar ratios and the total number of mole dosed per ton of ore.*

Pure or mixture of collectors	Collector or collector mixture labelled as:	Collector mixture (mole percent)	Total number of moles of pure or mixed collectors per ton of ore
Pure	530 g/t SIBX	SIBX : TTC or DTP 100% : 0%	2.55
Pure	530 g/t SIBX (80% in mill)	SIBX : TTC or DTP 100% : 0%	2.55
Pure	265 g/t SIBX	SIBX : TTC or DTP 100% : 0%	1.27
Pure	132.5 g/t SIBX	SIBX : TTC or DTP 100% : 0%	0.64
Mixture	6.25 % C_4 TTC	SIBX : C4 TTC 93.75% : 6.25%	2.55
Mixture	25 % C_4 TTC	SIBX : C_4 TTC 75% : 25%	2.55
Pure	100 % C_4 TTC	SIBX : C4 TTC 0% : 100%	2.55
Mixture	6.25 % C_{10} TTC	SIBX : C10 TTC 93.75% : 6.25%	2.55
Mixture	25 % C_{10} TTC	SIBX : C10 TTC 75% : 25%	2.55
Mixture	35 % C_{10} TTC	SIBX : C10 TTC 65% : 35%	2.55
Mixture	6.25 % C_{12} TTC	SIBX : C12 TTC 93.75% : 6.25%	2.55
Mixture	25 % C_{12} TTC	SIBX : C12 TTC 75% : 25%	2.55
Pure	100 % C_{12} TTC	SIBX : C12 TTC 0% : 100%	2.55
Mixture	DTP (2.27 mol.)	SIBX : DTP 56.1% : 43.9%	2.27
Mixture	DTP (1.28 mol.)	SIBX : DTP 56.1% : 43.9%	1.28
Mixture	DTP (0.64 mol.)	SIBX : DTP 56.1% : 43.9%	0.64

3.3.5. Depressant

Sodium carboxymethylcellulose (CMC) was used as depressant for all experiments. This reagent was obtained from Cellulose Derivatives (Pty) Ltd in Pretoria. This is the same company that supplies Mimosa plant with depressants and is sold under the

commercial name of Norilose 8058. Norilose comes as a yellowish granular powder, which is a soluble ionic colloid with particular thickening, film forming and soil suspending properties. According to the manufacturer's specification, the moisture is less than 7% with purity of not less than 56% and the pH of a 2% solution is not less than 10. The depressant was prepared as a bulk solution of 0.08 g/ml concentration and allowed to stand for two days before a fresh solution was prepared.

3.3.6. Activator

Copper sulphate ($CuSO_4$) was used as an activator, made up to a solution and dosed at 70 g/t.

3.3.7. Frother

Dowfroth 200 from Betachem (South Africa) was used as the frother during the entire experimental exercise.

3.3.8. Flotation Procedure

Figure 3.3 is a flow diagram of the batch process used. A dry 4kg of sample was crushed from 95.4% passing 9.5 mm with the laboratory cone crusher to 96% passing 2.36 mm. Once the sample was crushed, 3.3 kg of sample was the wet milled for wet milling, with the remaining portion kept for head sulphur and PGE+Au analysis.

The solids concentration in the mill was 60% by mass. The particle size was reduced to 70% passing 75µm during milling. The slurry from the mill was transferred to the 8-litre flotation cell. The initial slurry density was 1.27 g/ml. The cell was connected to a water supply system with the pulp level controller that ensured a constant pulp level in the cell for the duration of the experiments (Section 3.2.). Table 3.3 summarises the reagent dosing procedure followed during the experimental work.

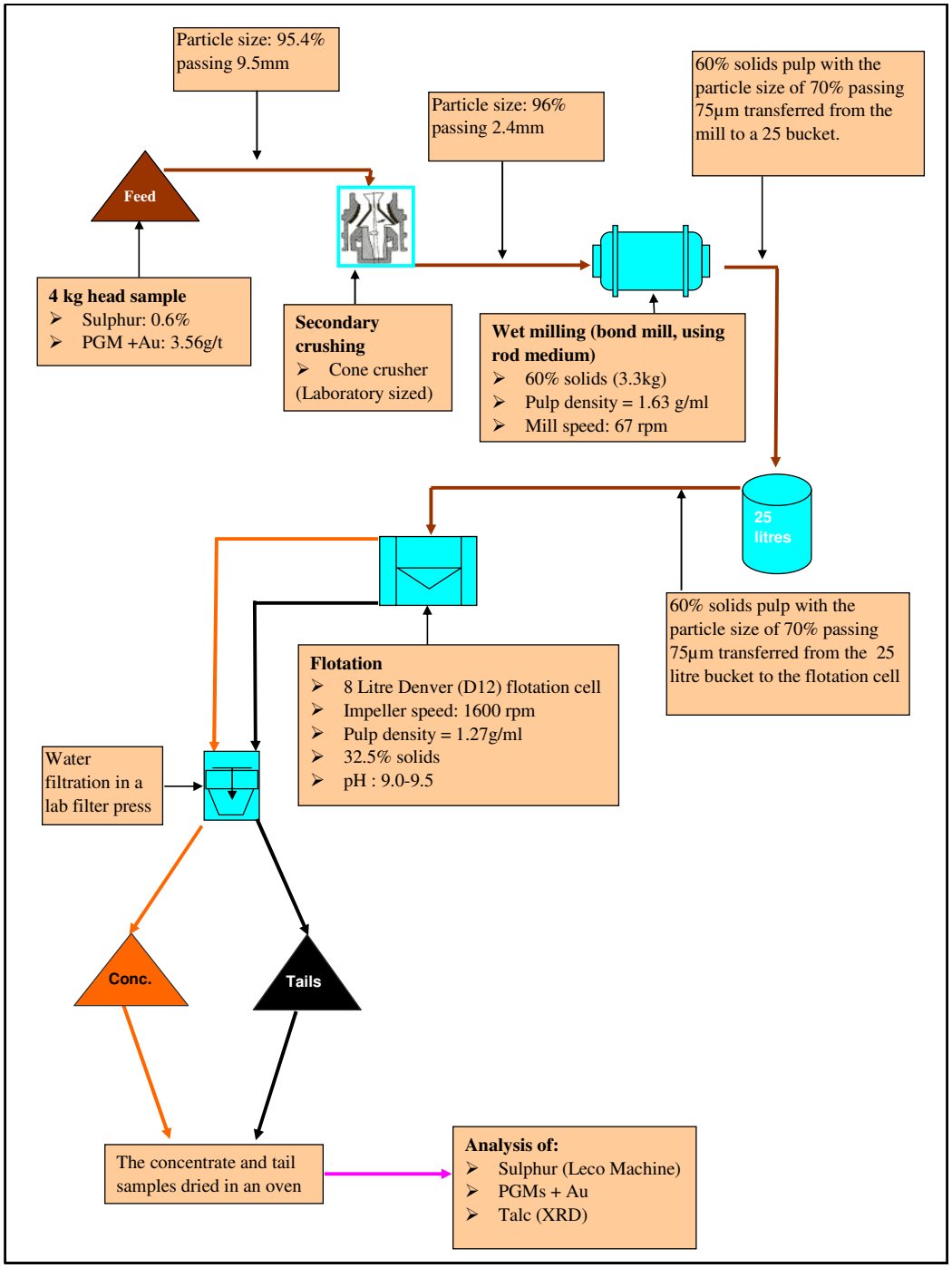

Figure 3.3: *Flow diagram of the experimental procedures followed.*

Table 3.3: *The flotation procedure*

	Conditioning time (Min)	**g/t**
Pulp Stirring	3	-
Activator ($CuSO_4$)	5	70
Collector (SIBX, TTC, DTP)	2	Variable
Depressant (CMC)	2	500
Frother (Dowfroth 200)	1	60

The slurry was stirred with the impeller running at 1600 rpm, with controlled air supply for three minutes to keep the pulp homogeneous prior to the dosing. The pH of the slurry was measured with the pH meter and it was recorded between the 9.0 and 9.5 range. After three minutes of stirring, 70g/t of the copper sulphate ($CuSO_4.5H_2O$) solution was added to the slurry. After conditioning the $CuSO_4$ for five minutes the collector (either a blend of SIBX and TTC, or DTP, or pure SIBX, or pure TTC) was added and was conditioned for an additional two minutes. The amounts of collector dosages are given both as grams per ton (g/t) and moles per ton (mol/t) in Appendix C.

The collector conditioning was followed by the addition of CMC depressant at 500g/t to the pulp. As soon as the depressant was conditioned for two minutes, it was followed by the addition of Dowfroth 200 at 60g/t and was conditioned for one minute. The dosing procedure is summarised in Table 3.3 and was repeated for all the subsequent experiments. The froth was manually removed from the slurry surface at constant height by a pair of scrapers at constant time intervals of 15 seconds. Incremental rougher concentrates were collected after 2, 7, 17 and 32 minutes each in a separate container and were weighed before filtering in the filter press. Figure 3.2 shows a picture of the containers that were used to collect the concentrates at the time intervals already indicated above. The concentrates labelled 1, 2, 3, and 4 were collected after 2, 7, 17, and 32 minutes respectively.

After the filtration, the tailings and the concentrate were dried in the oven at about 80^0C.

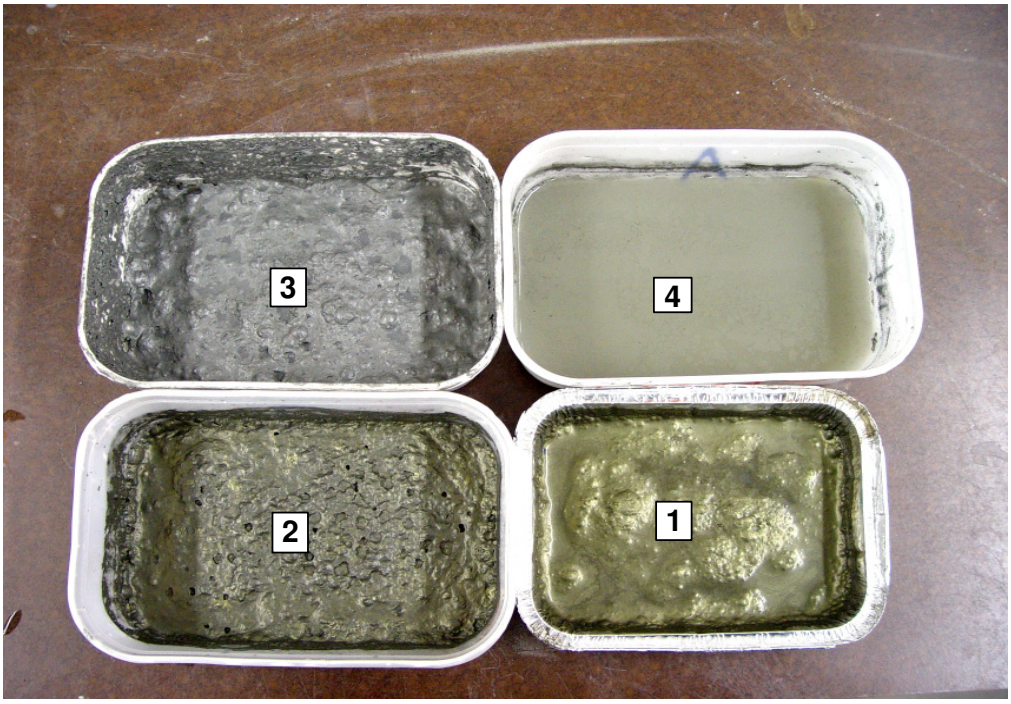

Figure 3.3: *Picture of the concentrates that were collected after 2, 7, 17, and 32 minutes, labeled as 1, 2, 3, and 4 respectively*

3.4. ANALYSIS

3.4.1. Sulphur Analysis

As soon as the concentrates and the tailings samples were dried they were placed in clearly labelled plastic bags. Once each sample was thoroughly mixed, small portions of representative sub-samples were taken for sulphur analysis.

Sulphur analysis was performed using the Leco S-144DR Sulphur Analyser shown in Figure 3.4 for all sulphur analysis in this report unless otherwise stated. 0.2 grams of the zinc sulphide standards were placed in a boat crucible and then pushed into the furnace for calibration. The calibration standards are given in Table 3.4. The calibration standard used was dependant on the percentage amount of sulphur to be analysed. For example, the 29% and the 32.8% sulphur standards were used for concentrates with the highest grades and they were collected during the first two minutes of flotation. The 13% sulphur standard was used for the concentrates that were collected during the seven minutes of flotation and are shown in container

number 2 in Figure 3.3. The last two concentrates, labelled 3 and 4 in Figure 3.3, together with the feed and tails, were analysed using the 0.56% sulphur standard.

Table 3.4: *The sulphur analyser calibration standards.*

Mintek Stds	Leco Stds (ZnS)
29% S	32.8 ± 0.2 % S
13% S	1.09 ± 0.05 % S
0.56% S	-

The Leco instrument analysed total sulphur by burning the sample at 1350^0C. The sulphur dioxide (SO_2) that released during the combustion was measured by an infrared detector and the data logged by a computer. Once the calibration was performed a 0,2 g representative sample of either the feed, the concentrate or the tails was analysed by putting the sample contained in a clean boat crucible in the furnace. The sample was then allowed to burn in the furnace. The burned sulphur reacts with oxygen to form SO_2. The sulphur percentage reading was then obtained from the computer. This procedure was repeated for all the representative sub-samples. The sulphur analysis was carried out in triplicates. The instrument was calibrated daily and each time a new set of samples was analysed. Spot checks using the standards shown in Table 3.4 were performed at regular intervals during the analysis of samples.

3.4.2. PGE + Au Analysis

The remaining portions of concentrate samples were sent to SGS Lakefield Research Africa (Pty) Ltd for PGE + Au analysis.

3.4.3. Talc Analysis

Four talc analysis samples were sent to Mintek and to the Department of Earth Sciences at the University of Pretoria for analysis. The results are provided and discussed in Chapter 4.

Figure 3.4: *Picture of the sulphur analyzer machine that was used for sulphur analysis*

CHAPTER FOUR

MIXTURES OF SIBX WITH iC_4-DTP AND TTCs

4.1. INTRODUCTION

A number of sulfide mineral flotation agents are of interest in this investigation. In particular, DTCs, DTPs and TTCs of varying chain lengths. The effect of combinations of these various collectors is also of interest. Earlier work by Slabert (1985), Van Rensburg (1987), Coetzer and Davidtz (1989), Steyn (1996), Davidtz (1998), Du Plessis *et al.* (1999), and Makanza (2005), have shown improvements in flotation activity with both short (C_3-C_6) chain TTCs, as well as long chain TTCs (C_{10} and C_{12}), and in particular C_{12} with SIBX and SIBX/TTC mixtures on Merensky ore (Breytenbach *et al.*, 2003, Vos *et al.*, 2007 and Venter and Vermaak, 2007). Current practice at most platinum mines is the combined use of DTPs with SIBX, and since only SIBX is used at Mimosa, it is also important to this study.

Grade-recovery and recovery–time data have been used to quantify molecular structure effects on flotation activity (Klimpel, 1980; Slabbert, 1985; Steyn, 1996). Similarly, such evaluations have been made in this investigation. The graphs shown compare percent cumulative sulphur grades with percent cumulative sulphur recovery, the time in minutes cumulative sulphur recovery, percent cumulative water recovery versus percent cumulative mass recovery and percent cumulative water recovery versus percent cumulative sulphur recovery. Table 4.8 summarizes the results of PGE+Au recovery and grade for the best collector mixture with SIBX for the various collector combinations and SIBX as standard collector. Mass and sulphur balance analysis data are summarized in Appendix A and Appendix B summarizes flotation results of the de-slimed ore.

4.2. RESULTS

4.2.1. Chemical Analysis of Mimosa Ore

Chemical analyses are given in Table 4.1. A detailed discussion on quantitative analysis of talc is given in Chapters 5 and 6.

Table 4.1: *Chemical analysis of Mimosa feed.*

Sulphur (%)	PGEs (g/t)	Talc (%)
0.6 ± .07	3.56 ± 0.2	15.93 ± 1,12

4.2.2. Effect of SIBX Concentration on Grade, Recovery and Rate

Effects of SIBX concentrations on grade, recovery and rate are reported in Figures 4.1 to 4.4 and Table 4.2. The standard dosage at Mimosa was 530 g/t and all flotation data refers to this concentration as the standard dosage. The grade-recovery curves in figure 4.1 show a progressive decrease as the SIBX dosage is reduced from 530 to 132.5 g/t. The final recovery decreased from 79.3 % to 76.2% and finally to 73.7%. A similar performance when dosages are decreased is also illustrated in Figure 4.2 and this agrees with cumulative sulphur recovery as a function of time for the three dosage levels. In the first minute, 50% of the total 80% sulphur is recovered at 530 g/t, compared to 25% of the 75% at lower dosages. The initial rate values are reported in Table 4.2 and follow the recovery sequence. This implies a higher initial rate and grade with the standard SIBX used. At any given time the highest sulphur recovery was obtained with 530 g/t SIBX. The water recovery versus the sulphur recovery given in figure 4.4 shows the slight improvement when the 530 g/t is used is mainly due to entrainment.

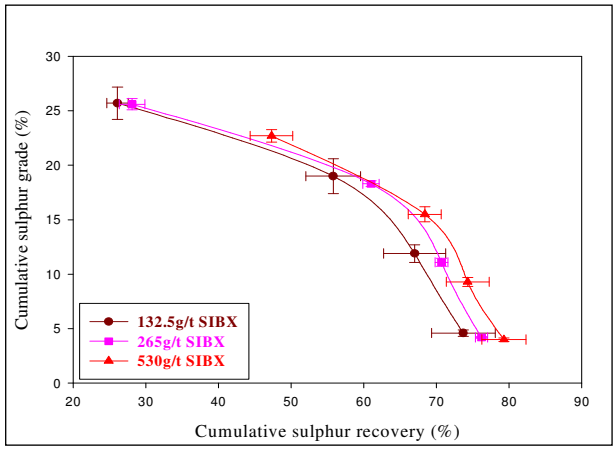

Figure 4.1: *Percent cumulative sulphur grade versus percent cumulative sulphur recovery.*

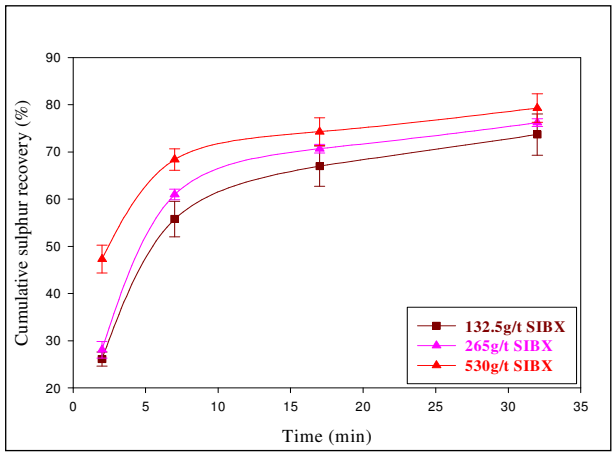

Figure 4.2: *Percent cumulative sulphur recovery versus time (minutes).*

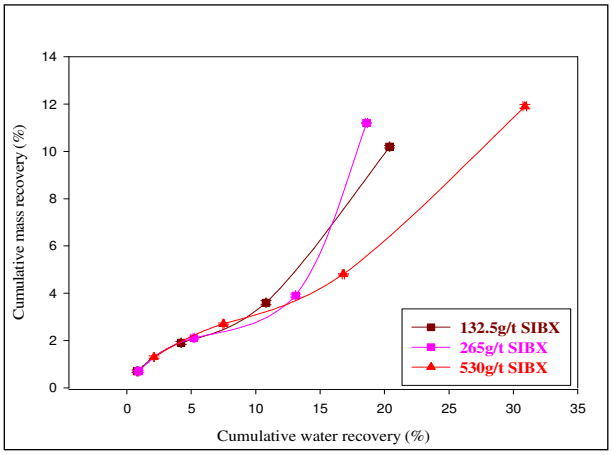

Figure 4.3: *Percent cumulative water recovery versus percent cumulative mass recovery.*

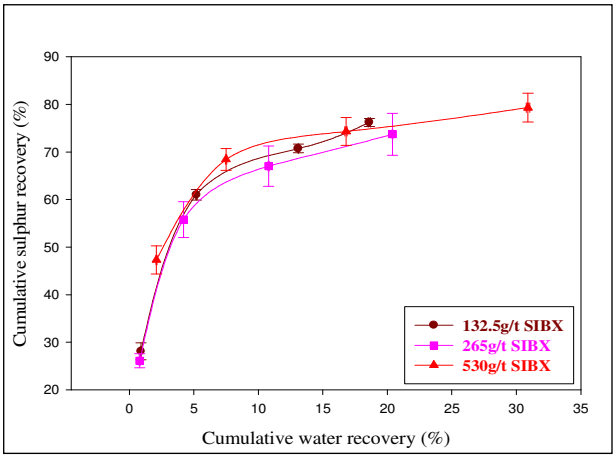

Figure 4.4: Percent cumulative sulphur recovery versus cumulative water recovery

Table 4.2: *Effect of SIBX concentrations on grade, recovery and rate*

Collector	SIBX dose (g/t)	Initial rate (min^{-1})	Final recovery (%)	Final grades (%)
530 g/t SIBX	530	23.7	79.3	4.0
265 g/t SIBX	265	14.1	76.2	4.2
132.5 g/t SIBX	132.5	13.1	73.7	4.6

4.2.3. Effect of SIBX Addition to Mill

Prior to flotation, 80% of the SIBX was added to the mill. Common practice is to add part of the reagent suite to the mill, especially under oxidative conditions. Fine-grained pyrite, pyrrhotite and pentlandite are prone to oxidation and improved recoveries are obtained by this practice. Copper sulphate was added to the mill as well. Comparisons were made between additions to the mill and direct addition to the cell prior to flotation.

After conditioning for 3 minutes, 80 % percent of 530 g/t SIBX and 80% $CuSO_4$ were added to the mill. The remaining 20% for both SIBX and $CuSO_4$ was added in the flotation cell. The same procedure described in Chapter 3, Section 3.3.7 was followed. The results are reported in Figures 4.5 to 4.8 and Table 4.3. Figure 4.5 shows the grade-recovery curves. When 80% of 530g/t is added to the mill, the grade-recovery curve is always lower than with 530g/t SIBX directly added to the cell.

Final grade and recovery values are the same irrespective of whether the collector is added in the mill or directly applied to the cell: this is in agreement with data in Figure 4.6. However, the initial rate was higher for direct dosing to the cell (Table 4.3). Cumulative water versus cumulative mass recovery graphs, in Figure 4.7, show that the 530 g/t SIBX was also more selective initially. Partial addition of collector and activator did not improve flotation activity; instead, the initial rates were reduced from 23.7 min^{-1} to 14.5 min^{-1}. Figure 4.8 shows that there is slightly less water for the same sulphur recovery when the collector is added into the mill.

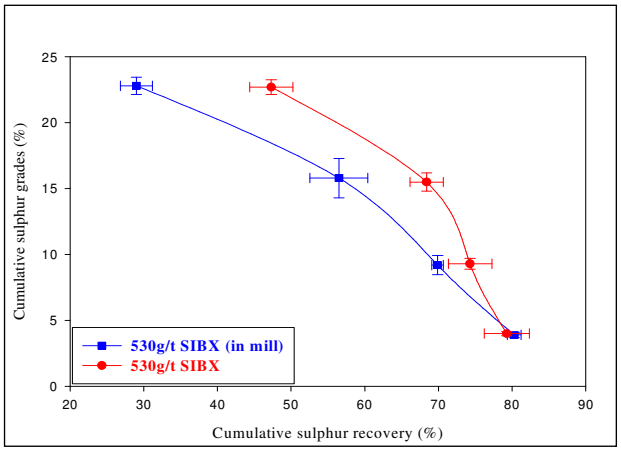

Figure 4.5: *Percent cumulative sulphur grade versus percent cumulative sulphur recovery. (For 530g/t SIBX (in mill), 80% of 530g/t SIBX and 80% of 70 g/t $CuSO_4$ was also added to the mill.*

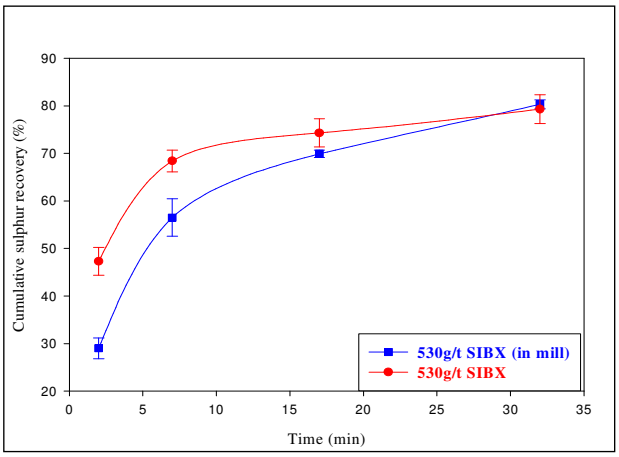

Figure 4.6: *Percent Cumulative sulphur recovery versus time (minutes).*

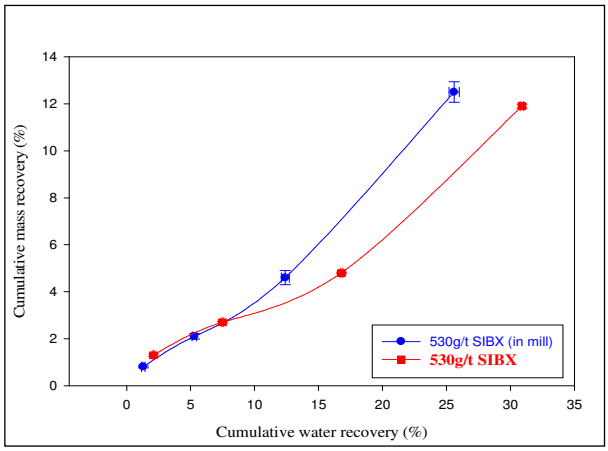

Figure 4.7: *Percent cumulative water recovery versus percent cumulative mass recovery.*

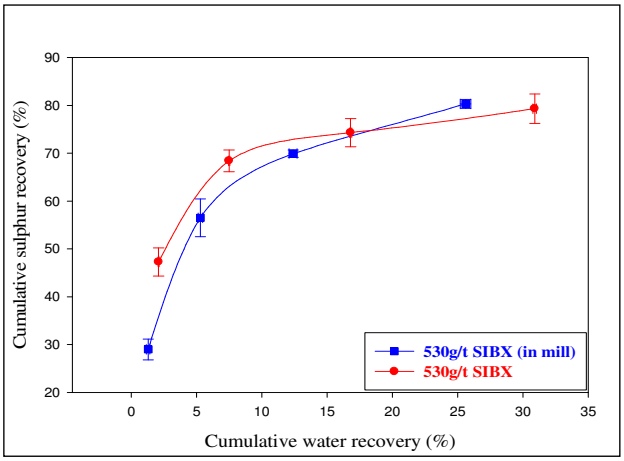

Figure 4.8: *Percent cumulative sulphur recovery versus water recovery.*

Table 4.3: *Effect of SIBX dosed in mill on grade, recovery and rate.*

Collector	Initial rate (min^{-1})	Final recovery (%)	Final grade (%)
530 g/t SIBX (in mill)	14.5	80.3	4.0
530 g/t SIBX	23.7	79.3	3.9

4.2.4. Blends of SIBX and TTCs

4.2.4.1. Blends of i-C$_4$ TTC and SIBX

Slabbert (1985) reported improvements in PGM recovery on an Impala-Merensky ore with mixtures of iC$_3$- and iC$_4$- TTCs with SIBX. Results reported are shown in Figures 4.9 to 4.12 and Table 4.4. The 530 g/t SIBX is the reference test.

On sulphur flotation, substitutions of SIBX by iC$_4$TTC were 6.25, 25 and 100%. The order of decreasing final recovery was 6.25%>25%>100%> 530g/t SIBX (Figures 4.9 to 4.12 and Table 4.9.). The standard was 79.3 % and the C$_4$TTC substitution may have shown a slight improvement in recovery. The time-sulphur recovery curves in Figure 4.10 were not significantly different. The cumulative water recovery versus mass recovery, shown in Figure 4.11, shows and increasing trend of mass recovery as water recovery is increased. The trend increases with an increase in the number of mole % of the C$_4$TTC substituting SIBX. Figure 4.12 shows no improvement of sulphur recovery as more water is recovered when 25% and 100% C$_4$TTC were used. Previous studies of short chain TTCs (C$_3$ to C$_6$) on Merensky ore, with 30 and 50 mole percent substitution of SIBX by short chain TTCs (Slabbert, 1985) gave higher grades and recoveries than the standard suite, which was an SIBX/DTP mixture. A major difference between Mimosa and Merensky ore is that Mimosa ore contains much more talc than the Impala-Merensky ore. This could be the reason the results are different from that achieved by Slabbert (1985) on the Merensky ore. A notable point of interest is that at 6.25 mole percent substitution of SIBX an increase in sulphur recovery is seen compared to the standard SIBX. At a later stage in this Chapter this point will be discussed again.

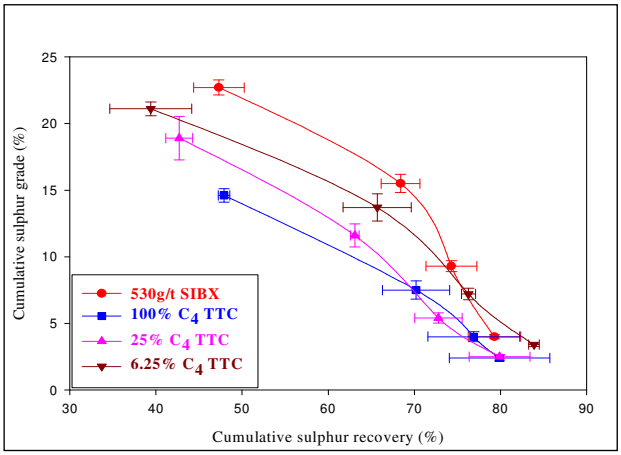

Figure 4.9: *Percent cumulative sulphur grade versus percent cumulative sulphur recovery.*

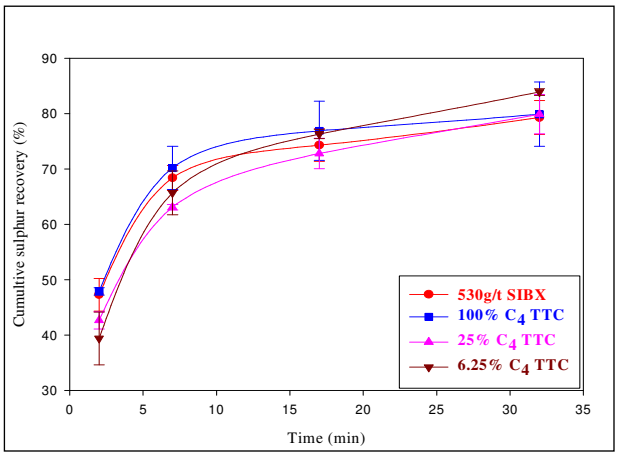

Figure 4.10: *Percent cumulative sulphur recovery versus time (minutes).*

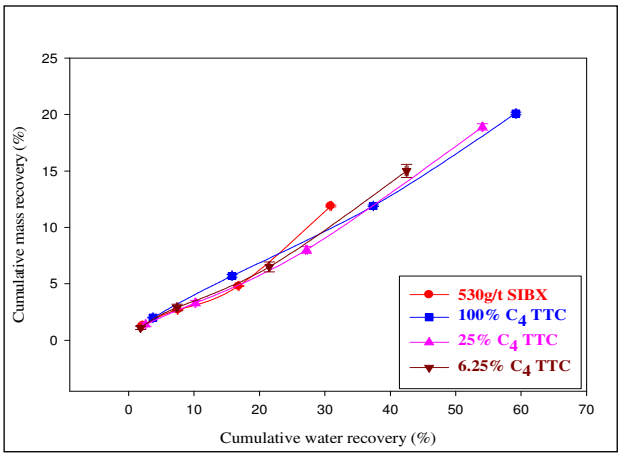

Figure 4.11: *Percent cumulative water recovery versus percent cumulative mass recovery.*

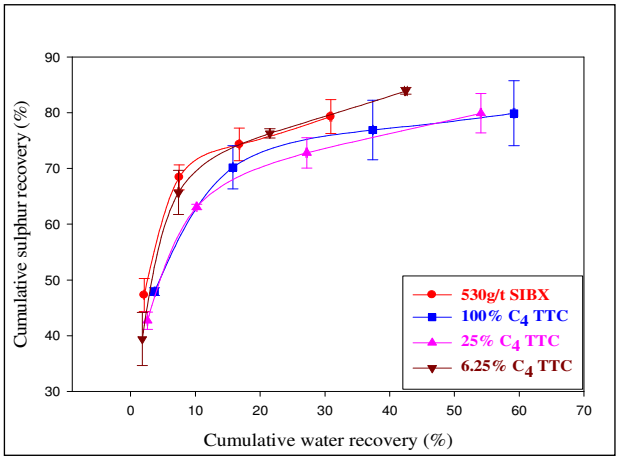

Figure 4.12: *Percent cumulative sulphur recovery versus water recovery.*

Table 4.4: *Effect of SIBX and SIBX blended with C$_4$ TTC on grade, recovery and rate.*

Collector	%	Initial rate (min^{-1})	Final recovery (%)	Final grades (%)
530 g/t SIBX	0	23.7	79.3	4.0
6.25% C_4 TTC	6.25	19.7	83.9	3.4
25% C_4 TTC	25	21.3	79.9	2.5
100% C_4 TTC	100	23.9	79.9	2.4

4.2.4.2. C$_{10}$ TTC blends with SIBX

In these tests, comparisons were made between the standard and 6.25, 25 and 35 mole percent substitutions of SIBX with C_{10} TTC (Figures 4.13 to 4.16 and Table 4.5). In final recoveries, no real significance can be seen between the chemical suites. It has been found that at relatively high pH values, such as found at Mimosa, long chain TTCs show strong frothing properties. This could explain the lower grade but higher final recovery of C_{10} TTC at 35% substitution and this is coupled to the lowest grade (Davidtz, 2007).

In summary, comparisons made between the standard and 6.25, 25 and 35 mole percent substitutions with C_{10} TTC are shown in Figures 4.13 to 4.16 and Table 4.5. Final recoveries given in Figure 4.13 are within the limit of experimental error. The lower grades were probably due to strong frothing. This fact is indicated by figure 4.16 which shows more water recovery for lesser sulphur recovered.

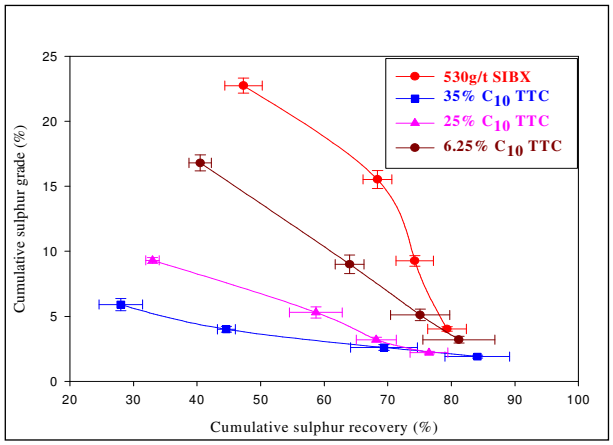

Figure 4.13: *Percent cumulative sulphur grade versus percent cumulative sulphur recovery.*

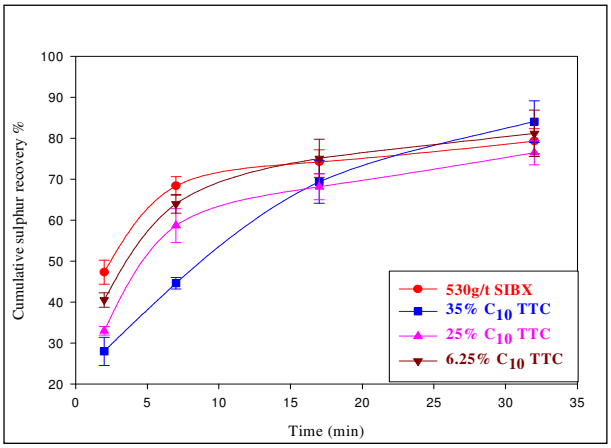

Figure 4.14: *Percent cumulative sulphur recovery versus time (minutes).*

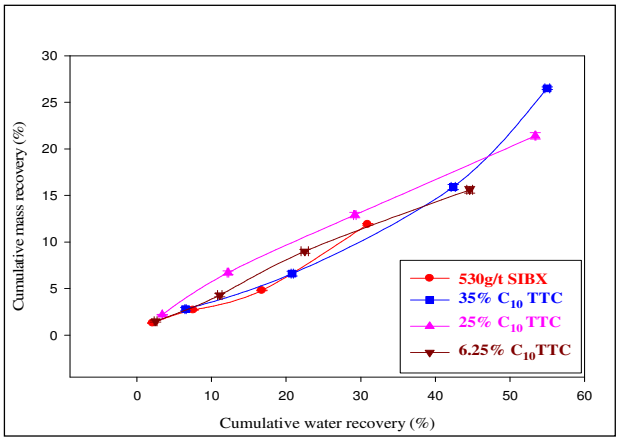

Figure 4.15: *Percent cumulative water recovery versus percent cumulative mass recovery.*

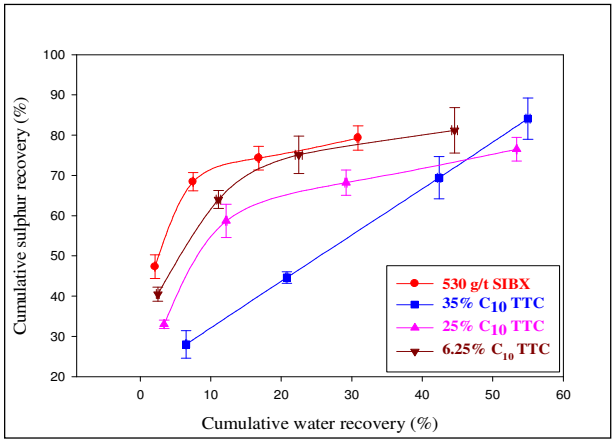

Figure 4.16: *Percent cumulative sulphur recovery versus cumulative water recovery.*

Table 4.5: *Effect of SIBX and SIBX blended with C_{10} TTC on grade, recovery and rate.*

Collector	TTC % fraction	Initial rate (min^{-1})	Final recovery (%)	Final grades (%)
530 g/t SIBX	0	23.7	79.3	4.0
6.25% C_{10} TTC	6.25	20.3	81.2	3.2
25% C_{10} TTC	25	16.5	76.5	2.2
35% C_{10} TTC	35	14.0	84.1	1.9

4.2.4.3. C_{12}TTC blends with SIBX

The following tests compare the 530 g/t SIBX standard to SIBX/C_{12}TTC blends. Molar C_{12}TTC substitutions were: 6.25, 25 and 100 mole percent. Figure 4.17 and 4.18 show that there is no clear difference between all the collector blends used. The final recoveries are with experimental error.

In general, the behaviour of SIBX/C_{12}TTC blends was similar to that of SIBX/C_{10}TTC blends, but there is a slight difference with i-C_4 and C_{12}TTC at 6.25 mole percent substitutions. There appears to be a slight increase in recovery relative to the standard around this concentration. Breytenbach *et al.* (2003) and Vos *et al.* (2006) have reported a similar synergistic behaviour that cannot fully be explained at present. This synergism has been observed with the Impala-Merensky ores.

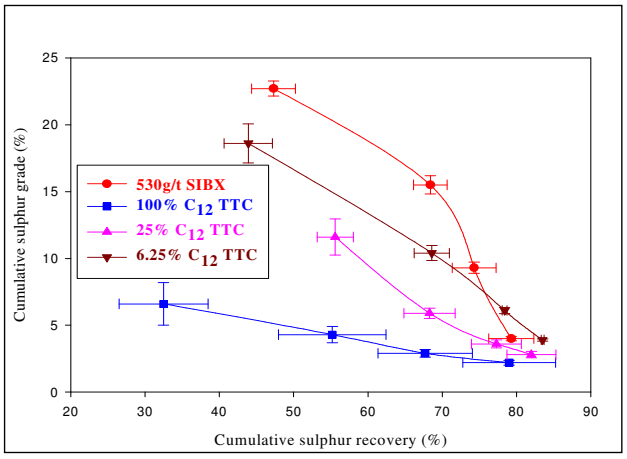

Figure 4.17: *Percent cumulative sulphur grade versus percent cumulative sulphur recovery.*

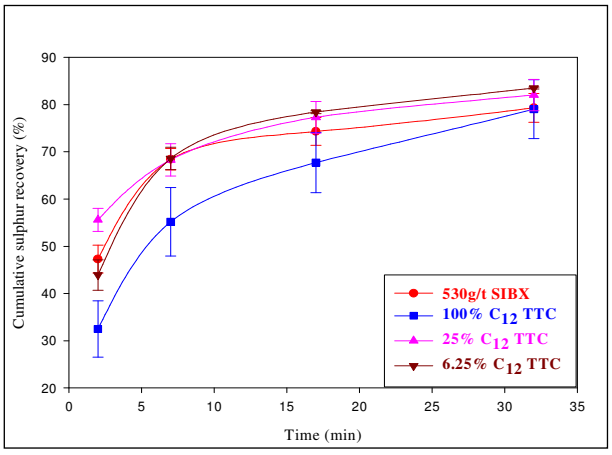

Figure 4.18: *Percent cumulative sulphur recovery versus time (minutes).*

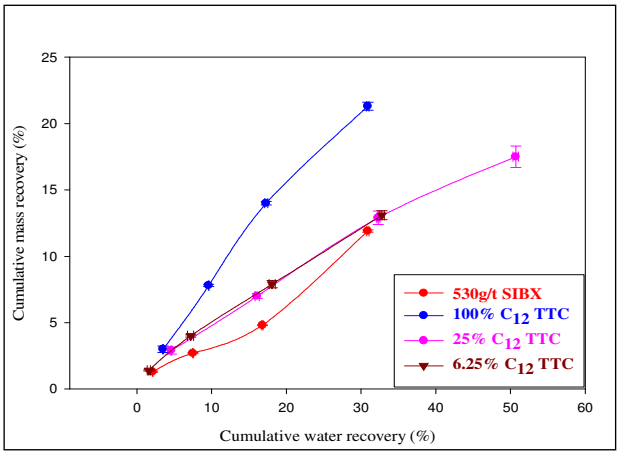

Figure 4.19: *Percent cumulative water recovery versus percent cumulative mass recovery.*

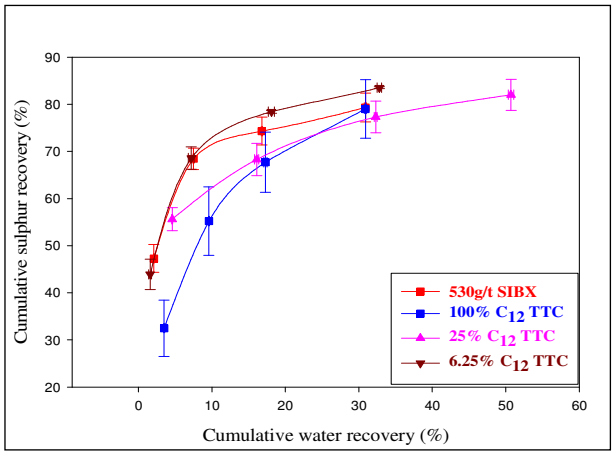

Figure 4.20: *Percent cumulative sulphur recovery versus cumulative water recovery.*

Table 4.6: *Effect of SIBX and SIBX blended with C_{12} TTC on grade, recovery and rate.*

Collector	TTC % fraction	Initial rate (min^{-1})	Final recovery (%)	Final grades (%)
530 g/t SIBX	0	23.7	79.3	4.0
6.25% C_{12} TTC	6.25	21.9	83.5	3.9
25% C_{12} TTC	25	27.8	82.0	2.8
100% C_{12} TTC	100	16.2	79.0	2.2

4.2.4.4. Blends of SIBX and DTP

Unlike Mimosa, mixtures of SIBX and DTP are generally the favoured collector combinations used in PGM recovery. The practice at Mimosa is to use SIBX as a single collector. Results of experimental data reported in this section show the effect of partial replacement of SIBX by DTP on Mimosa ore. Molar ratios of SIBX: DTP were kept constant at 1:1.3 respectively. At this fixed molar ratio the combined dosage varied from 2.55 moles of SIBX for the standard, to 0.64 total moles in the mixture. Dosage, initial rates, final recoveries and grade are reported in Table 4.7.

Figure 4.21 illustrates the grade-recovery curve for the 530g/t SIBX and the three SIBX/DTP mixtures (summarised in Table 4.7). Final sulphur recovery followed the order DTP (1.28 mol.) ≈ DTP (0.64 mol.) > DTP (2.27 mol.) > 530g/t SIBX. There is significantly a big difference shown by the DTP (1.28 mol.) and DTP (0.64 mol.).

This difference is seen right through figure 4.21 to 4.24. From figure 4.24 shows that the improvement of sulphur recovery is not simply due to entrainment but due to true flotation.

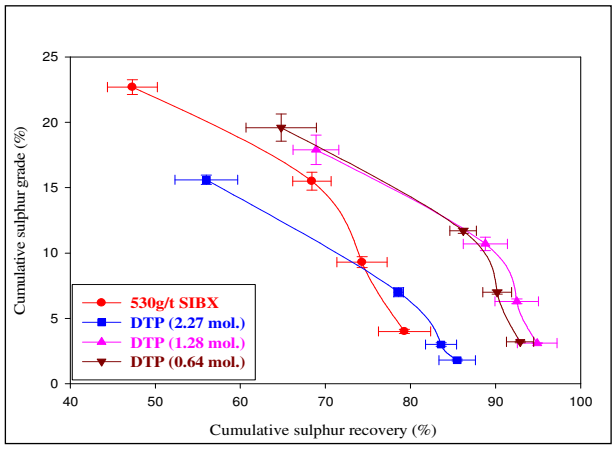

Figure 4.21: *Percent cumulative sulphur grade versus percent cumulative sulphur recovery.*

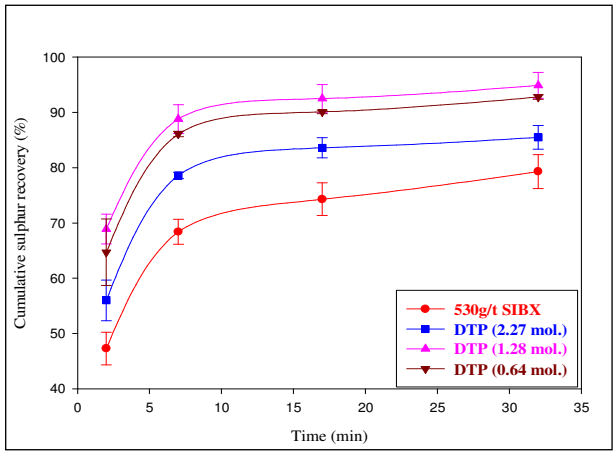

Figure 4.22: *Percent cumulative sulphur recovery versus time (minutes).*

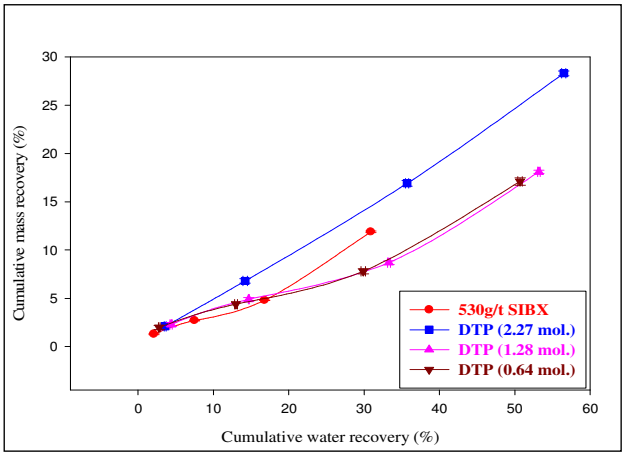

Figure 4.23: *Percent cumulative water recovery versus percent cumulative mass recovery.*

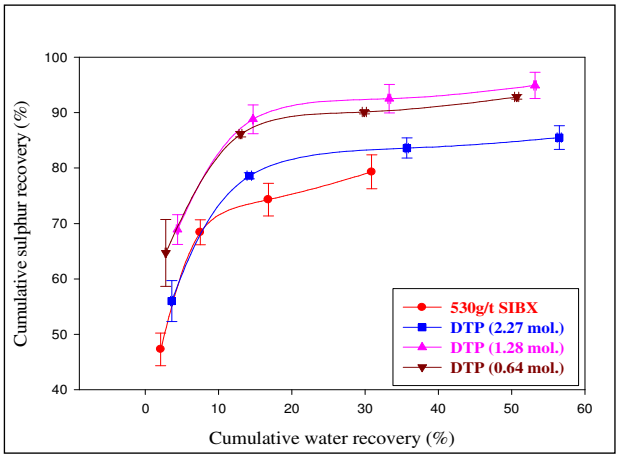

Figure 4.24: *Percent cumulative sulphur recovery versus cumulative water recovery.*

Table 4.7: *Effect of SIBX and SIBX blended with DTP on grade, recovery and rate.*

Collector	SIBX + DTP total mol/t	DTP mole fraction	Initial rate (min^{-1})	Final recovery (%)	Final grades (%)
530 g/t SIBX	2.55	0	23.7	79.3	4.0
DTP (2.27 mol.)	2.27	0.44	28.0	85.5	1.8
DTP (1.28 mol.)	1.28	0.44	34.5	94.9	3.1
DTP (0.64 mol.)	0.64	0.44	32.4	92.9	3.2

4.2.5. PGE + Au Flotation Data

Only a limited number of samples could be analysed for both PGEs+Au. Final recovery data listed in Table 4.8 shows final recovery and grades. Mass recovery and the grade per mass recovered are listed in Table 4.9 and will be discussed with the data in Table 4.8 for the selected collectors.

Table 4.8: *Final recovery and final grades for the PGE+Au of selected collector mixtures.*

Collector	Final PGE+Au recovery (%)	Final grades, (ppm)
DTP (1.28 mol.)	90.9	18.2
DTP (0.64 mol.)	89.0	18.7
C4 TTC (100%)	87.3	14.1
C12 TTC (6.25%)	84.3	22.5
530g/t SIBX	81.1	24.2
25% C12 TTC	80.4	16.5
6.25% C4 TTC	76.6	18.1
6.25% C10 TTC	69.3	13.8
DTP (2.27 mol.)	39.2	4.6

For PGE+Au, DTP (1.28 mol.) and DTP (2.27 mol.) have the highest recovery, but not the highest grades.

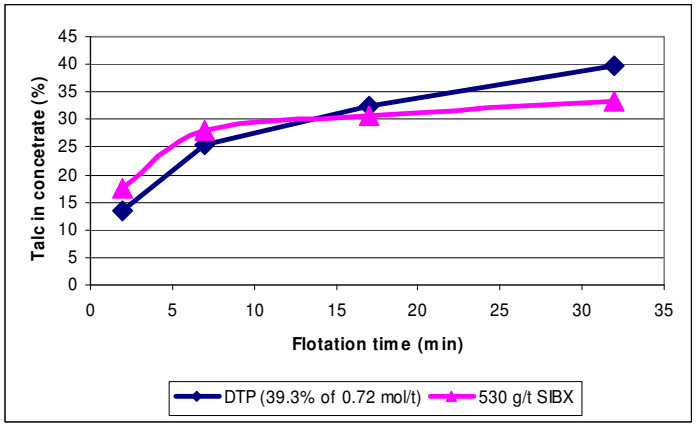

Figure 4.25: *Recovery of talc in concentrate versus time (min) for DTP (39.3% of 0.72 mol/t) and 530g/t SIBX.*

As seen in Figure 4.25, the initial recovery of talc is higher for the 530 g/t SIBX after the second concentrate: the rate of talc recovery exceeds that of the 530 g/t SIBX. The DTP has inherent frothing properties, so the lower grade and high gangue entrainment with increased water recovery could be the reason (Bandford, 1998) there is an increase in talc recovery beyond 15 minutes.

4.3. DISCUSSION OF RESULTS

In Table 4.9 the grade per mass recovered, which is a measure of selectivity, is listed. Based on this data, the standard SIBX and 6.25% C_{12} TTC are the best collectors. The high talc concentration in the feed is responsible for differences in final grade.

Table 4.9: *Summary data of final recoveries, final grades and rates in descending (top to bottom).*

Collector	Final sulphur recovery (%)	Final sulphur grades (%)	Sulphur initial rate (min^{-1})	Mass recovery (%)	PGE+Au grade/Mass rec. ratio	Sulphur grade/Mass rec. ratio
DTP (1.28 mol.)	94.9	3.1	34.5	18.1	1.03	0.2
DTP (0.64 mol.)	92.9	3.2	32.4	17.1	1.06	0.2
DTP (2.27 mol.)	85.5	1.8	28.0	28.3	0.16	0.1
35% C_{10} TTC	84.1	1.9	14.0	26.5	-	0.1
6.25% C_4 TTC	83.9	3.4	19.7	15.0	1.20	0.2
6.25% C_{12} TTC	83.5	3.9	21.9	13.1	1.72	0.3
25% C_{12} TTC	82.0	2.8	27.8	17.5	0.94	0.2
6.25% C_{10} TTC	81.2	3.2	20.3	15.6	0.88	0.2
530 g/t SIBX (in mill)	80.3	4.0	14.5	12.5	-	0.3
25% C_4 TTC	79.9	2.5	21.3	18.9	-	0.1
100% C_4 TTC	79.9	2.4	23.9	20.1	0.70	0.1
530 g/t SIBX	79.3	4.0	23.7	11.9	2.03	0.3
100% C_{12} TTC	79.0	2.2	16.2	21.3	-	0.1
25% C_{10} TTC	76.5	2.2	16.5	21.4	-	0.1
265 g/t SIBX	76.2	4.2	14.1	11.2	-	0.4
132.5 g/t SIBX	73.7	4.6	13.1	10.2	-	0.4

Table 4.9 shows that the initial rates for sulphur of the collectors under investigation decreased from the highest flotation kinetics given by DTP (1.28 mol.) to the lowest value given by 132.5 g/t SIBX. DTP (1.28 mol.) also shows the highest sulphur recovery while the final grades are lying in the middle of the pack. The highest final recovery could be due to enhanced pyrrhotite recovery with the use of DTP in the presence of copper sulphide. This is in agreement with the findings of Wiese *et al.* (2005). The lower final grades could be due to gangue entrainment (see water recovery versus sulphur recovery in figure 4.24) that results because of high initial

rate of flotation when DTP is used together with SIBX. The highest final grade given by 132.5 g/t SIBX is due to the fact that SIBX seems to be highly selective to sulphur, even though the recoveries are low.

Experiments on SIBX dosage levels have led to the following conclusions:

The optimum SIBX concentration of 530g/t agrees with that used by Mimosa. Grade recovery curves improved as the dosage of SIBX increased from 132.5 to 530 g/t. Rate and recovery increases were responsible for this improvement.

Addition of SIBX and $CuSO_4$ to the mill did not improve overall performance. Initial rates and final recoveries were similar. There were hints of increased final recovery, but in the early stages of flotation grade recovery relationship favoured direct addition to the flotation cell.

Mixtures of i-C_4TTC with SIBX showed no significant improvement in flotation performance compared to the standard.

With C_{10} and C_{12}TTC mixtures with SIBX there was generally no significant metallurgical improvement with respect to final grades and recoveries. However, the 6.25 molar percent substitution of SIBX by C_{12}TTC appeared to show some improvement on sulphur, but not on PGE+Au recovery and grade.

There are many different types of interactions that influence flotation activity. Interactions that dominate the mineral/water interfacial behaviour are probably the most significant ones. Collision efficiencies between both valuable mineral and gangue particles, with rising bubbles simplistically can explain differences between rates and grades as influenced by collector effects. This means that those physical factors that operate in rates of both gangue and mineral attachment and detachment are the ones that control both grade and rate (Davidtz, 2007).

A driving force to expel a particle from a solution is the key to effective bubble attachment. A loose term is “hydrophobicity”. Davidtz (2007) related a calculable thermodynamic quantity, the Gibbs Excess Free Energy” (G^{ex}), to the exclusion

energy of a collector coated particle from the water phase. The application of thermodynamic principles responsible for phase separation applies. In solution chemistry and a binary system, the mole fraction of two interacting solutions and their activity coefficients as a function of mole fractions are combined in the G^{ex} expression and this is related to miscibility of interacting phases. In the flotation system the two interacting phases are the surface adsorbed collector molecules and adjacent water. At maximum interaction between these components the respective mole fractions are assumed to be 0.5. The G^{ex} at this composition is assumed to be the maximum interaction energy. This value has previously been related to flotation rates and recovery, and eventually these quantify the flotation system. For constant temperature, the two variables are: the mole fraction of surface covered by collector molecules (X_i) and the activity coefficients γ_i of all interacting species *i* where water and mineral meet at temperature T.

$$G^{ex} = RT\sum_i X_i \ln \gamma_i \qquad (4.1)$$

Since attachment of a particle to a bubble requires a detachment of the particle from the water network, either an unstable state in solution or complete immiscibility is needed. This is what the G^{ex} quantifies.

The two variable parameters χ_i, γ_i, respectively are concentration and intensity factors, and consequently control miscibility of the collector-coated particle in water. This then is also a measure of hydrophobicity and surface tension. Best results are obtained at starvation concentrations and uniform distribution of collector molecules (Davidtz 2006). Not all molecules are immobilised on surfaces and there is migration of low polarity molecules both across the mineral surface and from one particle to another.

Complete or partial immobilization of and adsorbed collector is due to chemisorption. According to Bradshaw and O'Connor (1996) and Davidtz (1998) DTPs fit into the immobile species. The molecules are ionic and do not dimerize to produce non-ionic compounds under normal operating oxidation potentials. The mobile molecules in

turn are dimers such as dixanthogen - an essential component in sulphide mineral flotation.

Since larger G^{ex} value implies a higher flotation activity, either the mole fraction term χ_i or the activity coefficient term γ_i have to increase. But, in calculations of activity coefficients for interacting species G^{ex} for DTP is in fact smaller than the value for the SIBX dimer and this cannot be the reason for improved rate and recovery found in the presence of DTP. This implies an increase in χ_i. Although solubility data of collector molecules in water is often used to correlate flotation data, G^{ex} is related to solubility and is a thermodynamic quantity. The only explanation left is a specific interaction between the adsorbed DTP and the mobile dixanthogen (X_2). The final explanation is an accumulation of surface produced mobile (X_2) around the adsorbed ionic DTP. The result is an increased mole fraction χ_i .

High concentrations of talc: The Mimosa ore body has a high concentration of talc, a magnesium-silicate (oxide) gangue, and this magnifies interfering factors when attempts are made to optimise and describe the flotation system.

Some relevant physical and chemical factors that are involved in interactions between water, minerals (both valuable and gangue) and flotation chemicals are:

A high surface area and charge distribution on talc amplifies surface activity of talc. The associated physical and chemical interactions of both organic depressant and inorganic hydroxyl cations (copper and alkaline earth) reactions at the high pH feed values (>9.0) all influence flotation behaviour.

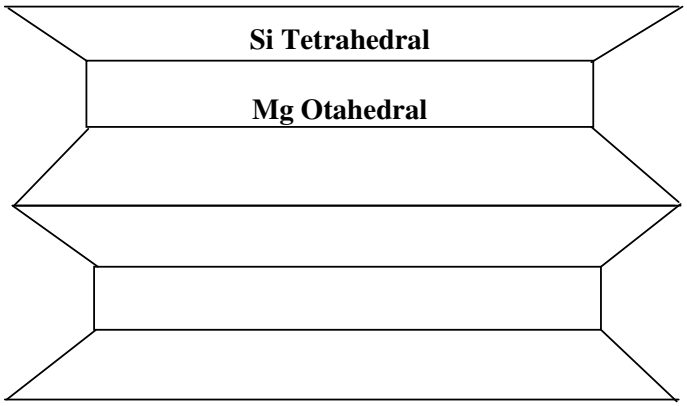

Figure 4.26: *Schematic representation of the layers of the talc structure.*

The conceptual structure of talc shown in Figure 4.21 shows that the predominantly hydrophobic basal planes, together with hydrophilic edges, interact differently with short and long chain collector molecules. Short chain collector molecules are much more water-soluble than long chain collector molecules and this implies a strong overall polarity of molecules such as SIBX and DTP. Long chain collector molecules, such as C_{10} and C_{12} TTC, are far less soluble in water and have a stronger hydrophobic bonding to talc basal planes via the long aliphatic group.

The high doses of reagents at Mimosa probably result from surface adsorption by talc. According to Davidtz (2007) the strong complexing character of divalent ions (Cu^{2+}) by thiol collectors results in a precipitation of salts from solution. These "collector salt precipitates" are no longer water-soluble and attach to surfaces too (Fornasiero and Ralston, 2004). This is in fact one method of producing the hydrophobic state with SIBX on pyrite surfaces (Davidtz, 2007).

In the case of TTCs, two molecules of TTC consist of six-sulphur atoms and no oxygen atoms. Two SIBX molecules in a dimer complex consist of four sulphur and two oxygen atoms and with DTP four sulphur atoms and four oxygen atoms form the complex. The ratios of O/S in the precipitates are therefore 0, ½ and 1 for TTC, DTC and DTP respectively. The affinity or interaction energy to produce metal sulphides follows the same sequence. Strong frothing behaviour by surfactants requires the frothing agent to be at the air/water interface and not attached to the mineral surface.

This is one reason for the natural frothing of DTP. At the other extreme, with TTCs, and especially with short chain TTCs, a very unstable froth forms.

This leads to the question: Why do long chain TTCs froth, and particularly at high pH values in the presence of talc and pyrophyllite? Part of the answer has to do with possible weakening of the polar group by calcium and magnesium ions and the formation of a strong frothing surfactant; but more important would be the increased hydrophobicity of these gangue particles after adsorption of the long chain collectors or collector precipitates. High frothing due to gangue only appears to result at high pH values in the presence of alkaline earth ions (Talc is a 2:1 magnesium silicate). With an increased attachment of gangue particles to bubbles and an overcrowding of drainage channels in the froth phase by these oxides, the float grade decreases.

Experiments on SIBX dosage levels have led to the following conclusions:

The optimum SIBX concentration of 530g/t agrees with that used by Mimosa. Grade recovery curves improved as the dosage of SIBX increased from 132.5 to 530 g/t. Rate and recovery increases were responsible for the improvement.

Addition of SIBX and $CuSO_4$ to the mill did not improve overall performance. Initial rates and final recoveries were similar. There were hints of increased final recovery, but in the early stages of flotation grade recovery relationship favoured direct addition to the flotation cell.

Mixtures of iC_4TTC with SIBX when compared to the standard showed no significant improvement in flotation performance.

With C_{10} and C_{12} TTC mixtures with SIBX there was generally no significant metallurgical improvement with respect to final grades and recoveries. However, the 6.25 molar per cent substitution of SIBX by C_{12}TTC appeared to show some improvement on sulphur but not on PGE + Au recovery and grade.

CHAPTER FIVE

EXPERIMENTAL (PART II)

TALC DE-SLIMING

5.1. INTRODUCTION

As already discussed in the literature survey in Chapter 2, the high level of talc is responsible for the high depressant consumption at Mimosa concentration plant. The objective of this test was to de-slime talc using 36.9 mm and 76.0 mm cyclones prior to flotation. Since talc is fragile, it breaks finer during milling compared to the silicates (consists of approximately 90% of the ore) and therefore it is expected to concentrate to the finer fraction of the ore. This makes it easy to de-slime in a water medium using a de-watering cyclone. The talc de-sliming would also be enhanced by the fact that talc has a lower density and hydrophobic, hence it would be easy to de-slime.

The primary objective of this chapter is to discuss the experimental methods followed during the execution of this research and the type of equipment used. Section 5.3 gives a short description of the equipment used while Section 5.4 gives the method or procedures followed. Under the methods, Section 5.4.1 describes in detail the method followed to calibrate and analyse the samples for talc using the XRD instrument and Section 5.4.2 gives the procedure of the XRF method that was followed to confirm the XRD results.

5.2. ORE

The sample preparation was done as already discussed in Chapter 3. A portion of the milled head samples was sent for size analysis at Lakefield Research Africa (Pty) Ltd (South Africa). The aim of this analysis was to determine the deportment of talc as a function of size.

5.3. THE EQUIPMENT

5.3.1. De-sliming Equipment

The de-sliming equipment is shown in Figure 5.1 and consisted of the following units:

1. Pachuca tank of about 150-litre capacity.
2. A 7.5 kW pump motor.
3. Three valves.
4. Fitted cyclone (36.9 mm or 76.0 mm).
5. Pressure gauge.
6. The steel piping system.

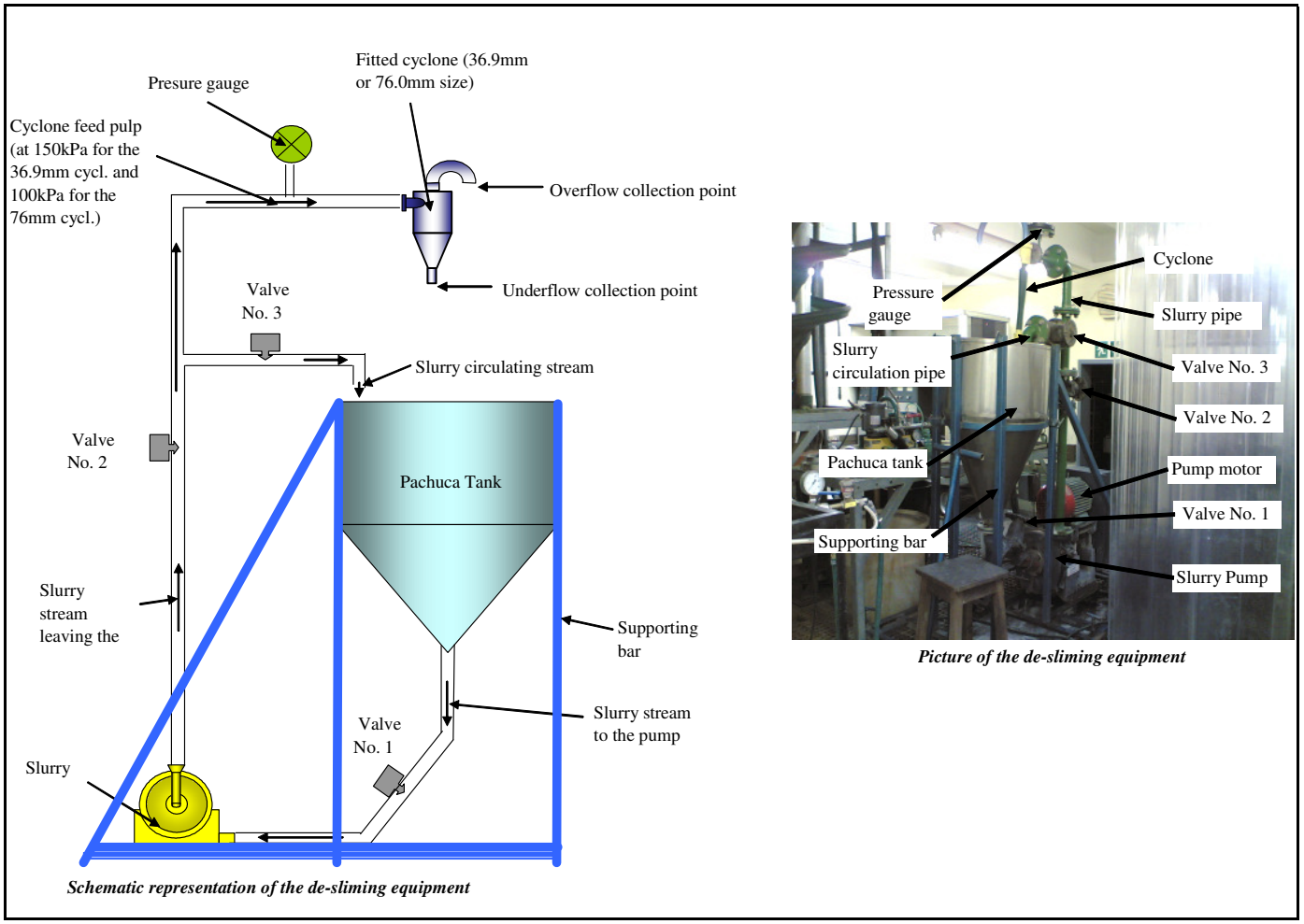

Figure 5.1: *Schematic (not drawn to scale) and pictorial representation of the de-sliming equipment*

5.3.2. Cyclones

The cyclones were supplied by Multotec (South Africa) and were made from polyurethane. The spigot for both the 36.9 mm and the 76.0 mm cyclone were measured and were found to be 8.8 mm and 11.72 mm respectively. The two spigot sizes were chosen after testing a series of three spigots for both cyclones. They were chosen based on the fact that they provided the best separation performance. The other two spigots were either providing a spray or rope discharge for each cyclone. The vortex finders were 14.8 mm for the 36.9 mm cyclone and 23.04 mm for the 76.0 mm cyclone.

5.3.3. Flotation Equipment

The flotation cell used for flotation is described in Chapter 3.

5.4. METHODS

5.4.1. Quantitative X-ray Diffraction (XRD) Analysis of Talc

5.4.1.1. Introduction

Talc is a very difficult mineral to quantify due to its complex mixture with other minerals in the Mimosa ore. QEM SCAN and X-ray diffraction analysis are some of the analytical methods that are employed to semi-quantitatively analyse for talc. In this study, XRD was used to quantify talc in the cyclone overflow and underflow, as this method is sensitive to crystallographic structure of individual phases and is not influenced by textural features, such as fine intergrowth with other phases. Quantification of clay minerals by X-ray diffraction can be difficult since clay minerals can produce overlapping peaks and subsequently require more work for accurate analysis. In addition the chemical composition and therefore the structure of talc are also important factors to consider in the quantification.

5.4.1.2. Experimental

Samples were milled in a swing mill using a WC-milling vessel followed by a micronising step in a McCrone micronising mill. The samples were prepared for XRD analysis using the back loading preparation method. They were analysed with a PANalytical X'Pert Pro powder diffractometer with X'Celerator detector and variable divergence and receiving slits each set at 15mm, scanned from 2 to 90 °2θ. The radiation was Fe filtered Co-Kα radiation. The phases were identified using X'Pert Highscore plus software. The relative amounts were estimated by Rietveld method using the Autoquan/BGMN Rietveld Program (Kleeberg & Bergmann, 1998 & 2002) employing the fundamental parameter approach. Autoquan/BGMN is GE Inspection Technologies' program for quantitative analysis by the Rietveld method that enables full automatic analysis of multiphase samples by use of the advanced BGMN program, including the application of the Fundamental Parameter Approach for peak shape modelling and a prepared collection of start structure models (Verryn, 2006).

5.4.2. Loss On Ignition and XRF Analysis to Confirm the XRD Results

Mass Loss On Ignition (LOI) was performed to confirm the XRD talc analysis results and XRF was used to confirm these results. The samples were ground to <75µm in a Tungsten Carbide milling vessel, roasted at 1000ºC to determine LOI value and, after adding 1g sample to 6g $Li_2B_4O_7$, fused into a glass bead. Major element analyses were executed on the fused bead using the ARL9400XP+ spectrometer. Table 6.3 in Chapter 6 summarises the Mass LOI values obtained by performing XRF analysis.

5.4.3. De-sliming Procedure

Figure 5.2 shows a flow diagram that illustrates the batch process followed during the experimental procedure. The crushing and milling procedure followed is described in Chapter 3 Section 3.1.2. For one de-sliming session, 16.5 kg of solids was milled in batches of 3.3 kg samples. The pulp generated at each milling session for the five sessions was poured in a 25-litre drum. The slurry was kept under constant agitation and bubbling with nitrogen. Nitrogen was bubbled through the slurry to prevent

oxidation while the rest of the samples for the de-sliming experiments were being milled.

As soon as the total milled slurry sample was transferred into the 25-litre drum, the content of the drum was transferred to the de-sliming equipment pachuca tank after ensuring that valve number 1 was closed. Once all the drum contents had been transferred to the pachuca tank, dilution water was added to the tank and the tank was filled to the 100-litre mark in order to achieve the final a pulp density of 1.1 g/ml in the pachuca tank.

After ensuring that valve numbers 2 and 3 were opened, the slurry circulation pump was started (see Figure 5.1). The slurry was allowed to circulate back to the pachuca tank for about three minutes. This was to ensure that the solids in the slurry were uniformly suspended in the Pachuca tank and the pipes and that they did not settle in the pump sump.

As soon as the three minutes has lapsed, valve number 2 was closed slightly and valve number 3 was carefully adjusted to increase the pulp pressure in the upstream that goes to the cyclone inlet. Valves number 2 and 3 were carefully controlled in order to achieve the appropriate pressure in the cyclone inlet for non-roping or non-spraying cyclone discharge. The cyclone pressures were controlled at 150 kPa and 100 kPa for 36.9 mm cyclone and 76.0 mm cyclone respectively throughout the experiment.

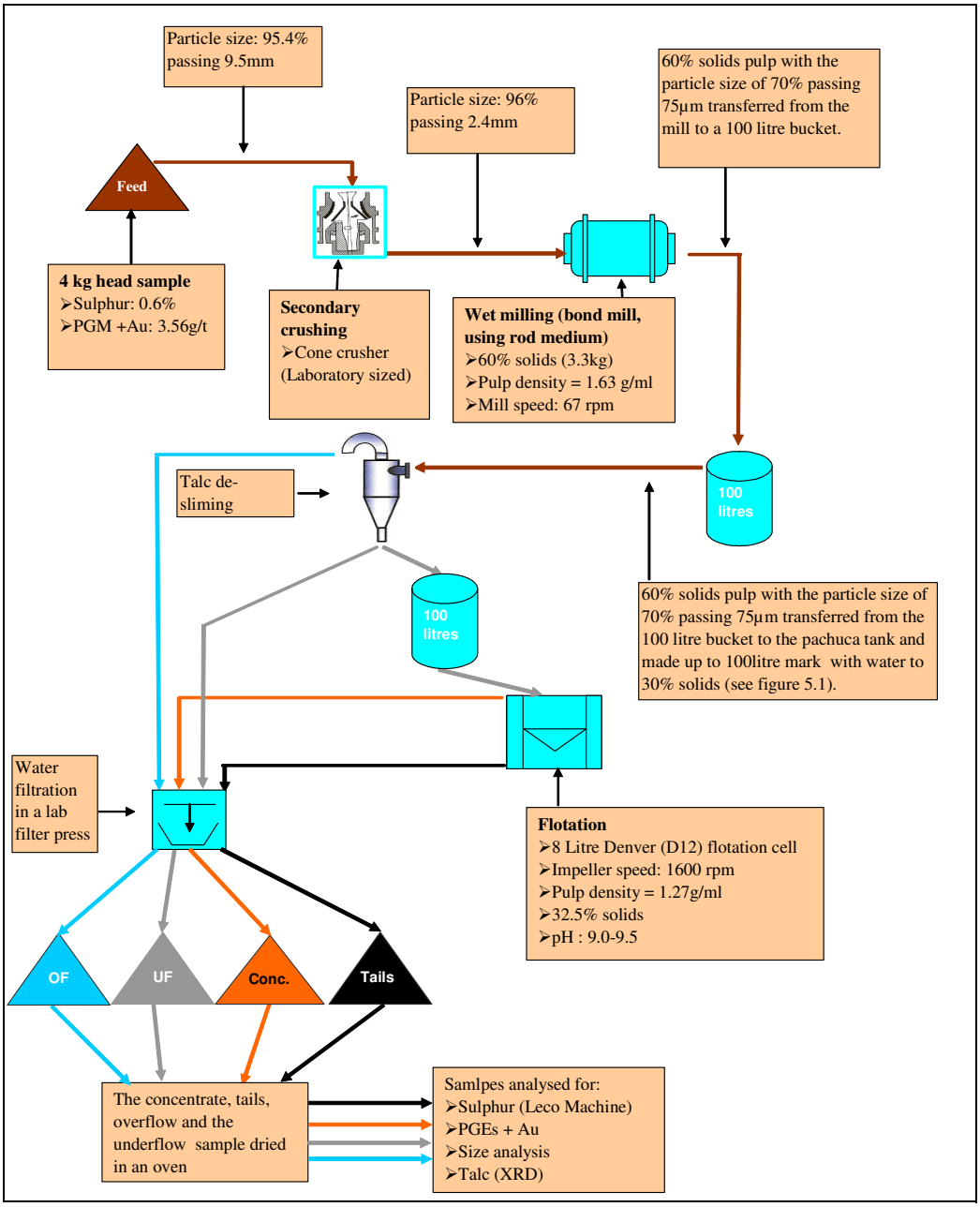

Figure 5.2: *The flow diagram for the procedure followed during the experimental work (OF is overflow and UF is underflow)*

Figure 5.3 shows the picture of the de-sliming setup taken during de-sliming using the 76.0 mm cyclone. The cyclone discharge of the underflow from the spigot and overflow are shown in the picture. The recirculation stream is also shown.

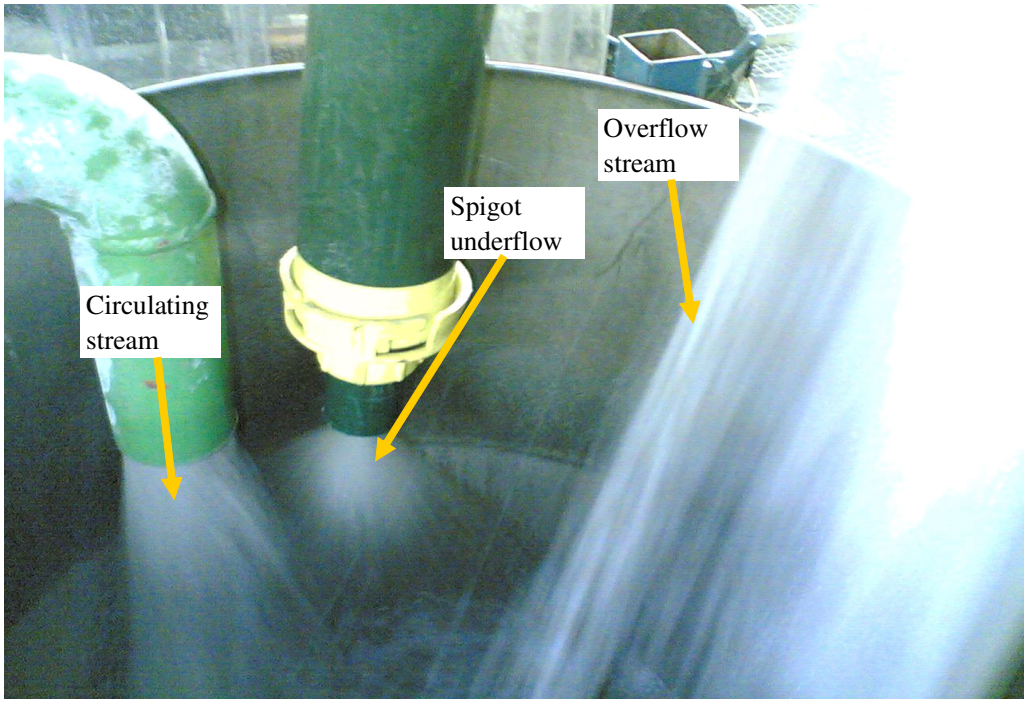

Figure 5.3: *The inside view of the de-sliming pachuca tank. Also seen is the underflow slurry from the 76.0 mm cyclone spigot and the recirculation stream pipe.*

5.4.4. Underflow and Overflow Rate Measurements and De-sliming

The flow rate was measured by simultaneously collecting the underflow (UF) and overflow (OF) slurry samples using the slurry holder shown in Figures 5.4 and 5.5. The time taken to fill the overflow container was measured using a stopwatch. The overflow containers filled faster than the underflow because they consisted mainly of water. As soon as the overflow container was filled the two containers were removed simultaneously, the stopwatch was stopped at the same time and the time taken to fill the container was recorded. The mass of the pulp in the containers (both UF and OF) were weighed and recorded. The same procedure was repeated three more times for both the 36.9 mm and the 76.0 mm cyclones. The time and the mass measurements were later used to calculate the flow rates of the slurry in tons per hour (t/h) (Appendix E) using the following formula:

$$F_{slurry} = \frac{W_{slurry} \times 3600}{T \times 1000} \qquad (5.1)$$

F_{slurry} = flow rate of the slurry

W_{slurry} = weight of the slurry and
T = time taken to fill the overflow slurry holder.

Once the masses were recorded the UF and OF slurry samples were later filtered in the laboratory filter press and dried in an oven. The dried solid samples were weighed and the masses recorded (Appendix E). The values obtained together with the flow rates were used to calculate the mass balance of sulphur, PGE+Au and talc.

As soon as the samples were taken to determine flow-rates and cyclone mass balance, the underflow discharge was collected by filling the slurry holders shown in Figure 5.4. The underflow discharge was collected until the discharge changed from the normal cyclone discharge (i.e. discharge (2) shown in Section 2.3) to a spray discharge (labelled (3) in Section 2.3.).

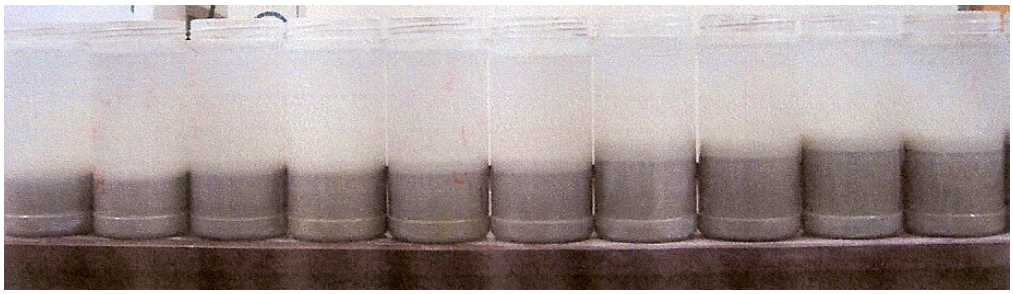

Figure 5.4: *The one-litre containers containing the cyclone underflow slurry.*

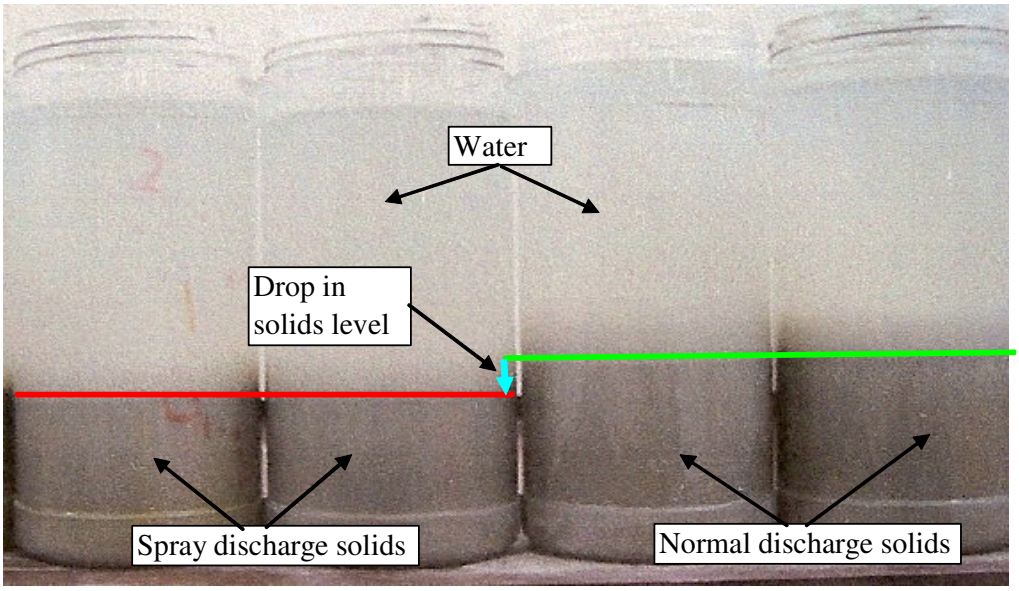

Figure 5.5: *Slurry holders used to determine the cyclone change from normal discharge to spray discharge.*

In order to distinguish the exact change between the normal underflow discharge and spray discharge, the containers were put next to one another and a drop in the solids level provided an indication of the exact point of change, as shown in Figure 5.5. Once this point was reached, the de-sliming process was stopped and all the slurry obtained before the solids level dropped (i.e. normal discharge) was transferred to a 25-litre container. The pulp density in the 25-litre bucket was measured by taking a representative slurry sample with a known volume of 100ml from the bulk slurry in the 25-litre bucket and weighing it. The procedure was done in triplicate in order to achieve reproducibility. The following formula was then used to calculate the slurry density:

$$\rho_{pulp} = \frac{M_{pulp}}{V_{pulp}} \tag{5.2}$$

where ρ_{pulp} is the slurry density; M_{pulp} is the slurry mass and V_{pulp} is the slurry volume.

The three representative samples were then filtered and dried in an oven to determine the solids percentage of the slurry. In the meantime the bulk slurry in the 25-litre

bucket was constantly agitated with nitrogen bubbling to minimise oxidation. The percent solids were then determined by using the following formula:

$$\%Solids = \frac{Dried\ \ solids\ \ mass}{Slurry\ \ mass} \times 100 \qquad (5.3)$$

As soon as the solids percentage was determined, slurry consisting of 3.3kg solids was taken from the bulk slurry in the 25-litre bucket to the 8-litre Denver D12 flotation cell. The slurry in the cell was adjusted to 1.27 g/ml by diluting it with water up to the 8-litre mark. Once this was achieved, flotation was performed as discussed in Chapter 3 using DTP (3) as the collector mixture and variable depressant dosages, as discussed later.

5.5. SAMPLES ANALYSIS

5.5.1. Introduction

The following section deals with the analysis of the products of the de-sliming tests.

5.5.2. Sample Preparation

Once the underflow and overflow samples were dried, the samples were weighed and thoroughly mixed to obtain a homogeneous sample. After mixing, the samples were divided into sub-samples by quartering and coning and stored in special sample containers to prevent contamination. The sub-samples were subsequently analysed by employing the following: *Malvern particle size analysis*, *total sulphur analysis*, *PGE analysis*, *X-ray diffraction analysis* of talc and *QEM SCAN analysis* of the overflow sample. Full descriptions of these techniques are given below.

5.5.3. Particle Size Analysis

The most common method of representing the cyclone efficiency is by constructing a performance or partition curve (also a Tromp curve). This method relates the weight

fraction or percentage of each particle size in the feed, which reports to the cyclone underflow to the particle size. The Malvern size analyser reports results as volume fraction. Therefore, in order to convert the volume fractions to mass fractions, it was assumed that the density or specific gravity of the various mineral components is the same as that of talc, which is around 2.7 g/cm^3. This assumption is close to the true value, since the finer fraction of the ore consists mainly of talc. The particle size distribution was measured by SGS Lakefield Research Africa (Pty) Ltd (South Africa) and the University of Pretoria by employing Malvern particle size analysers (Malvern Mastersizer 2000).

5.5.4. Sulphur Analysis

The total sulphur content of the sample was measured using the Leco S-144DR Sulphur analyser as described in detail in Chapter 3.

5.5.5. PGE Analysis

Platinum-group element content of the samples was assayed by SGS Lakefield Research Africa (Pty) Ltd in Johannesburg by employing fire assay.

5.5.6. QEM SCAN Analysis of the Overflow Samples

As will be seen later in Chapter 6, from the sulphur mass balance determined for each cyclone it was clear that there are some PGMs that would report to the overflow. In order to determine whether the PGMs lost to the overflows were recoverable or not, 100g of each sample (overflows from the 36.9mm and 76.0mm cyclones) were sent to Mintek for PGM and gold analysis using the QEMSCAN analysis technique. The results obtained from this type of analysis are discussed in Chapter 6.

5.6. FLOTATION AFTER DE-SLIMING

Once the 1.27g/ml slurry was prepared, as described in Section 5.4.4, the flotation process was initiated and the procedure followed was the same as discussed earlier in Chapter 3, unless otherwise stated. DTP (0.64 mol.) (See Chapter three for the SIBX:

DTP mixtures) was used as a collector for the flotation. $CuSO_4$ was used as an activator and it was dosed at 70g/t. The variable component of the reagent suit was the depressant (CMC). Sodium carboxymethylcellulose (CMC) was used as a depressant for the entire experimental work. The manufacturer's specifications are described in Chapter 3. However, in this experimental exercise, the CMC concentration was varied by dropping the dose rate according to the following sequence: 500, 400 and 300 g/t. Dowfroth 200 from Betachem (South Africa) was used as the frother during the entire experimental exercise. The concentrate was manually removed with two hand scrapers as described in Chapter 3 and the concentrate was collected after two and 10 minute time intervals.

As soon as flotation was completed, concentrate was air filtered in the filter press and dried in an oven. The dried concentrate was then sent for further analysis of sulphur. The results obtained are discussed in Chapter 6.

5.7. FLOTATION OF TALC PRIOR TO THE PGM FLOTATION

5.7.1. Introduction

The aim of this experimental exercise was to draw a rough comparison between de-sliming of talc and flotation of talc prior to the PGM mineral flotation. As has already been discussed in Chapter 2, talc is hydrophobic in nature; hence it is easy to float. In this test work a simple talc flotation exercise was performed. As a method of comparison, the talc concentrates were analysed for sulphur in order to establish whether there were some PGEs reporting to the talc concentrate. The following section details the experimental procedure.

5.7.2. Experimental Procedure

The ore sample was prepared and milled in the same way as already discussed in Chapter 3, Section 3.1. Dowfroth 200 from Betachem (South Africa) was used to enhance talc floatability. A Denver D12 flotation machine fitted with an 8-litre cell was used for the first rougher float of talc. Then the talc concentrate was floated with a 2-litre cell fitted to the Denver D12 machine.

As soon as milling (described in Chapter 3, Section 3.1.1) was completed, pulp consisting of 3.3kg solids was transferred to the 8-litre flotation cell and filled to the mark with water. The slurry was agitated with the cell impeller for three minutes, after which 60g/t of frother was added. No depressant was added in order to avoid talc depression.

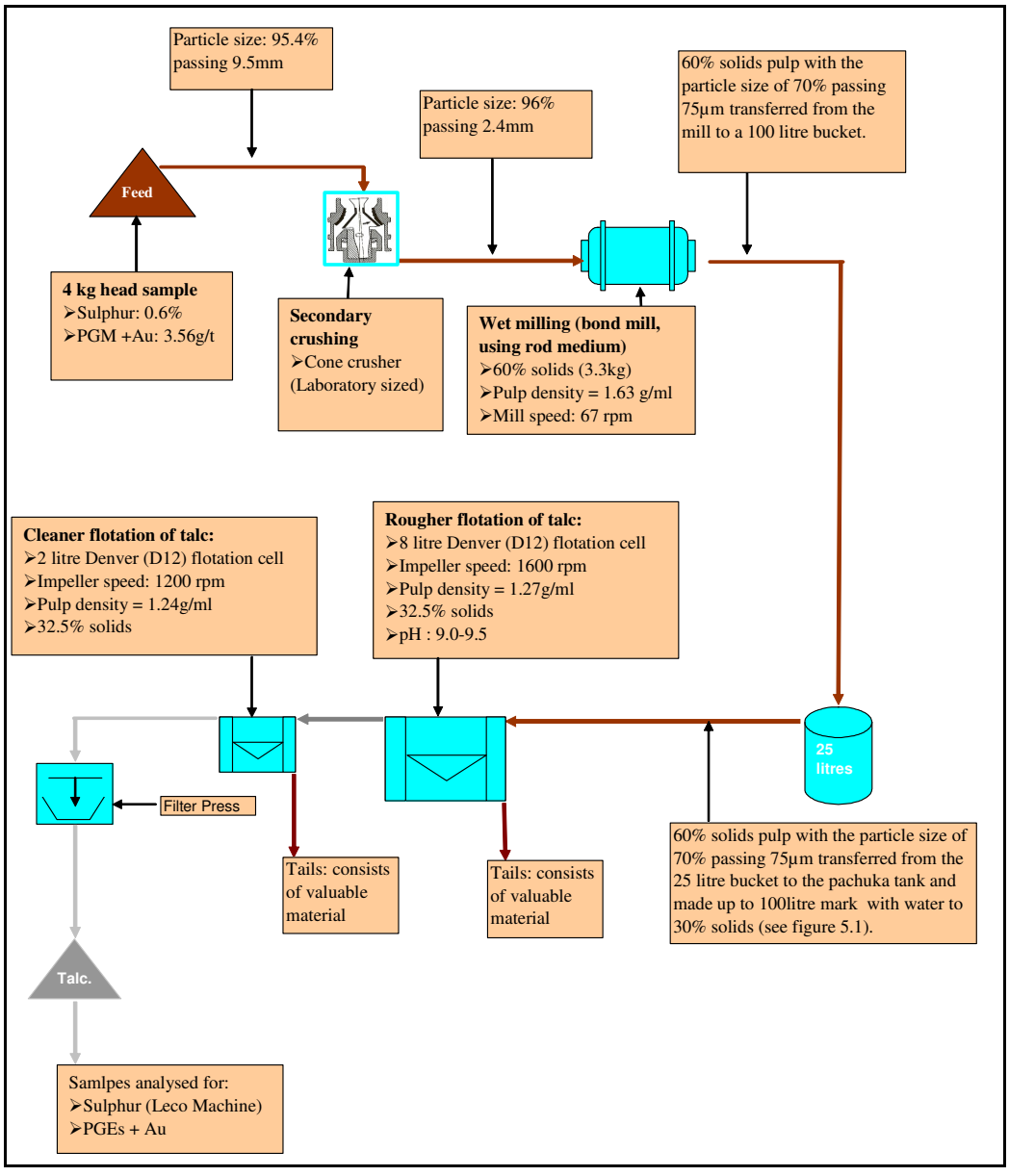

Figure 5.6: *Flow diagram for the procedure followed during the experimental work.*

The frother was conditioned for one minute. As soon as the one minute had elapsed the aeration valve was opened and flotation of talc commenced. The talc was

manually removed from the surface with two hand scrappers at ten seconds intervals and collected in containers.

Figure 5.7: *Picture of the 8-litre flotation cell with talc being floated using Dowfroth 200 frother.*

The scraping process was continued for 10 minutes. The talc concentrate was then filtered and dried in an oven. The dried concentrates were then thoroughly mixed and a representative portion was taken and kept aside for further analysis of sulphur and talc. The rest of the portion was split into three and each portion was added into the 2-litre flotation cell. The cell was then filled with water to the 2-litre mark. The pulp was stirred for a minute and then 60g/t of frother was added and conditioned for one minute. As soon as the one minute had elapsed, the aeration valve was opened and manual scrapping of the concentrate was initiated. The concentrate was scraped off every 10 seconds for five minutes. As soon as flotation was completed, the concentrate was air filtered in the filter press and dried in an oven. The dried samples were taken for further analysis of sulphur and PGEs and the results are discussed in Chapter 6.

CHAPTER SIX

REMOVAL OF TALC FROM MIMOSA ORE

6.1. RESULTS AND DISCUSSION

6.1.1. Introduction

The aim of this chapter is to discuss the methods used to remove talc (by de-sliming) and the results obtained during the de-sliming of talc. Finally, the de-sliming of talc is compared to the pre-floating of talc prior to the flotation.

6.1.2. Quantification of Talc

Preferred orientation is a challenge associated with the quantification of talc by XRD analysis. When this clay mineral is pressed in the sample holder for XRD analysis, the mineral forms flat sheets that are orientated perpendicular to the c-axis of the crystallites and these sheets are presented preferentially to the X-ray beam. In order to establish standards, as well as to determine the chemical composition of talc by micro probe analysis, a sample as high as possible in its talc content was required. Sourcing of pure talc with a composition resembling that of the talc found at Mimosa Mine was very difficult. Alternatively, it was decided to employ collectorless flotation of Mimosa ore to obtain a high grade talc concentrate. The concentrate of the first stage was subjected to two stages of cleaning to maximise the talc content. The quantitative analysis of the final talc concentrate (re-cleaner concentrate) is shown in Table 6.1 and is compared to the foam (formed on top of the talc concentrate during filtration of the concentrate) obtained during the flotation. It is believed (judging by visual appearance) that the foam consists of a higher grade of talc compared to the re-cleaner concentrate, based on the fact that the foam appeared brighter. Table 6.1 shows that a final talc grade of around 39.4% was obtained after two stages of cleaning and 38.3 was obtained when the talc foam was analysed.

The structural modification of the talc reference in the Rietveld quantification and the accuracy of the XRD results were tested by spiking the samples with Si powder; the

samples were spiked with 15% (by mass) Si powder (Aldrich 99% purity) before micronizing.

Table 6.1: *Quantitative XRD-analysis results of talc concentrate samples extracted from Mimosa feed ore.*

Composition	Re-cleaner concentrate (3rd Float)	Std dev.	Foam of Re-cleaner concentrate	Std dev.
Calcite	6.51	1.26	4.48	0.69
Chlorite IIb-2	14.94	2.19	5.72	0.69
Diopside	2.44	0.96	5.09	0.69
Hornblende, Magnesium Iron	7.22	1.44	7.44	0.9
Hypersthene	13.85	2.28	19.01	1.38
Plagioclase Oligoclase An16	1.36	1.59	4.43	1.14
Silicon	14.28	1.59	16.82	0.78
Talc C-1_Fe	39.4	2.3	38.3	3.6

Figures 6.1 and 6.2 show back-scattered electron images of the talc-rich flotation concentrate. These figures clearly indicate the association of the talc with a complex mixture of other clay minerals such as mica, in Figure 6.1, and also base metal sulphides locked in talc, as shown in Figure 6.2. Given the association, a very pure talc concentrate is therefore not possible. The base metal sulphides that are intergrown with talc will probably be lost with the talc during de-sliming. However considering the size of the base metal sulphides it would probably be impossible to recover them by any means. Hence, one of the aims of this chapter was to investigate the amount of PGE lost during de-sliming and use this as a criterion to evaluate the de-sliming process.

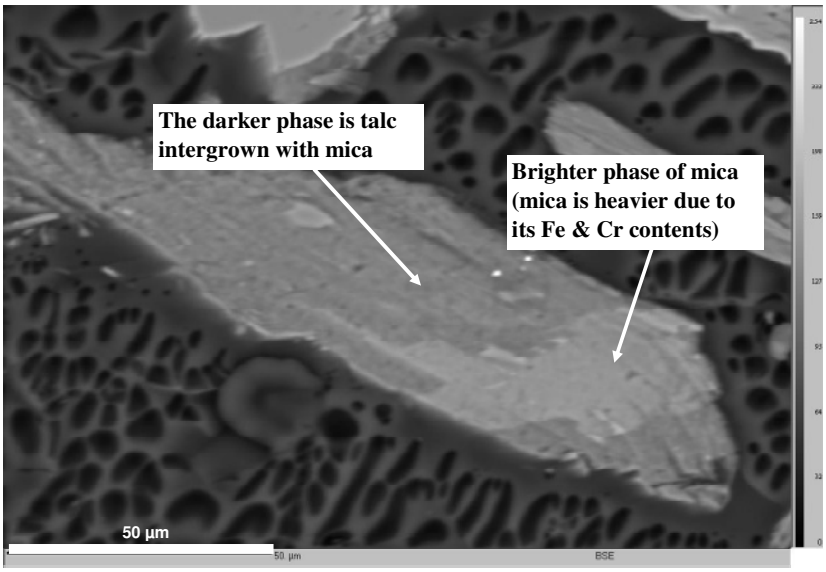

Figure 6.1: *Back-scattered electron image of the Mimosa talc concentrate.*

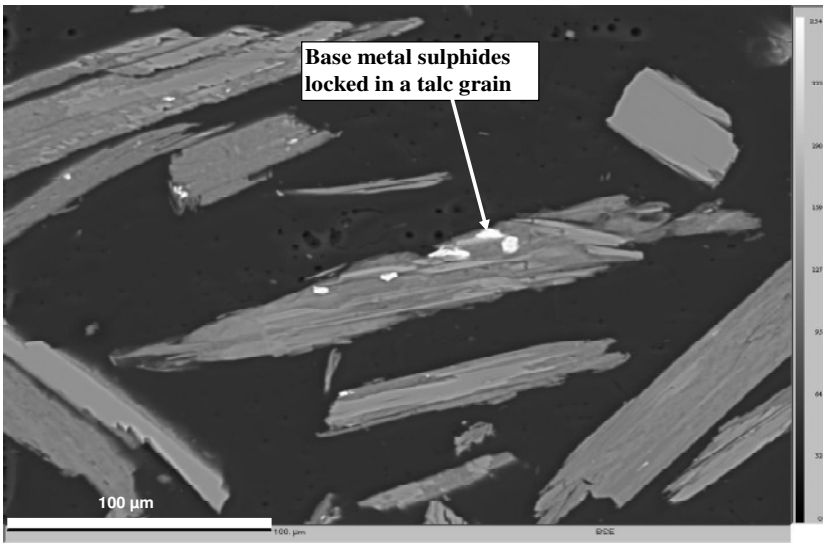

Figure 6.2: *Back-scattered electron image of the Mimosa talc concentrate.*

During the preliminary analysis it was found that talc is very finely intergrown with hornblende and biotite. The initial modelling of talc using the Rieveld method by way of Autoquan/BGMN software showed large errors in the results (Verryn, 2006). It was subsequently discovered by electron microprobe analysis (Table 6.2) that the Mimosa talc has a high iron (Fe) content compared to the talc found in the Merensky reef and it is different from the pure natural talc structure (Perdikatsis, 1981) used in

the Rietveld quantification software. After incorporating Fe into the talc structure, the results improved significantly.

Table 6.2: *Electron microprobe analysis of Mimosa talc and comparison with the talc from Merensky and Uitkoms deposits. Talc 1, 2 and 3 refers to the chemical analysis of three separate talc samples.*

	Mimosa talc 1	Mimosa talc 2	Mimosa talc 3	Average Merensky	Average Uitkoms
SiO_2	64.13	64.06	64.13	61.161	32.40
Al_2O_3	1.47	1.40	1.20	0.731	16.11
MgO	27.99	28.16	28.48	29.003	28.08
FeO	6.40	6.37	6.20	4.038	10.20
MnO				0.033	0.16
Cr_2O_3				0.172	0.36
NiO				0.094	0.06
TiO_2				0.027	0.14
CaO				0.031	0.19
Na_2O				0.068	0.04
K_2O				0.065	0.13
Cl				0.018	0.01
F				0.120	0.12

The following section discusses the talc analysis of Mimosa feed after milling as described in Section 3.1.2.

6.1.3. Quantification of Talc in the Mimosa Feed

Before the underflow and overflow samples were analysed for the talc, five representative samples of the Mimosa ore were taken at random and were sent for quantitative talc analysis by XRD. The results obtained are presented in Figure 6.3. The talc grade obtained ranges between 14.55% and 17.37% by mass with overlapping standard deviations as shown in Figure 6.3. For the purposes of this study, an average of 15.93% was taken, as shown in Figure 6.3.

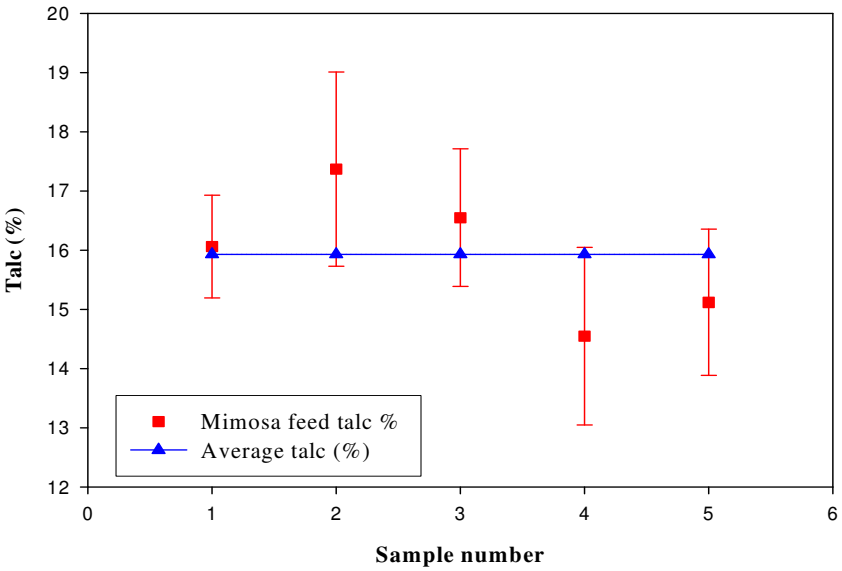

Figure 6.3: *Quantitative analysis of talc for various samples of Mimosa feed ore and the average talc grade (% by mass).*

The following section discusses the analysis of talc distribution in the various particle size fractions after milling the Mimosa ore as described in Section 3.1.2. Also given is the talc concentration found in these various size fractions.

6.1.4. Talc Distribution in the Various Particle Size Fractions

There are three factors that could be associated with the efficiencies of mineral separations in mineral processing (Kelly and Spottiswood, 1989). The factors encountered could be attributed to three broad sources, namely:

1. Mineral limitation, which is often associated with the properties of the mineral. These properties can be physical or chemical properties.
2. Equipment limitation, which prevents the maximum separation efficiency of the equipment.
3. Human failure to minimize these inefficiencies.

The focus of the following sections of this chapter is on the first two factors. Figures 6.4 –to 6.7 show the size analysis and the talc analysis in each size fraction for the Mimosa ore sample milled in the laboratory using the bond rod mill, as described in Section 3.1.2. The size analysis was performed by using tailor sieves for the larger

fractions, whilst the cloth screens were used for the smaller fractions. The cloth screens were submerged in ultra-sonic baths and the size fractions are represented graphically in Figures 6.4 and 6.5 while Figures 6.6 and 6.7 show the graph of the analysis when the cyclosizer was used instead of the cloth screen. For the cyclosizer analysis, only -53µm size fraction was sent for analysis. All the size analysis was performed at Lakefield Research Africa (Pty) Ltd (South Africa) and the different size fractions were then sent to the Geology Department at the University of Pretoria for quantitative XRD analysis of talc in each fraction.

It can be seen from Figure 6.4 that the talc grade is almost uniformly distributed in all size fractions with the exception of -10+5 µm and +150 µm sizes. Figure 6.5 plots the cumulative mass percentage and talc grade passing a specific screen size. It can be seen that the curve for the pure talc closely resembles that of the particle size distribution (PSD) of the Mimosa milled ROM. This is indicative of constant talc:ore ratio for each of the size intervals. The outcome is clearly in contradiction to our hypothesis, which is the basis of this study; which states that talc is softer and more friable compared to the rest of the material components of the ore and that it would therefore report mostly to the finer fractions.

Screen separation is based on size only. The flakiness and sheet like structure of talc composites, as indicated in Figures 6.1 and 6.2 result possibly in the blinding of the screen apertures and therefore makes it difficult to screen finer fractions. A very long time of ultrasonic treatment is required to overcome screen blinding and obtain good separation efficiencies. Therefore it is concluded that results obtained from screening cannot be used to predict the separation of talc from the ore using cyclones.

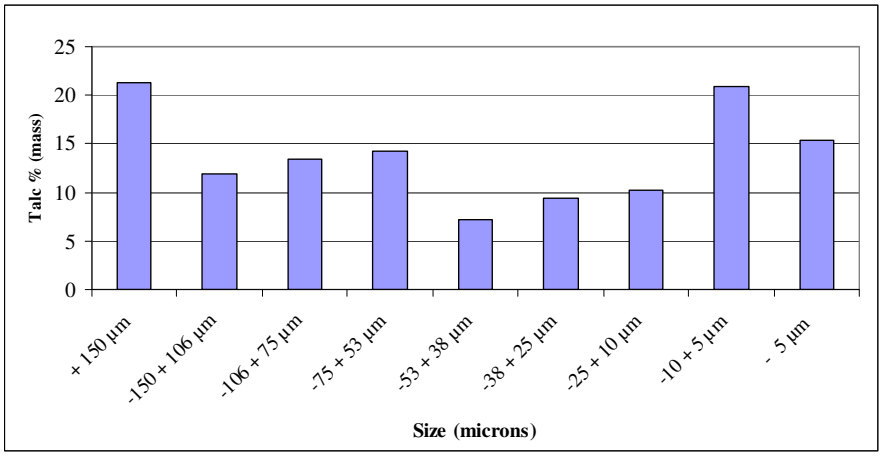

Figure 6.4: *Talc grade (%) in the various size fractions of the screen product.*

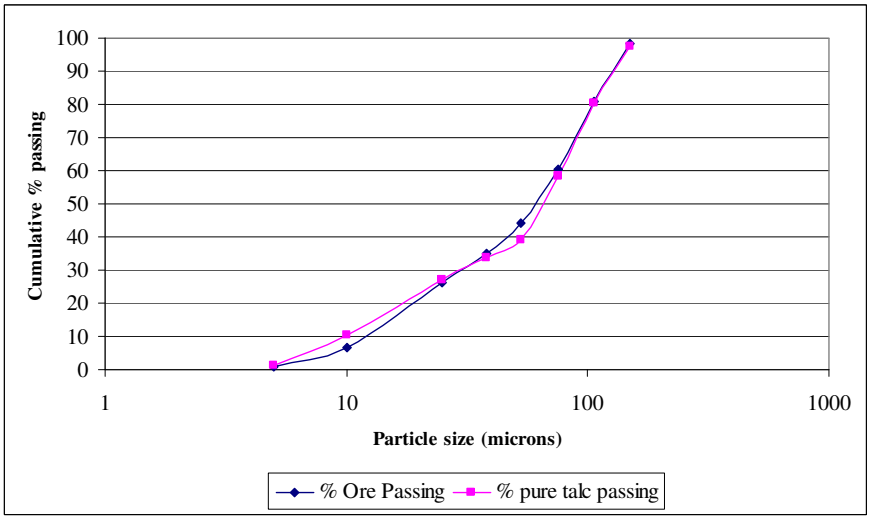

Figure 6.5: *Talc and mass size distribution (by mass) of milled ore samples subjected to sieve size analysis.*

Cyclosizer separation should be more representative of the cyclones since the same separation mechanism is employed by de-sliming cyclones. Figures 6.6 and 6.7 summarise the mass and talc distribution of the milled Mimosa ore sample. Just like cyclones, cyclosizers separate based on the densities and size of the constituents. For material of the same density, density plays a lesser role than size.

From Figure 6.6 it is clear that there is an increasing trend towards the finer fractions, which is an indication that more talc is liberated. Therefore Figure 6.7 can be used to

estimate the percentage of talc that can be removed by removing a certain size fraction of the ore. As an example, in order to remove about 40% of talc at a cut size of 16µm, about 25% of the ore will report to the slimes.

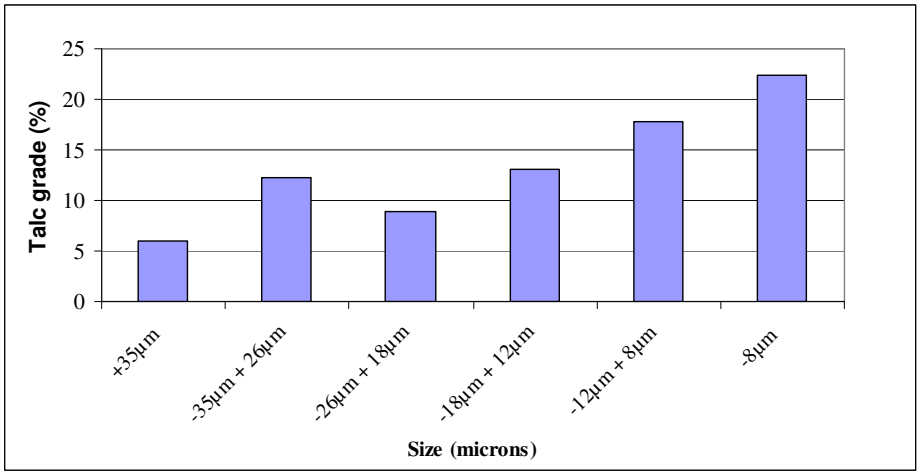

Figure 6.6: *Talc grade (%) in the various size fractions of the cyclosizer product.*

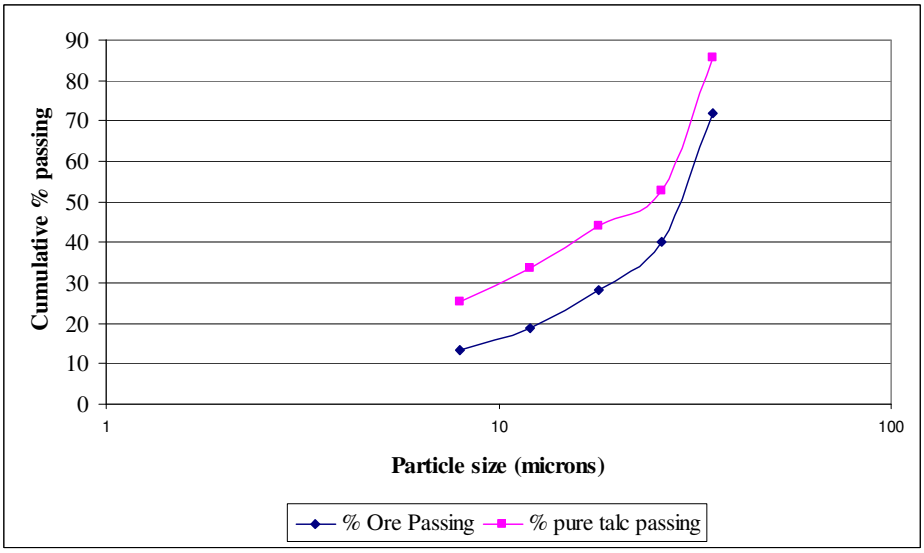

Figure 6.7: *Talc and mass size distribution (by mass) of milled ore sample subjected to cyclosizer size analysis.*

The concentration of talc in the finer fractions is expected to be worse in an industrial process, since ball mills are employed. Ball mills break ore particles indiscriminately, which is in contrast to the rod mills employed by this study. The reason for selecting rod mills in this study is that the size distribution of a rod mill resembles that of a ball

mill classifier combination (see Figure 3.2). Figure 6.7 plots the PSD of the talc and the ore and clearly the talc is finer than the ore.

The following section gives a detailed discussion of talc de-sliming using the de-sliming equipment and hydro-cyclones described in Sections 5.3.2 and 5.3.3.

6.2. DE-SLIMING USING HYDRO-CYCLONES

6.2.1. Determination of the Cyclone Cut-point

Before any experimental results can be discussed, it is important to determine the cut-point and discuss the efficiency of both cyclones that were used for the de-sliming. Performance curves are a common method used to determine the cyclone efficiency and cut-point. Figures 6.8 and 6.9 show the graphs for the performance curves of the 36.9 mm and the 76.0 mm cyclones respectively. These graphs show the actual performance curve and the corrected performance curve.

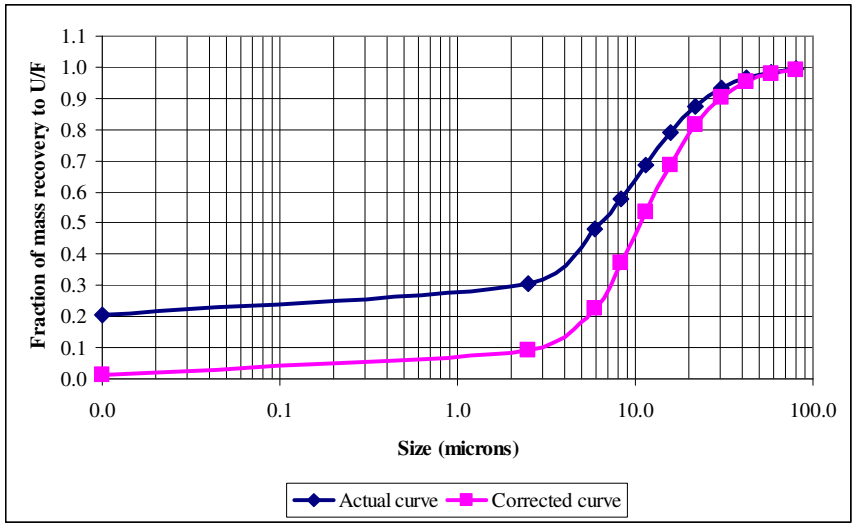

Figure 6.8: *The corrected and uncorrected partition curves for the 36.9 mm cyclone.*

The actual performance curve is a plot of the actual data for the underflow material and it also exhibits the imperfections of the cyclone. For ideal separation, the mass fraction to the underflow should be zero when the particle size is zero. However, in practice this is never the case because of short circuiting of the fine particles with the

water to the underflow. The short circuiting water is called the α-water (Section 2.3 and Figures 2.19a and b). For the 36.9 mm cyclone, the α-water fraction is about 0.20; while for the 76 mm cyclone the fraction is 0.17 (see Figure 6.8 and 6.9.). The α-water obtained for both the 36.9 mm cyclone and the 76 mm cyclone compares well within the experimental error to the values obtained by performing mass balances later in Table 6.6 and 6.8.

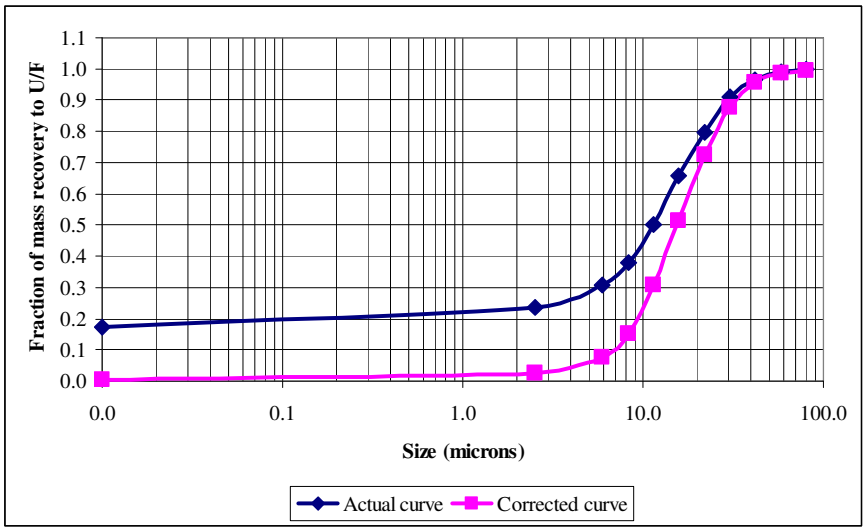

Figure 6.9: *The corrected and uncorrected partition curves for the 76.0 mm cyclone.*

The primary objective of plotting Figure 6.8 and 6.9 was to determine the cut-point (d_{50}) for the two cyclones from the corrected curves. In order to obtain an accurate estimate of the d_{50}, the actual partition curve had to be corrected in order to take into account the unclassified feed material to the underflow. From the corrected partition curves the cut sizes or d_{50}-values were obtained: 10.9 μm for the 36.9 mm cyclone and 15.5 μm for the 76.0 mm cyclone. Using Figure 6.7 in Section 6.1, it can be predicted that about 35% of talc will be removed with the 36.9 mm cyclone and 40% with the 76.0 mm cyclone. These results are confirmed by mass balances of talc for each of the cyclones.

On an industrial scale, cyclones such as these can be used in clusters. However, operating these small cyclones in clusters could pose problems such as blockages and splitting of the feed slurry prior to de-sliming. The imbalances in splitting could cause

a pressure drop for individual cyclones in a cluster and therefore cause inefficiencies when it comes to the de-sliming of talc.

The following section investigates the results obtained from the analysis of the UF and the OF of the Mimosa ore.

6.2.2. Cyclone Underflow and Overflow Analysis of Talc by Quantitative XRD Analysis

Figures 6.10 and 6.11 show the bar graphs for the quantitative XRD analysis of talc and other minerals recovered to both the UF and OF fractions for the 36.9 mm and 76.0 mm cyclones respectively.

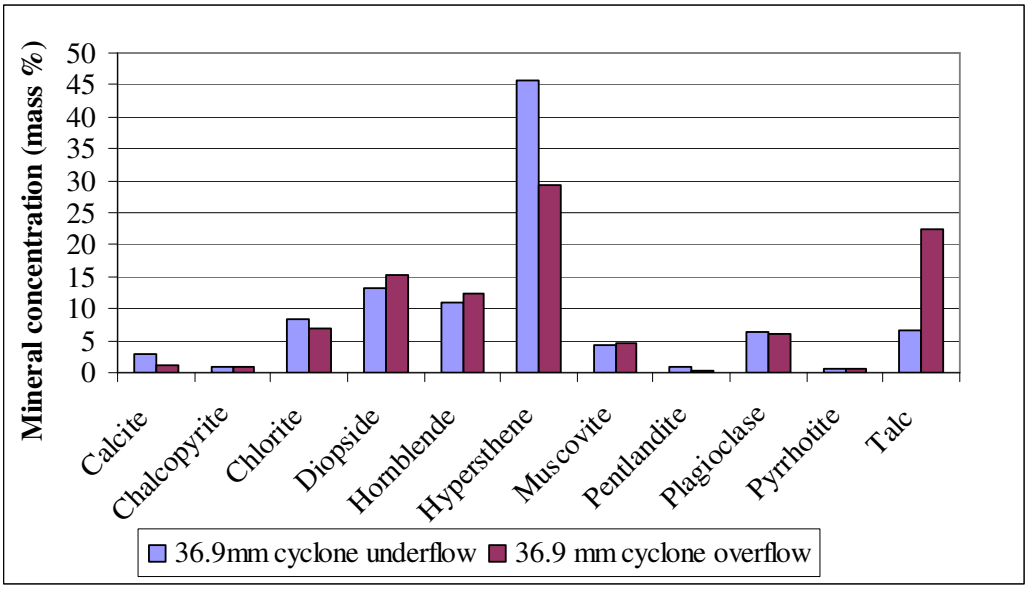

Figure 6.10: *Graphic representation of the XRD quantitative analysis results of the 36.9 mm cyclone UF and OF.*

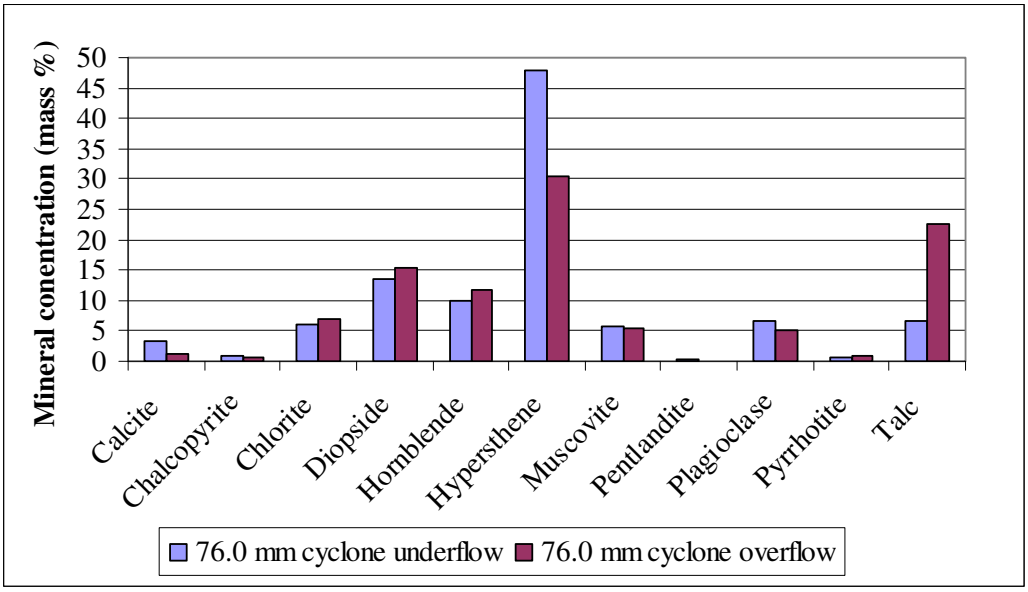

Figure 6.11: *Graphic representation of the XRD quantitative analysis results of the 76.0 mm cyclone UF and OF.*

It is clear from the two graphs in Figures 6.10 and 6.11 that the talc concentration in UF for both the 36.9 mm and the 76.0 mm cyclone has been reduced compared to the talc concentration in the feed. The talc concentration was reduced from 15.93% to an average of 6.7% when the 36.9 mm cyclone was employed and to an average of 6.5% when the 76.0 mm cyclone was used. The talc concentration to the OF was upgraded to 22.4% when the 36.9 mm cyclone was used and to 22.5% 76.0 mm cyclone.

From these results it can be concluded that the talc concentration can be reduced by de-sliming using a de-watering cyclone.

In order to confirm the results of talc analysis, shown above, LOI and XRF analyses were performed, as discussed in Chapter 5 Section 5.4.2.

6.2.3. Loss on Ignition Results

LOI is the sum of all the changes that occur in a sample at a temperature of 1000°C, expressed as a weight percentage of the original sample weight. Samples usually contain some volatile elements, like Br, Cl, S, F, C, which are lost at 1000°C. A gain on ignition can also be measured when, for example, FeO is oxidised to Fe_2O_3 (Loubser, 2007). LOI has to be brought into consideration if the analytical oxide total

is to be used as an indication of analytical reliability. This method is not always foolproof, as some sulphur as sulphate, fluorine as fluoride and even some apatite, carbon dioxide or hydroxide will remain in some materials (Loubser, 2007). Table 6.3 shows the results obtained when LOI was performed to the UF and OF samples of the 36.9 mm and the 76.0 mm cyclones. Table 6.3 shows the comparison between experimental LOI and theoretical LOI. The theoretic LOI was arrived at by first obtaining the percentage OH group in pure talc. The figure was achieved by using the following calculation:

$$OH\ \%\ in\ pure\ talc = [\frac{(OH\ \ molar\ mass)\ \times 2}{Talc\ molar\ mass}] \times 100 \qquad (6.1)$$

Then the theoretical LOI (or OH percentage in the whole sample) was obtained from the following calculation:

$$Theoretical\ \ LOI = [\frac{(\frac{OH\ \%\ \ in\ \ pure\ \ talc}{100}) \times talc\ \ mass\ \ in\ \ sample}{Sample\ \ mass}] \times 100 \qquad (6.2)$$

where:

$$talc\ \ mass\ \ in\ \ sample = talc\ \ \%\ \ in\ \ sample\ \ \times sample\ \ mass$$

and the talc percentage in the sample is obtained from Figures 6.8 and 6.9 for both the UF and OF of the 36.9 mm and 76.0 mm cyclones.

Theoretical LOI assumes that only talc in the whole sample analysed consists of the hydroxide (OH) group and there are no other volatiles present. However, from the practical values it can be seen that the LOI is a little higher than the theoretical ones. The small difference in the results therefore suggests that there are other volatiles associated with the other mineral components of the samples, as shown in Figures 6.10 and 6.11. However, the consistency of these results confirms that the XRD analysis performed to quantify talc is trustworthy.

Table 6.3: *Chemical composition of cyclone overflow and underflow samples of Mimosa ore.*

%	76 mm cyclone UF	76 mm cyclone OF	36.9 mm cyclone UF	36.9 mm cyclone OF
SiO_2	52.77	49.61	50.83	49.71
TiO_2	0.20	0.20	0.22	0.21
Al_2O_3	3.99	4.25	3.87	4.64
Fe_2O_3	12.21	14.34	13.88	14.09
MnO	0.21	0.25	0.26	0.24
MgO	23.20	21.60	22.61	21.08
CaO	5.43	5.15	5.89	4.96
Na_2O	<0.01	<0.01	<0.01	<0.01
K_2O	0.21	0.28	0.26	0.22
P_2O_5	<0.01	<0.01	<0.01	0.02
Cr_2O_3	0.42	0.52	0.49	0.59
NiO	0.28	0.47	0.35	0.51
V_2O_5	0.04	0.02	0.03	<0.01
ZrO_2	<0.01	<0.01	<0.01	<0.01
LOI	0.83	2.87	0.84	3.33
TOTAL	99.78	99.56	99.54	99.61

Table 6.4: *Comparison between experimental LOI and theoretical LOI on the underflows and overflows.*

	76 mm cyclone UF	76 mm cyclone OF	36.9 mm cyclone UF	36.9 mm cyclone OF
Experimental LOI	0.83	2.87	0.84	3.33
Calculated LOI	0.59	2.01	0.60	2.01

As has been discussed in Chapter 2 Section 2.2.10, a cyclone separates minerals based on density and size. Although it was assumed in Chapter 2 that talc will break finer compared to the valuable minerals such as the base metal sulphides and the PGMs. In practice one would expect some of the valuable minerals, such as the BMS carrying the PGMs, to also break finer than anticipated and therefore be lost to the overflow stream. It can be seen from Figures 6.10 and 6.11 that some base metal sulphides such as chalcopyrite, pentlandite and pyrrhotite have reported to the overflows of the two cyclones. This is clearly a disadvantage of de-sliming. The following section therefore discuses the mass and chemical balances of the valuable minerals being discussed.

6.3. ANALYSIS OF THE OVERFLOW SLIMES

6.3.1. Mass and Chemical Balance for the 36.9 mm and 76.0 mm Cyclones

Tables 6.5 and 6.6 summarise the mass and chemical balances for the two cyclones under investigation. Tables 6.7 and 6.8 summarise the percentage recoveries to the UF and OF for both cyclones. Based on the amount of sulphur that reports to the OF, it was expected that losses of PGMs to the OF would occur. In order to quantify PGE losses to the OF, representative samples of the OF material from both cyclones were sent to SGS Lakefield Research Africa (Pty) Ltd for PGE analysis and the results obtained are shown in Tables 6.7 to 6.8.

Table 6.5: *Mass and chemical balance tables for the 36.9 mm cyclone.*

	Feed	Underflow	Overflow
Solids (t/h)	0.58	0.50	0.08
Sulphur (kg/h)	3.39	2.89	0.50
(PGE + Au) (g/h)	2.29	2.02	0.27
Talc (t/h)	0.05	0.03	0.02

Table 6.6: *Mass and chemical balance tables for the 76.0 mm cyclone.*

	Feed	Underflow	Overflow
Solids (t/h)	2.21	1.8	0.4
Sulphur (kg/h)	12.57	9.8	2.8
(PGE + Au) (g/h)	6.49	5.0	1.5
Talc (t/h)	0.21	0.1	0.1

Table 6.7: *Percent recoveries to 36.9 mm cyclone underflow and overflow.*

Consituent	Recovery to UF	Recovery to OF
Solids (wt%)	85.8	14.2
Water recovery (wt%)	17.8	82.2
Sulphur (wt%)	85.1	14.9
(PGE + Au) (wt%)	88.0	12.0
Talc (wt%)	64.4	35.6

Table 6.8: *Percent recoveries to 76.0 mm cyclone underflow and overflow.*

Consituent	Recovery to UF	Recovery to OF
Solids (wt%)	80.4	19.6
Water recovery (wt%)	12.8	87.2
Sulphur (wt%)	77.6	22.4
(PGE + Au) (wt%)	77.2	22.8
Talc (wt%)	54.4	45.6

The analysis of talc based on the data obtained from the XRD, shows that the 36.9 mm cyclone removes about 35.6 wt% of talc to the OF, while the bigger cyclone removes about 45.6 wt% of talc from the Mimosa ore. These figures are similar to the predictions in Section 6.2.1. Both cyclones seem to be removing a significant amount of talc, with the bigger one removing more than the smaller one. The reason the bigger cyclone seems to remove more talc is because it is less selective compared to the smaller one. It can also be seen from Tables 6.7 and 6.8 above that metal accounting indicates that 12% of PGE + Au reports to the OF of the 36.9 mm cyclone and 22.8% PGE + Au reports to the OF for the 76.0 mm cyclone. This clearly shows that the talc obtained with the 36.9 mm cyclone has a higher grade than the talc from the 76 mm cyclone. The objective was ideally to selectively remove talc without losing the valuable PGMs. Table 6.9 shows an example of the cut size of PGM and base metal sulphides in comparison with the talc for both cyclone sizes. The cut sizes for the PGMs and the base metal sulphides were determined using the equation 6.3 as indicated by Plitt's model. The smaller cyclone with the lower cut-point (10.9 μm for talc) is more selective than the bigger one of 15.5 μm. This is due to the lower cutpoint, as was already seen in Figure 6.8.

$$d_{50PGM} = d_{talc}\left[\frac{\rho_{talc} - \rho_e}{\rho_{PGM} - \rho_e}\right]^{0.5} \qquad (6.3)$$

Table 6.9: *Calculated cut sizes for various minerals with known densities.*

		36.9 mm cyclone.	76.0 mm cyclone.
Mineral	**ρ**	**d_{50} (µm)**	**d_{50} (µm)**
Talc	**2.8**	**11.9**	**15.80**
PGM (PdBiTe)	**8.5**	**5.83**	**7.74**
Pentlandite	**4.8**	**8.19**	**10.87**
Pyrrhotite	**4.6**	**8.41**	**11.17**

Using equation 6.3, it is possible to theoretically predict the PGM sizes lost to the OF of the two cyclones. PGMs of about 6 µm and less were expected to be removed with the slimes for the 36.9 mm cyclone. PGMs of about 8 µm and less were expected to be lost to the OF for the 76.0 mm cyclone. The following section gives a more detailed discussion on the reasons for the loss of the PGM and BMS with the slimes to the OF of the cyclones.

6.3.2. PGM Grain Size Distribution in the Cyclone Overflow

Figure 6.12 summarises the PGM grain size distribution in the OF of the 36.9 mm and the 76.0 mm cyclones. The particle size of the PGMs and the BMS are expressed as Equivalent Circle Diameter (ECD): the diameter of a circle covering an area equal to that of the measured PGM grain. The PGM grain sizes vary from less than 3µm to just above 6 µm. The average PGM particle size is 3.65µm for the OF sample for the 36.9 mm cyclone and is close to an average size of 3.76 µm for the 76 mm cyclone. Therefore the average PGM size approximates the size predicted in Table 6.9 using equation 6.3.

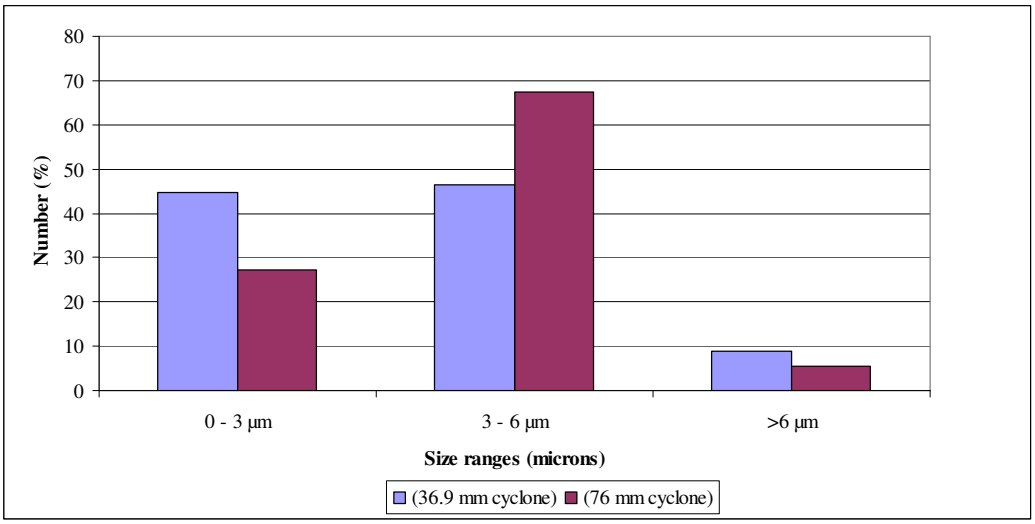

Figure 6.12: *PGM grain size distribution for the 36.9 mm and 76 mm cyclones overflows.*

6.3.3. Distribution of PGM Types

The types of PGMs observed for the 36.9 mm and 76.0 mm cyclone OF are summarized in Table 6.10. Most of the PGMs shown in Table 6.10 belong to PGE-Bi-Te and PGE-As-S classes. These results exclude Ruthenium, Osmium and/or Iridium bearing phases, such as laurite [Ru (Os, Ir)-Sulfide], since these species do not contribute to the assayed PGE content (McLaren, 2003). Pd-Bi-Te has the highest contribution of PGM type for both cyclone size OF samples and is followed by $PtAs_2$. For the 36.9 mm cyclone sample, the Pd-Bi-Te contributed 28 grains out of 56 analysed, followed by the 17 grains of the $PtAs_2$ classes. 24 and 16 grains, out of the 55 grains analysed, belong to the Pd-Bi-Te and the PtAs for the 76 mm cyclone OF sample, respectively. The fact that Pd-Bi-Te forms the largest percentage PGM type in the fines that report with the cyclones overflows is in agreement with a study conducted by Vermaak (2005), whereby it was shown that the poor recovery of the Pd-Bi-Te is possibly caused by the small particle size rather than the lack of collector interaction with the mineral surface.

Table 6.10: *Summary of distribution of PGM type in 36.9 mm cyclone overflow and 76 mm cyclone overflow.*

	(36.9 mm cyclone OF)		
PGM type	**PGM (vol %)**	**No of PGMs**	**Average ECD (µm)**
PdBiTe	28.4	16	3.59
PtAs	17.3	9	3.80
PtRhAsS	8.8	5	3.54
PtBiTe	8.0	7	3.06
PdHgAs	7.6	3	4.48
AuAg	6.0	3	4.11
PtPdBiTe	5.4	1	6.77
PtFeCu	5.4	2	4.69
RhAsS	3.8	2	3.98
PdBi	3.1	2	3.55
RhPtAsS	2.8	1	4.86
PdAsSb	1.0	1	2.98
PtPdSbAs	0.8	1	2.58
Au	0.7	1	2.43
PtS	0	0	0
PtPdNiS	0	0	0
PtBi	0.4	1	1.92
PtFe	0.3	1	1.72
Total		**56**	
	(76 mm cyclone OF)		
PGM type	**PGM (vol %)**	**No of PGMs**	**Average ECD (µm)**
PdBiTe	38.7	24	3.43
PtAs	32.4	16	4.09
PtRhAsS	13.5	6	4.32
PtBiTe	0	0	0
PdHgAs	0	0	0
AuAg	3.9	2	4.11
PtPdBiTe	3.9	2	4.02
PtFeCu	0	0	0
RhAsS	0.3	1	1.49
PdBi	0	0	0
RhPtAsS	0	0	0
PdAsSb	0	0	0
PtPdSbAs	0	0	0
Au	0	0	0
PtS	4.9	2	4.56
PtPdNiS	1.9	1	4.03
PtBi	0	0	0
PtFe	0.5	1	2.10
Total		**55**	

6.3.4. PGM Grain Liberation and Floatability Indexes

The purpose of this investigation was to obtain data information concerning (a) the type, (b) the mode of occurrence and (c) the liberation of the discrete PGM and BMS particles in the cyclone OF. Table 6.10 (McLaren *et al*., 2003) shows an example of a conceptual representation of the PGM grain modes of occurrence. The abbreviations in the top row of the table are defined at the bottom of the table. For example, the columns labelled SG and G show the mean PGMs associated with BMS locked in silicate gangue particles and PGMs locked within silicate gangue particles respectively. If, for instance, the valuable minerals are locked in the silicates, as indicated conceptually in Table 6.11 columns SG and G, it can be concluded that they will be lost in any case even if flotation is to be employed without de-sliming.

Table 6.11: *Schematic diagram of PGM grain modes of occurrence (McLaren, 2003).*

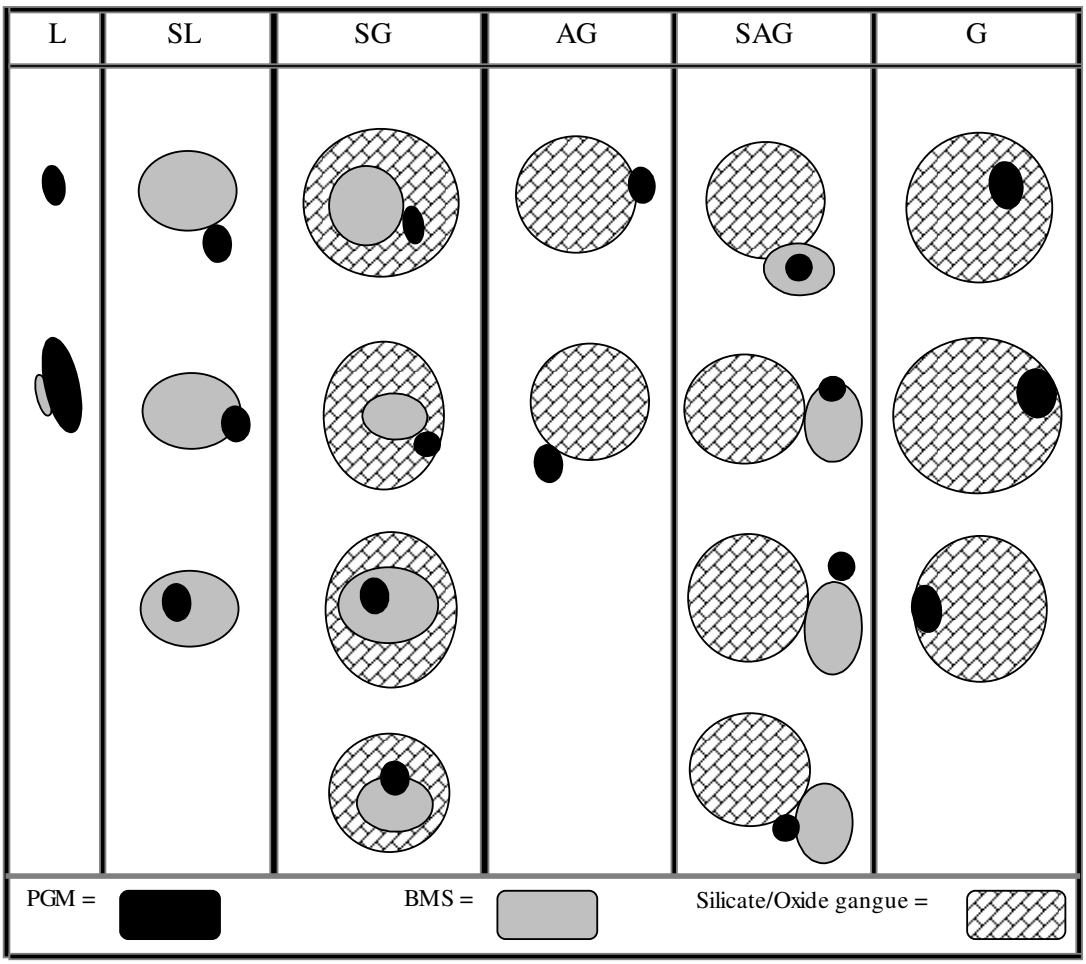

L	Liberated PGMs
SL	PGMs associated with liberated BMS (Base Metal Sulphides)
SG	PGMs associated with BMS locked in Silicate gangue particles
AG	PGMs attached to Silicate gangue particles
SAG	PGMs associated with BMS attached to Silicate gangue particles
G	PGMs locked within Silicate gangue particles

Figures 6.13 and 6.14 summarise graphically the mode of occurrence of the PGM grains in the cyclone OF streams. From the graphs, it can be seen that for the 36.9 mm cyclone, 74 (v/v) % of the PGMs lost to the OF are liberated, while 83% of the liberated PGMs are lost to the OF when the 76.0 mm cyclone is used.

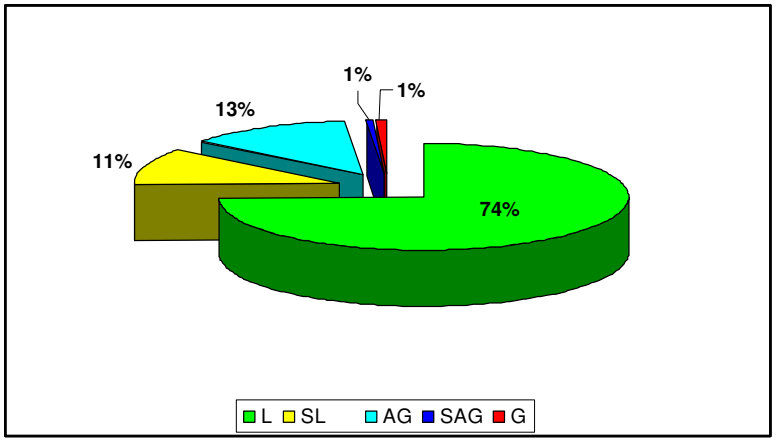

Figure 6.13: *PGM grain modes of occurrence for the 36.9 mm cyclone overflow, (the abbreviations shown are summarized in Table 6.11).*

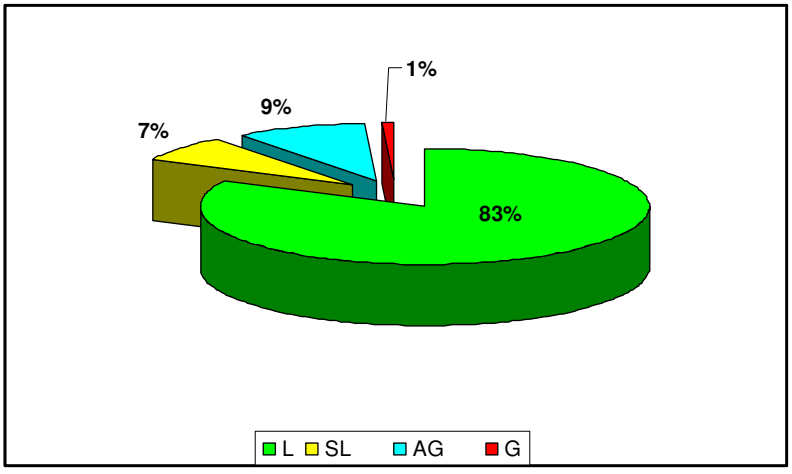

Figure 6.14: *PGM grain mode of occurrence for the 76.0 mm cyclone overflow (the abbreviations shown are summarized in Table 6.11).*

Combine Liberation Index (CLI) is the measure of PGM grain liberation and is calculated by dividing the area of potentially floatable component (PGM + BMS) by the total area of the particle (PGM + BMS + Silicate Gangue). It gives an indication of possible recovery during rougher flotation and is defined as:

$$CLI = \frac{Area\ of\ floatable\ \text{min}eral\ in\ particle}{Total\ area\ of\ particle} \tag{6.4}$$

where CLI = combined liberation index.

The resultant figure will range between 0 and 1, the latter indicating either a liberated PGM grain or one associated with a liberated BMS particle. In contrast, the liberation index of a BMS-barren silicate particle (low probability of flotation) will approach zero (McLaren et al., 2003).

Table 6.12: *Summary of PGM grain liberation index 36.9 mm cyclone OF and 76 mm cyclone OF.*

	PGM grain liberation index (36.9 mm cyclone OF)		
Index	**No of PGMs**	**PGM Vol %**	**Num %**
<0.2	1	0.70	1.8
0.2 - 0.4	1	1.66	1.8
0.4 - 0.6	5	12.22	8.9
0.6 - 0.8	0	-	-
0.8 - 1.0	49	85.43	87.5
Total	**56**	**100.0**	**100.0**
	PGM grain liberation index (76 mm cyclone OF)		
Index	**No of PGMs**	**PGM Vol %**	**Num %**
<0.2	3	3.4	5.5
0.2 - 0.4	2	2.1	3.6
0.4 - 0.6	2	4.8	3.6
0.6 - 0.8	0	-	-
0.8 - 1.0	48	89.7	87.3
Total	**55**	**100.0**	**100.0**

Table 6.12 shows the data on the liberation of the PGM minerals. The data shows that the minerals with a high possibility of PGM recovery exist to the cyclone OF of the two cyclone sizes used during de-sliming. The mineral grains with a liberation index

of 0.8-1.0 were 87.5% for the 36.9 mm cyclone OF and were based on the 56 grains that were observed. For the 76 mm cyclone OF, 87.3% out of 55 grains was observed with the index of 0.8-1.0. From Table 6.13 it can be seen that the flotation response is very much dependent on size.

Table 6.13: *Summary of PGM grain floatability index of de-slimed Mimosa ore.*

		36.9 mm cyclone OF	
	Particle Characteristics	**PGM Vol %**	**No of PGMs**
Fast Floating	Liberated PGMs >3µm ECD	59.8	24
	Liberated BMS >10µm ECD	5.2	3
Slow Floating 1	Liberated PGMs <3µm ECD	15.0	18
	Liberated BMS <10µm ECD	5.4	4
	PGMs >3µm ECD attached to gangue	12.6	4
	BMS >10µm ECD attached to gangue	0.8	1
Slow Floating 2	PGMs <3µm ECD attached to gangue	0.5	1
	BMS <10µm ECD attached to gangue	-	0
No Floating	PGMs and/or BMS locked in gangue	0.7	1
Total		**100.0**	**56**
		76 mm cyclone OF	
	Particle Characteristics	**PGM Vol %**	**No of PGMs**
Fast Floating	Liberated PGMs >3µm ECD	74.0	32
	Liberated BMS >10µm ECD	4.7	2
Slow Floating 1	Liberated PGMs <3µm ECD	8.5	12
	Liberated BMS <10µm ECD	2.4	2
	PGMs >3µm ECD attached to gangue	8.9	4
	BMS >10µm ECD attached to gangue	-	0
Slow Floating 2	PGMs <3µm ECD attached to gangue	0.5	1
	BMS <10µm ECD attached to gangue	-	0
No Floating	PGMs and/or BMS locked in gangue	0.9	2
Total		**100.0**	**55**

The floatability index (FI) is a method based not only on the size of PGM and host particles, but also on their modes of occurrence. This index is used with the particle size to establish the predicted flotation response of the particles (McLaren *et al.*, 2003). The PGM grains and PGM-bearing particles are classified either as fast-floating, slow-floating 1, slow-floating 2 or no-floating, according to the listed particle characteristics. There is 59.8 (v/v) % of the fast floating PGM minerals with a grain size greater than 3µm Equivalent Circle Diameter (ECD) for the 36.9 mm

cyclone OF, while for the 76.0 mm cyclone the (v/v) % is 74. The slow floating particles can be recovered after a longer resident time. However, the flotation index does not take the surface hydrophobic state into account, which can be a strong function of: type and amount of collector, reaction of the mineral surface, oxidation tendency, pulp conditions (pH, E_h and temperature), grinding conditions, circuit design and contamination of products. The flotation index therefore assumes particles with the correct size and liberation properties should be recoverable, which is not always the case.

6.3.5. Flotation of the De-slimed Mimosa Ore at Different Depressant Dosages

Once the Mimosa ore was de-slimed, the cyclone UF material was sent for bench flotation tests to investigate possible improvement in the recoveries and reagent consumption since most of talc and other fines had been removed during de-sliming. The second and most important purpose of the flotation test was to investigate whether the depressant dosage could be lowered as a result of de-sliming. The results shown in Figures 6.15 and 6.16 were obtained after floating the de-slimed ore using various dosages of the depressant, starting from 300g/t to 500 g/t CMC. As has been explained in Chapter 5 Section 5.6, the flotation was performed at two and ten minute intervals.

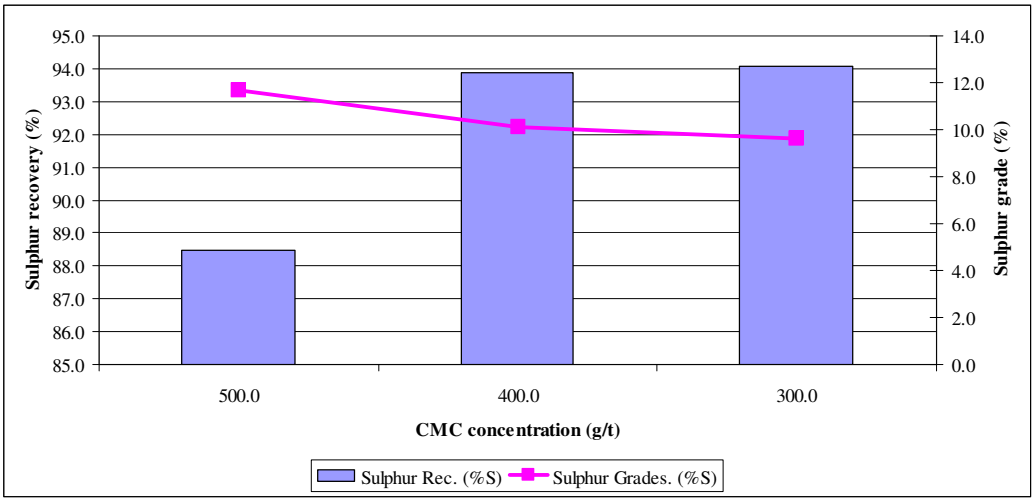

Figure 6.15: *Sulphur recovery and grade plots against depressant dosages for the 36.9 mm cyclone de-slimed ore.*

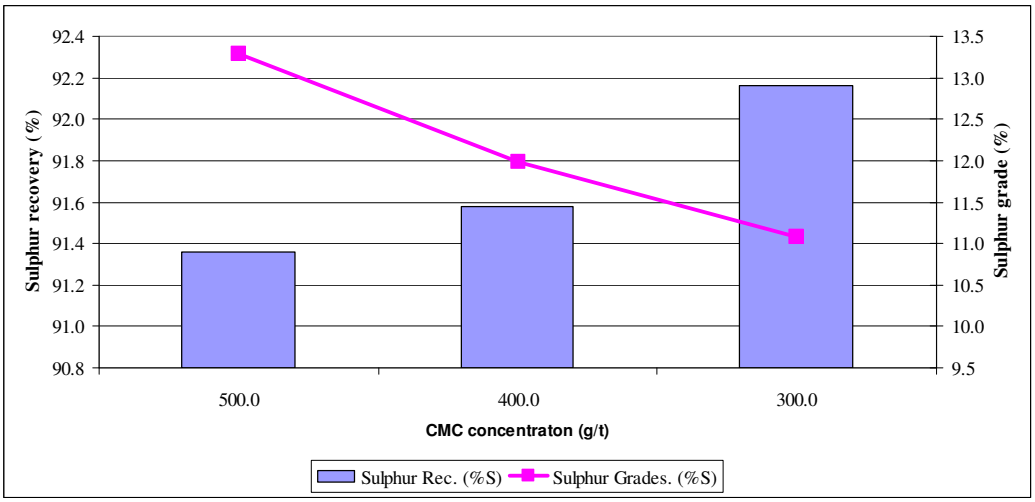

Figure 6.16: *Sulphur recovery and grade plots against depressant dosages for the 76 mm cyclone de-slimed ore.*

Both Figures 6.15 and 6.16 show that as soon as the flotation feed ore is de-slimed to remove talc it was possible to drop the dosage levels up to 300 g/t without significantly decreasing the final sulphur grade. The sulphur recovery increased to as high as 94%.

The decrease in dosage levels proves that the high doses of reagents at Mimosa were a result of adsorption by talc.

Figure 6.17 shows the cumulative sulphur grade (%) versus cumulative sulphur recovery (%) relationship, comparing the de-slimed flotation results with the standard collector suite as well as DTP (0.64 mol.) for the de-slimed ore. The flotation was carried at 300 g/t CMC depressant dosage.

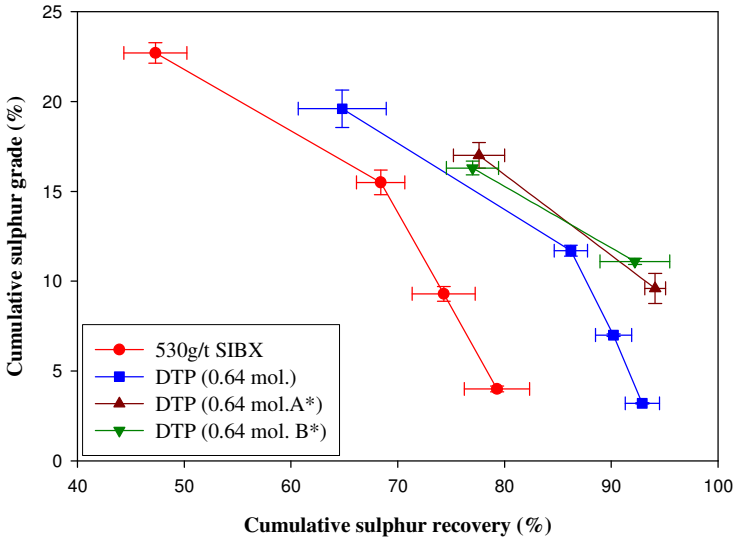

Figure 6.17: *Cumulative sulphur grades and recovery curves for the ore de-slimed with the 36.9 mm cyclone. A* = DTP (0.64 mol.) used for the ore de-slimed with 36.9 mm cyclone. B* = DTP (0.64 mol.) used for the ore de-slimed with 76 mm cyclone.*

The summary of results in Table 6.14 above shows that when the ore was de-slimed, the recoveries were improved by between 20.3 and 22.4% from about 72% when the standard SIBX was used on non-de-slimed ore. This translates to between 4 and 6% improvement of recoveries from that obtained when the DTP (0.64 mol.) is used on the non-de-slimed ore. The initial rates also improved from 23.7 min^{-1} to about 39 min^{-1}. Note that, unlike in the first part (Chapters 3 and 4) of this report, flotation results were only taken for 10 minute flotation periods, as opposed to 32 minute periods in the first part of this thesis (i.e. Chapters 3 and 4).

As has already been indicated in Tables 6.6 and 6.7, about 14.9% of sulphur is lost when 36.9 mm cyclone is used for de-sliming and 22.4% is lost when the 76 mm cyclone is used. It can therefore be concluded that the sulphur recovery improvement shown in Table 6.14 is offset by the sulphur lost during de-sliming. For example, when the ore was not de-slimed, with the SIBX being used as a collector, the recovery was 71.8% and when DTP (0.64 mol.) was used the recoveries improved to 88.5% with a slight drop of grades by 1% after ten minutes of flotation. The highest net improvement in sulphur recovery was realised when DTP (0.64 mol.) was used in non-de-slimed ore with just a slight decrease in grades of 1%. The initial rate change

for DTP (0.64 mol.) is not the highest when compared with DTP (0.64 mol. A*) and DTP (0.64 mol. B*), but it brings about an increase of 8.8 min^{-1} when compared with the standard collector (530 g/t SIBX).

Table 6.14: *Initial rate, final recovery and final grades for flotation of de-slimed and non-de-slimed ore.*

Collector	530 g/t SIBX	DTP (3)	DTP (3A*)	DTP (3B*)
Initial rate (min^{-1})	23.7	32.4	39.5	38.5
Final recovery (%) (After 10 min)	71.8	88.5	94.1	92.2
Final grades (%) (After 10 min)	13.0	12.0	9.6	11.1
Improvement (%) on recoveries	0.0	16.7	22.3	20.4
Loss due to de-sliming (%)	0.0	0.0	14.9	22.4
S non-recovered during flotation (%)	28.2	11.5	5.9	7.8
Total loss of S (%)	28.2	11.5	20.8	30.2
Net improvement in S (%) recovery	0.0	16.7	7.4	-2.0
Grade change (%)	0.0	-1.0	-3.4	-1.9
Initial rate change (min^{-1})	0.0	8.8	15.9	14.9

A = DTP (0.64 mol.) used for the ore de-slimed with 36.9 mm cyclone.*
B = DTP (0.64 mol.) used for the ore de-slimed with 76 mm cyclone.*

6.4. DISCUSSION OF THE RESULTS

The results given from Section 6.3.1 to 6.3.4 confirm three important aspects, as follows:

1) There are PGM grains that are lost to the cyclone OF during de-sliming (Section 6.3.1.).

2) The PGM grains lost to the cyclone OF hardly exceed 6 μm in size and are liberated (Section 6.3.2 and 6.3.4 respectively).

3) These PGM particles ought to be recovered during flotation since most of them are fast-floating, as defined by McLaren (2003) in Table 6.13. However, the definition of fast-floating by McLaren (2003) does take the surface hydrophobic state into account.

Electrochemical and contact angle measurements conducted by Vermaak and Pistorius (2005) showed that there is a strong interaction of the Pd-Bi-Te and $PtAs_2$ - which are the majority of the PGM minerals lost with the fines (see Table 6.10) - and the ethyl xanthate used as collector. Vermaak and Pistorius (2005) confirmed the co-presence of xanthate and dixanthogen on the surface of Pd-Bi-Te and $PtAs_2$, which is

an indication that these minerals are supposed to float in the presence of xanthate collector, but it is not happening. It is a well known fact that in many flotation circuits it is often difficult to recover minerals in the fine particles below 10 μm (Pease *et al.*, 2005). The key question to ask is why fine PGMs are difficult to recover? One of the bases of work performed by Vermaak and Pistorius (2005) was due to the very fact that previous mineralogical investigations performed on the effluent flotation streams of Mimosa Mine indicated appreciable amounts of PGMs that were not recoverable. Vermaak and Pistorius (2005) also found that over 70% of the PGMs were liberated and most belonged to the Pt-Pd-Bi-Te class. This discovery was similar to the results obtained in Sections 6.3.1 to 6.3.4.

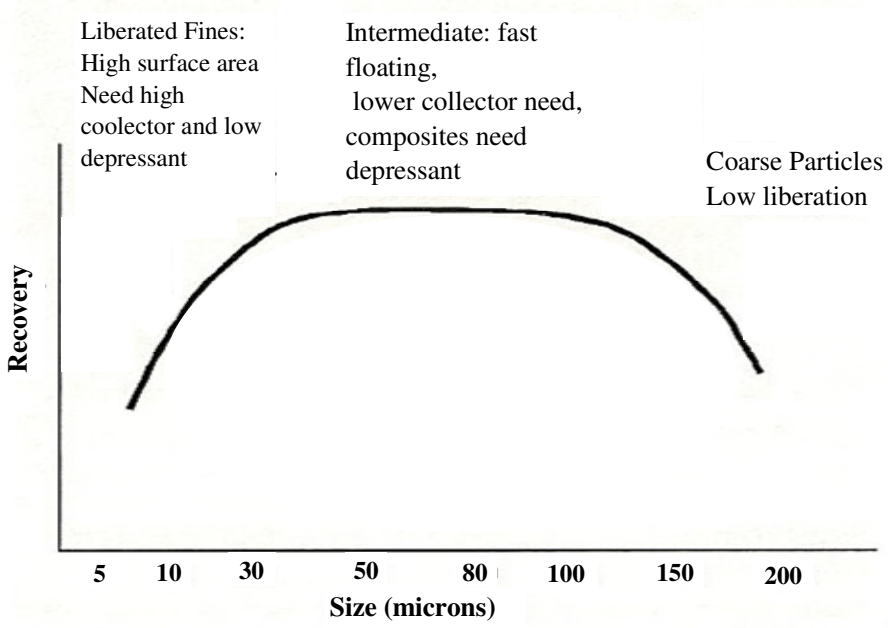

Figure 6.18: *Conventional view - 'fines don't float' (Pease et al., 2005).*

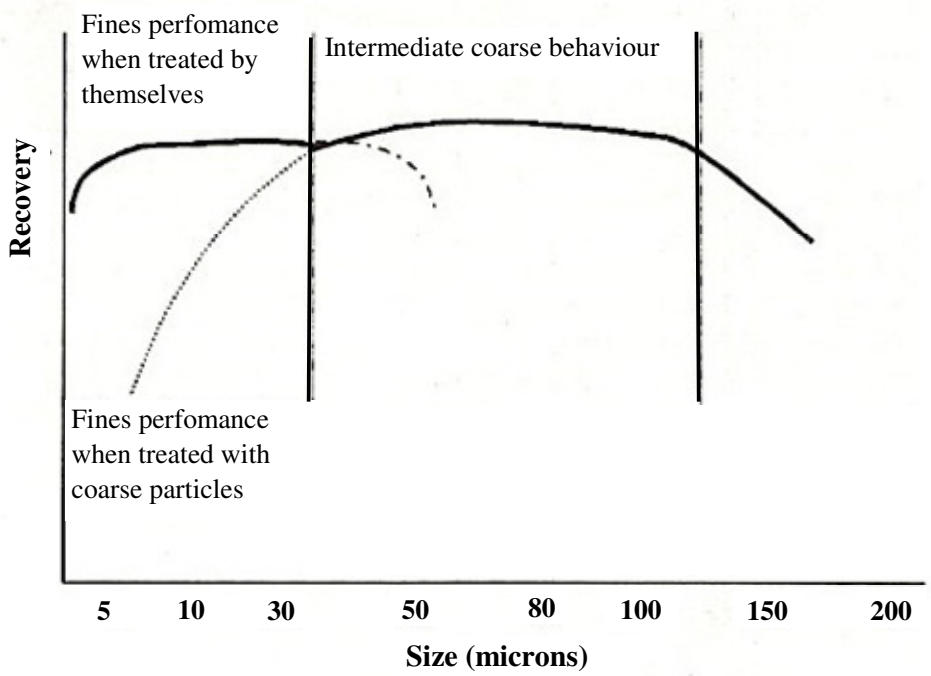

Figure 6.19: *Proposed conceptual staged grind-float circuit performance (Pease et al., 2005).*

Based on their investigations Vermaak and Pistorius (2005) concluded that small particle size (< 5 μm) is a probable cause for low recoveries of Pd-Bi-Te at platinum concentrators along the Great Dyke of Zimbabwe. This conclusion by Vermaak and Pistorius (2005) is confirmed by Pease et al. (2005), who were able to show that the reason fines do not float well in many circuits is because they are mixed with coarse particles (Figure 6.18). Figure 6.19 is a conceptual staged grind-float circuit performance proposed by Pease et al. (2005). Based on the work by Pease et al. (2005) it can therefore be concluded that given the wide particle size distribution of the milled Mimosa ore, the fine PGMs lost to the cyclone OF during de-sliming of talc would be difficult to recover in any case. De-sliming therefore provides an opportunity to separate the fine PGM (<10 μm) from the coarse particles (>10 μm) and treat them on their own. When this exercise is used with the Mimosa ore it must be borne in mind that the OF will consist mainly of talc. Therefore an innovative method of dealing with fines that are mixed with talc will have to be investigated. However, the latest research indicates the depression of PGMs in the presence of the base metal sulphides. It is believed that some of the oxidation products of the base metal sulphides can render these particles slow-floating (Vermaak *et al.*, 2007). It can

therefore be concluded that the PGM particles lost to the cyclone OF during de-sliming are likely to be lost by conventional flotation methods.

6.5. FLOTATION OF TALC USING A FROTHER PRIOR TO FLOTATION OF THE PGM

6.5.1. Introduction

Removing talc by de-sliming is an alternative method to other methods such as: (1) pre-flotation of talc prior to the flotation of the PGMs, (2) depression of talc (currently being used in most industrial operations) and (3) dispersion of talc in the water using a dispersant such as sodium silicate or sodium hexametaphosphate. The pre-flotation of talc was investigated in this chapter and this section provides a discussion of the results. The author believes that further thorough investigation will have to be conducted in order to make a meaningful contribution to this method of talc removal. For example, various frothers and other reagents that are more selective to talc might have to be developed or investigated. Therefore the author did a high level investigation of the talc pre-float. The aim of this investigation was therefore to determine whether removing talc by flotation prior to the flotation of the PGMs using the standard frother results in the loss of PMGs and, if it does, to what extent does it do so compared to de-sliming.

6.5.2. Mass and Chemical Balance of the Talc Concentrates

Table 6.15 gives the mass balance around the 8-litre flotation cell during rougher flotation. The experimental method for this section was detailed in Chapter 5 Section 5.7.

As has already been described by the experimental method, only the frother was used in order to float as pure a talc as possible.

Table 6.15: *The mass balance of the 8-litre cell for the talc rougher concentrate.*

	Feed (ore)	Rougher conc. (talc)	Tails
Dry solids (kg)	3.3	0.77	2.55
Sulphur mass (g)	0.020	0.003	0.017
PGE + Au (g/t) grade	3.56	2.75	3.80
PGE + Au (g)	0.0117	0.0021	0.0096

Table 6.16 shows the chemical qualities of the talc concentrate and the tails. Note that the tails in this case would be used as the feed to the PGM flotation cell and the talc concentrate would be discarded or subjected to further processing.

Table 6.16: *Chemical qualities of the talc concentrate and tails.*

	Rougher conc. (talc)	Tails
Sulphur Grade (%)	0.36	0.67
S recovery (wt %)	14.15	85.85
PGE + Au recovery (%)	18.1	82.5

Mass balance around the 2-litre cell is detailed in Table 6.17. Note that the feed material is the rougher talc concentrate from the 8-litre cell from above. The aim of this second stage flotation was to achieve as pure a talc as possible.

Table 6.17: *The mass balance of the 2-litre cell for talc cleaner concentrate.*

	Rougher talc conc. (Feed to 2-litre cell)	Cleaner Concentrate (talc)	Talc cleaner tails
Dry solids (kg)	0.825	0.459	0.367
Sulphur mass (g)	0.003	0.0010	0.0017
Total PGE + Au (g/t)	2.75	2.063	3.260
PGE + Au (g)	0.0021	0.0009	0.0012

Performing a simple mass balance, as shown in Table 6.15, indicates that a total of 14.15 wt% of sulphur was lost to the talc concentrate during the rougher flotation of talc. A total of about 18.1 wt % of PGE + Au reported to the talc rougher concentrate. When the rougher talc concentrate was subjected to further treatment, the talc cleaner

concentrate consisted of a total of 5 wt % sulphur and a total of 8.1 wt % PGE + Au (Table 6.10).

Table 6.18: *Summary of recoveries to the cleaner concentrate and loss to the tailings.*

	Cleaner Concentrate (talc)	Talc cleaner tails
Sulphur Grade (%)	0.2	0.47
Sulphur recovery (wt %)	5.0	8.75
PGE + Au recovery (%)	8.1	10.2

It is believed that the PGM was lost together with the BMS locked within the talc particles as indicated by the back-scattered electron image of the Mimosa talc concentrate shown earlier in Figure 6.2. It can therefore be concluded that pre-flotation of talc prior to the flotation of the PGMs seems to result in a lower loss of the PGE + Au compared to the de-sliming method. However, this method does require intensive investigation and further quantification of talc before a firm conclusion can be made.

CHAPTER SEVEN

CONCLUSION AND RECOMENDATION

7.1. COLLECTOR TESTS

Experiments on SIBX and SIBX mixture with TTCs or DTP dosages have led to the following conclusions:

- The optimum SIBX concentration of 530g/t agrees with that used by Mimosa. Grade recovery curves improved as the dosage of SIBX increased from 132.5 to 530 g/t. Rate and recovery increases were responsible.

- Addition of SIBX and $CuSO_4$ to the mill did not improve overall performance. Initial rates and final recoveries were similar. There were hints of increased final recovery, but in the early stages of flotation grade recovery relationship favoured direct addition to the flotation cell.

- Mixtures of iC_4 TTC with SIBX showed no significant improvement in flotation performance when compared to the standard.

- The C_{10} and C_{12} TTC mixtures with SIBX generally showed no significant metallurgical improvement with respect to final grades and recoveries. However, the 6.25 molar per cent substitution of SIBX by C_{12}TTC appeared to show some improvement on sulphur but not on PGE+Au recovery and grade.

- DTP mixed with the SIBX at 1:1.3 mole ratio at a total number of moles of 0.64 and 1.28 moles gave the best results in terms of sulphur and PGE +Au recoveries. The difference was well within the experimental error.

7.2. TALC DE-SLIMING

After de-sliming the Mimosa ore using a de-watering cyclone, the following conclusions were reached:

- One of the reasons the PGM recoveries are low at Mimosa Mine is because the particle size distribution is too wide, with the fine particles mixed with the coarse particles. Therefore de-sliming provides an opportunity to separate the fine PGM (<10 μm) from the coarse particles (>10 μm) and treat them on their own.

- De-sliming the ore helped to reduce the depressant up to 300 g/t as opposed to 530 g/t that was used as the standard dosage. Therefore the high doses of reagents at Mimosa probably result from surface adsorption of dixanthogen by talc. This is a non-ionic molecule with a high degree of hydrophobicity associated with it. Non-polar (hydrophobic bonding) between $(DTC)_2$ and non-polar talc basal planes can act as a sink of this collector molecule. The complexing character of divalent ions associated with gangue by thiol collector molecule could also reduce collector attachment to the base metal sulphide mineral.

7.3. RECOMMENDATION

- DTP mixed with the SIBX at 1:1.3 mole ratio at a total number of moles of 0.64 and C_{12} TTC should be tested at pilot plant levels to verify the results obtained in chapter 4.

- Since the objective of this thesis was to optimise the collector suite and remove the talc by de-sliming using hydro-cyclones, it is recommended that a detailed study that focuses solely on recovering fine PGMs in the talc slimes be conducted.

REFERENCES

Ackerman, P. K., Harris, G. H., Klimpel, R. R., and Aplan, P. P., 2000, *Use of xanthogen formats as collectors in the flotation of copper sulphides and pyrite.* International journal of mineral processing, Vol. 58, pp 1-13.

Aquarius Platinum Limited., 2002, *Aquarius projects*, Project- Mimosa Platinum Mine. http://www.aquariusplatinum.com/ProjectsDetail.asp?ID=mimosa.

Banford, A. W., Aktas, Z., and Woodburn, E. T., 1998, *Interpretation of the effect of froth structure on the performance of froth flotation using image analysis,* Powder Technology, vol. 98, pp. 61-73.

Beattie, D. A., Huynh, L., Kaggwa, B. N., and Ralston, J., 2005, *The effect of polysaccharides and, polyacrylamides on the depression of talc and the flotation of sulphide minerals*, Minerals engneering, vol. 19, pp. 598-608.

Bergmann, J., Kleeberg, R., Haase, A., Breidenstein, B., 2000, Advanced fundamental parameter model for improved profile analysis. Mat. Sci. Forum, Vols. 347-349(2) pp. 303-308.

Belzile, N., Chen, Y. W., Cai, M. F. and Li, Y. 2004, *A review on pyrrhotite oxidation,* Journal of geochemical exploration, vol 84, pp 65-76.

Berry, L. G., Mason, B., Dietrich, R. V., 1983, *Mineralogy*, concepts description determinations, 2nd Edition, Printed in theUnited States of America, San Francisco, W.H. Freeman and Company, February.

Bozkurt, V., Xu, Z., and Finch, J. A., 1990, *Effect of depressants on xanthate adsorption on Pentlandite and pyrrhotite: Single vs. mixed minerals*, Canadian metallurgical quarterly, vol. 38, Issue 2, pp. 105-112.

Bozkurt, V., Xu, Z., and Finch, J. A., 1998a, *Pentlandite/Pyrrhotite Interaction.* Xanthate Adsorption in Presence of Ni Ions, Processing of Complex Ores, Met Soc. CIM, Sudbury, vol. 52, pp. 101-114.

Bozkurt, V., Xu, Z., and Finch, J. A., 1998b, *Pentlandite/pyrrhotite interaction and xanthate adsorption*, international journal of mineral processing, vol. 52, No. 4, pp. 203-214.

Bozkurt, V., Xu, Z., and Finch, J. A., 1998c, *Xanthate adsorption on pentlandite and pyrrhotite: effect of mineral interactions, Innovations in Mineral and Coal Processing*, Proc. 7th international mineral processing symposium, Eds. S. Atak G. Önal and M.S. Çelik, Istanbul, Turkey, pp. 93-98, September 15-17.

Bradshaw, D. J., Buswell, A. M., Harris, P. J., Ekmekci, Z., 2005a, *Interactive effect of the type of milling media and copper sulphate addition on the flotation performance of sulphide minerals from Merensky ore Part I*: Pulp chemistry. International journal of mineral processing, vol. 78, pp. 164-174, December.

Bradshaw, D. J., and O'Connor, C. T., 1996, *Measurements of sub-process of bubble loading in flotation*, Mineral engineering, vol. 9, pp. 443-448.

Breytenbach, W., Vermaak, M. K. G., and Davidtz, J. C., 2003, *Synergistic effects among dithiocarbonates (DTC)*, Dithiophosphate (DTP) and trithiocorbonate (ttc) in the flotation of Merensky ores, South African institute of mining and metallurgy, December.

Bryson, M., 2006, Mintek, South Africa, Personal communication.

Bühmann, D., 1998, *The phyllosilicates of clays and their X-ray identification,* The mineralogical association of South Africa, Clay workshop.

Buswell, A. M., and Nicol, M. J., 2002, *Some aspect of the electrochemistry of the flotation of pyrrhotite,* Journal of applied electrochemistry, vol. 32, pp.1321-1329.

Chen, G., Grano, S., Sobieraj, S., and Ralston, J., 1999, *The effect of high intensity conditioning on the flotation of a nickel ore part1: Size by size analysis,* Minerals engineering, vol. 12 pp 1185-1200.

Cilliers, J. J., Neethling, S. J., 2002, *The entrainment of gangue into a flotation froth*, International journal of mineral processing, vol. 64, pp. 123-1134, July 2.

Cilliers, J. J., Wang, M., and Neethliing, S. J., 1999, *Measuring flowing foam density distributions using ERT,* 1st World congress on industrial process topography, Buxton, Menchester, pp. 108-112.

Coetzer, G., and Davidtz, J. C., 1989, *Sulphydryl collectors in bulk and selective flotation Part 1. Covalent trithiocarbonate derivatives*, Journal of South Africa institute of mining and metallurgy, vol. 89, pp. 307-311.

Cramer, L.A., 2001, *The extractive metallurgy of south africa's platinum ores*, Platinum group metals, Overview JOM, pp. 14-18, October.

Crosbie, R., Robertson, C., Smit I., and Ser, V., 2005, *The benefits of inter-particle comminution on flotation* Anglo American research laboratory, Crown Mines Johannesburg.

Dai, Z, Fornasiero, D., and Ralston, J., 1999, *Particle–bubble attachment in mineral flotation,* Journal of colloid and science, vol. 217, pp 70-76.

Davidtz, J. C., 1998, *Design of molecules of specific to base mineral recovery in typical PGM containing ores,* 8th International platinum symposium, Rustenburg 28 June-3 July 1998.

Davidtz, J. C., 2003, Personal Communication

Davidtz, J. C., 2005, Personal Communication

Davidtz, J. C., 2007, Personal Communication

De Lucas, A., Rodrigues, L., Lobato., J. and Sanchez, P., 2002, *Synthesis of crystalline δ-$Na_2Si_2O_5$ from sodium silicates solution for use as a builder in detergents,* Chemical engineering science, vol. 57, Issue 3, pp. 479-486, February.

Drake, J. E., and Yang J., 1993, *Synthesis and Spectroscopic characterization of s-ethyl, s-isopropyl s-n-propyl, and s-n-butyl trithiocarbonate(trixanthate) derivatives of try methyl- and triphenylgermane and diphenylgermane, Crystal Structure of $Ph_2Ge[S_2CS(u\text{-}Pr)]_2$.* Department of Chemistry and Biochemistry, University of Windsor, Windsor, Ontario, Canada N9B 3P4. Received June 16.

Du Plessis, R., Davidtz, J. C., and Miller, J., 1999, *Preliminary examination of the electrochemical and spectroscopic features of trithiocarbonate collectors for sulphide mineral flotation,* Proceeding of an international workshop on electrochemistry of flotation of sulphide minerals.

Du Plessis, R., Miller, J. D., and Davidtz, J. C., 2003, *Thiocarbonate collectors in pyrite flotation fundamentals and applications,* Accepted for presentation: XXII International mineral processing congress, Cape Town South Africa.

Ebbing, D. D., 1993, *General Chemistry*, Fouth eddition, By Houghton Miffin Company.

Ekmekci, Z., Bradshaw, D. J., Harris, P. J., Buswell, A. M., 2006, *Interactive effect the type of milling media and $CuSO_4$ addition on the flotation performance of sulphide minerals from Merensky ore part II: Froth stabilty,* International journal of mineral processing, vol. 78 pp164-174.

Feng, D., and Aldrich, C., 2004, *Effect of ultrasonication on the flotation of talc*, Industrial engineering chemistry research vol. 43, pp. 4422-4427.

Feng, Q. M., Liu, G. S., Yu, Z. J., Lu, Y. P., Ou, L. M., Andzhang, G. F., 2006, *Influence of mechanism of ferric and ferrous ions on flotation of talc,* Zhongan daxue xuebao (Ziran kexue ban), Journal of central south university (science and technology), vol. 37, pp. 476-480.

Flintoff, B. C., Plitt. L. R., Turak, A. A., 1987, *Cyclone modelling: a review of present technology,* Modelling technology. CIM Bulletin, September.

Fornasiero, D., Montalti, M., and Ralston, J., 1995, *Kinetics of adsorption ethyl xanthate on pyrrhotitie: in situ uv and infrared spectroscopic studies,* Journal of colloid and interface science, vol. 172 pp 467-478.

Fornasiero, D., and Ralston, J., 2004, *Cu (ii) and Ni (ii) activation in the flotation of quarty lizardite and chlorite,* International Journal of Mineral Processing, vol. 76, pp 75-81.

Forrest, K., Yan, D., and Dunne, R., 2000, *Optimisation of gold recovery by selective gold flotation for copper–gold–pyrite ores,* Minerals engineering, vol. 14 pp227-241.

Fuerstenau, M. C., 1982, *Chemistry of collectors in solutions*, Principles of flotation. South African institute of mining and metallurgy, Monograph series no. 3. pp 1-16.

Fuerstenau, M. C., Kuhn, M. C., and Eligillani, D. A., 1968, *The role of dixanthogen in xanthate flotation of pyrite*, AIME, Trans. SME, 241, 148-156.

Fuerstenau, M. C., Valdivieso, A. L., and Fuerstenau, D. W., 1988, *Role of hydrolysed cations in the natural hydrophobicty of talc,* International journal of mineral processing, vol. 23, pp. 161-170.

Goncalves, K. L. C., Andrade, V. L. L., and Peres, A. E. C., 2003, *The effect of grinding conditions on the flotation of a sulphide copper ore*, Minerals engineering, vol. 16, pp. 1213-1216(4).

Guongming, L., and Hongen, Z., 1985, *The chemical principles of flotation, activation and depression of arsenopyrite,* Processing of complex ores, The department of mineral engineering, Northeast university of technology, Shengang, lidoning, Peoples Repulic of China.

Harris, P. J., 1982, *Frothing phenomena and frothers in principles of flotation*, SAIMM, Johannesburg, chapter 13, pp. 237-250.

Implats, 2004, Annual Report, *Impala Platinum Holdings Limited (http://webmineral.com/determin.shtml)*

Jenskins, P., and Ralston, J., 1998, *The adsorption of polysaccharides at the talc-aqueous solution, Colloids and surfaces A*: Physical and engineering aspects, vol. 139, Issue 1, pp. 27-40.

Kelebek, S., 1987, *Wetting behaviour polar characteristics and flotation of inherently hydrophobic minerals,* Mineral processing and extractive metallurgy, vol. 96, pp. c103-c107.

Kelebek, S., Yoruk, S., and Smith, G. W., 2001, *Wetting behaviour of molybdenite and talc in lignosulphonate/MIBC solutions and their separation by flotation,* Separation science and technology vol. 36(2), pp 145-157.

Kelly, E.G., and Spottiswood, D. J, 1989, *Introduction to Mineral Processing*.

Kelsall, D F, 1953, *A further study of the hydraulic cyclone,* Chemical engineering science, vol. 2, pp. 254-272.

Khraisheh, M., Holland, C., Creany, C., Harrs, P., and Parolis, L., 2005, *Effect of molecular weight and concentration on the adsorption of cmc onto talc at different strengths,* International journal of mineral processing, vol. 75, pp 197-206.

Klassen, V. I., and Mokrousov, V. A., 1963, *An Introduction to the Theory of Flotation*. English translation by J. Leja and G. W. Poling. Butterworths, London. 1963.

Kleeberg, R., Bergmann, J., 1998, *Quantitative Röntgenphasenanalyse mit den Rietveldprogrammen BGMN und AUTOQUANT in der täglichen Laborpraxis*. Ber. DTTG Greifswald 6: 237-250.

Kleeberg, R., and Bergmann, J., 2002, Quantitative *Phase Analysis Using The Rietveld Method and a Fundamental Parameter Approach*, In: S.P. SenGupta & P. Chatterjee (Eds.) Powder Diffraction. Proc. II Int. School on Powder Diffraction, IACS, Kolkata, Allied Publishers Ltd, 63-76.

Klimpel, R. R., 1980, *Selection of chemical reagents for flotation*, in Mular, A. and Bhappu, R. (Eds), Mineral processing plant design, 2nd Eddition, AIME, NY, pp. 907-934.

Klimpel, R. R., 1984, *Froth Flotation: The Kinetic Approach,* Proceedings of the international conference on Mineral Science and Technology, Sandton, South Africa, vol. 1, pp 385-392.

Klimpel, R. R., 1994, *A discussion of traditional and new reagent chemistries for the flotation of sulphide minerals* [A] in Mulukutla P S ed. Reagents for better Metallurgy [C] 59-66.

Kusaka, E., Amano, N., and Nakahiro. Y., 1997, *Effect of hydrolysed aluminium (iii) and chromium (iii) cation on the lipophilicityof talc,* International journal of mineral processing, vol. 50, pp. 243-253.

Kursun, H., and Ulusoy, U., 2006, *Influence of shape characteristics of mineral on the column flotation behaviour,* International journal of mineral processing, vol. 78 pp 262-268.

Laskowski, J. S., 2003, *Fundamental properties of flotation frothers,* Proceedings of the 22nd international mineral processing congress, Cape Town, South Africa.

Leja, J., 1982, *Surface Chemistry of Froth Flotation,* New York, A division of plenum publishing corporation, Plenum Press.

Liu, G., Feng, Q., Ou, L., Lu, Y., and Zhang, G., 2005, *Adsorption of polysacxharide onto talc*, Mineral engineering, vol. 19, pp 147-153.

Liu, G., Feng, Q., Ou, L., Lu, Y., and Zhang, G., 2005, *Influence and mechanism of copper ions and nickel ions on flotation of talc,* Kuei Suan Jen Hsueh Pao/ Journal of Chinese ceramic society, vol. 33, pp. 1018-1022.

Longwider, G., 2002, Lonmin Platinum, *PGE Mineralogy/ Metallurgy*, Information from plant visit.

Loubser M, 2007, Personal Communication.

Luzenac, Talc for the World, http://www.luzenac.com/geology.html

Magwai, K. M., and Bosman, J., 2007, *Fundamentals on the spigot capacity of dense medium cyclones*, Minerals engineering, Department of Material Science and Metallurgical Engineering, University of Pretria, Gauteng, 0002, South Africa.

Makanza, A. T., 2005, *Flotation of auriferous pyrite using a mixture of collectors* Submitted In Partial Fulfilment of The Requirements for the Degree in Masters of Metallurgical Engineering. Faculty of Engineering, Build Environment and Information Technology, University Of Pretoria, South Africa.

Marais, P., Mugoshi, J., Escorcio, P. A., Valenta, M. M., 1992, *Mimosa Mine Platinum project*, vol. 1, January.

Mathur, S., Singh, P., and Mondgil, B.M., 2000, *Advances in selective flocculation technology for solid- solid separations*, International journal of mineral processing, vol. 58, Issue 1-4, pp. 201-222, February.

McHardy, J., and Salman, T., 1974, *Some aspects of the surface chemistry of talc flotation,* Both of the department of mining and metallurgical engineeing, McGill University, Montreal, Quebec, Canada.

Michot, L J., Villieras, F., Francois, M., Le Dred, R., Yvon, J., and Cases, J M., 1994, *The structural microscopic hydrophilicity of talc,* Langmuir, vol. 10 pp. 3765-3773.

McLaren, C. H., Bushell, C. L., Duarte, V. H. M., Duarte, J. C., Clark, W., Kleyenstüber, A. S. E., and Mazhakata, J., 2003, *Mineralogical Inverstigation of the Platinum-Group Minerals in Flotation products from Mimosa Platinum Mine*, Mintek, Specialist in mineral and metallurgical technology, Communication, April.

McNeil, M. Rao, S. R., and Finch J. A., 1994, *Oxidation of Amyl Xanthate by Pentlandite*, Can. Met. Quart. 33 (2), pp. 165-167.

Mieleczarski, J., and Yoon, R. H., *Orientation of thiol collectors on chalcocite*, Department of mining and minerals engineering, Virginia polytechnic institute and state university Blackburg.

Miller, J D, Li, J., Davidtz, J C, and Vos, F 2005 *A Review Of Pyrrhotite Flotation Chemistry In The Processing Of PGM Ores,* Mineral Processing, vol. 18, pp. 855-865.

Moore, D. M., and Reynolds, R. C. J., 1989, *X-Ray Diffraction and the Identification of Clay Minerals*, Oxford New York, Oxford University Press (Inc.)

Morris, G. E., Fornasiero, D., and Ralston, J., 2002, *Polymer depressant at the talc–water interface: adsorption isotherm, microflotation and electrokinetic studies,* International journal of mineral processing, pp. 1-17. April, 30.

Nagaraj, D. R., Basilio, C., and Yoon, R. H., 1987, *The chemistry and structure –activity relationships for new sulphide collectors*; Processing of Complex Ores; pp 157-166, 20-24 August.

Neesse, T., Schneider, M., Dueck, J., Donhauser, F., Regler, J., and Tiefel, H., 2003, *Computer controlled hydro-cyclone battery with maximum solids recovery,* Proceedings: XXII international Mineral Processing Congress, pp. 1552-1560.

Neethling, S. J., and Cilliers, J. J., 2004, *The entrainment of gangue into a flotation froth,* International journal of mineral processing, vol. 64, pp. 123-134.

Nemecz, E., 1981, *Clay Minerals*, Member of Hungarian Academy of Sciences. Budapest, Akadémiai Kiadó.

Norwitz, G., and Gordon, H., 1979, *Improved scheme for analysis of high-purity talc,* Talanta, vol. 24, pp159-162.

Oberthür, T., 2002a, *Platinum-Group element mineralization of the Grate Dyke, Zimbabwe*. Federal Institute for Geosciences and Natural Resources (BGR) Hannover, Germany, pp. 483-506.

Oberthür, T., Davis, D. W., Blenkinsop, T. G., and Höhn-Dorf, A., 2002b, *Precise U-Pb mineral ages, Rb-Sr and Sm-Nd systematic for The Great Dyke, Zimbabwe* – constraints on late Archean events in the Zimbabwe Craton and Limpopo Belt. Precambrian research, 113, pp. 293-305.

Oberthür, T., Melcher, F., Weiser T. W. and Gast, L., 2002c, *Distribution of PGE and PGM in oxidized ores of the Main Sulphide Zone of the Great Dyke,* Zimbabwe, Proceedings: 9th International Platinum Symposium, Billings, Montana, USA, 21-25 July.

Oberthür, T., Thorolf, W., Weiser, and Kojonen, K., 2002d, *Local Variations and Trends in PGE Geochemistry and Mineralogy in the Main Sulphide Zone of the Great Dyke,* Zimbabwe, Proceedings: 9th International Platinum Symposium, Billings, Montana, USA, 21-25 July.

Oberthür, T., Weiser, T. W., and Gast, L., 1999, *Mobility of PGE and PGM in the supergene environment at the Hartley Mine, Great Dyke, Zimbabwe- A case study. In* Mineral Deposit: Processes to Processing, pp.763-766.

Oberthür, T., Weiser, T.W., Muller, P., Lodziak, J., Klosa, D., and Cabri, L. J., 1998b, *New Observation on the distribution of the Platinum Group Element (PGE) and Platinum Group Minerals (PGM) in the MSZ at Hartley, Great Dyke, Zimbabwe*, In 8th International Platinum Symposium, South African South African Institute of Mining and Metallurgy, Symposium Series S18, pp. 293-296.

Oberthür, T., Weiser, T.W., Thorolf W., Gast, L., Lodziak, J., Klosa, D., and Wittich, C., 1998a. *Detrital platinum group minerals in rivers along the Great Dyke, and in the Somabula Gravels,* In 8th International Platinum Symposium. South African Institute of Mining and Metallurgy, Symposium Series S18, pp. 289-292.

O'Connor, C. T., Bradshaw, D. J., and Upton, A. E., 1990, *The uses of dithiophosphates and dithiocarbonates for the flotation of arsenopyrite,* Minerals engineering, vol. 3, No 5, pp.447-459.

O'Connor, C.T., Dunne, R. C., and Botelho de Souse, A. M. R., 1984, *The effect of temperature on the flotation of pyrite,* Journal of South African Institute of Mining and. Metallurgy, vol. 84, pp. 389-394.

O'Connor, C. T., and Van Zyl, A., 1985, *The separation of kerogen from pyrophyllite by flotation*. Journal of South African Institute of Mining and. Metallurgy, vol. 85, pp. 357-360.

Parekh, B. K., and Miller, J. D., 1999, *Advances in Flotation Technology,* Printed in the United States of America, Society for Mining, Metallurgy, and Exploration, Inc.

Pease, J. D., Curry, D. C., and Young, M. F., 2005, *Designing flotation circuit for high fines recovery*, Centenary of flotation symposium, Brisbane, QLD. June, 6-9.

Penberthy, C. J., 1999, *Mineralogical and chemical evaluation of Mimosa floatation feed, concentrate and tailings sample*, Mintek, November.

Perdikatsis, B., and Burzlaff, H., 1981, *Strukturverfeinerung am talc* $Mg_3[(OH)_2Si_4O_{10}$. Zeitschrift fur Kristallographie, vol. 156, pp 177-186.

Plitt L. R., 1971, *The Analysis o solid-solid separations in Classifiers.* CIM Bulletin. April.

Prendergast, M. D., 1990, *Platinum-group minerals and hydrosilicate'alteration' in Wedza-Mimosa platinum deposit, Great-Dyke,* Zimbabwe, Genetic and metallurgical implication, pp. B91-B105, May-August.

Prendergast, M. D., 1988, *The geology and economic potential of the PGE-rich Main Sulphide Zone of the Great Dyke,* Zimbabwe. In Geo-platinum 87, pp. 281-302.

Prestidge, C. A., Ralston, J., 1994, *Contact angle studies of galena particles,* Journal of colloid and interface science, vol. 172, pp. 302-310.

Pugh, P. J., 1988a, *Macromolecular Organic Depressants In Sulphide Flotation* –A Review 1: Principles, types and applications, International journal of mineral processing, vol. 25, pp.101-130.

Pugh, P. J., 1988b, *Macromolecular organic depressants in sulphide flotation* –A Review 2: Principles*, Theoretical analysis of the forces involved in the depressant action,* International journal of mineral processing, vol. 25, pp.131-146.

Rao, S.R., 1985, *Xanthates and related compounds*, Marcel Deckker, New York,

1971, p. 504.

Ross, V. E., 1991, *The behaviour of particles in flotation froths,* Minerals engineering, vol. 4, No. 7-11, pp. 959-974.

Slabbert, W., 1985, *The role of trithiocarbonates and thiols on the flotation of some selected South African sulphide ores.* MSc. Dissertation, Potchefstroom University, South Africa.

Smart, S. St. C., 1991, *Surface layers in base metal sulphide flotation*, Minerals engineering, vol. 4, Nos. 7-11, pp. 891-909.

Steenberg, E., and Harris, P. J., 1984, *Adsorption of carboxymethylcellulose guar gum, and starch onto sulphides, oxides and salt-type minerals,* South African journal of chemistry, vol. vol. 37, No. 3, pp. 85-90.

Styn, J. J., 1996, *The role of collector functional groups in the flotation activity of Merensky Reef sample*, Dissertation.

Sutherland, K. L., and Wark, I. W., 1955, *Principles of flotation*, Melbourne: Australian institute of mining and metallurgy (Inc.).

Szymula, M., and Szczypa, J., *Investigation on mechanism of sorption and aggregation properties of long –chained thior collectors in application to polymineral copper ores*, Depertment of radiochemistry,maria curie-sklodowska university,20-031 lublin poland

Teague, A. J., Swaminathan, C., and Van Deventer, J. S. J., 1998, *The behaviour of gold bearing minerals during froth flotation as determined by diagnostic leaching,* Minerals engineering, vol. 6, pp. 523-533.

Teague, A. J., Van Deventer, J. S. J., and Swaminathan, C., 1999, *The effect of copper activation on the behaviour of free and refractory gold during froth flotation,* International Journal of Mineral Processing, vol. 59, pp. 113-130.

Teague, A. J. Van Deventer, J. S. J., and Swaminathan, C 1999 *The effect of galvanic interaction on the behaviour of free and refractory gold during froth flotation* International journal of mineral processing, vol. 57, pp. 243-263.

Thang, S. H., Chong, Y. K., Mayadunne, R. Y. A., Moad, G., and Rizzardo, E., 1999, *A novel synthesis of functional dihioesters, dithiocarbamates, xanthates and trithiocarbonates,* Tetrahedron letters, vol. 40, pp. 2435-2438.

Tjus, K., and Pugh, R. J., 1989, *Depressant action of low molecular weight non- ionic surfactants on talc,* Processing of complex ores, Proceedings of international symposium on proceedings of complex ores: Halifax, Canada, 20-24 August.

Van Runsburg, A. R. J., 1987, *A quantitative evaluation of sulphydral in noble metal recovery,* Masters of engineering dissertation, University of Potchefstroom, South Africa.

Venter J.A. and Vermaak, M. K. G., 2007, *Dithiocarbonate and trithiocarbonate interactions with pyrite,* South African Journal of Science, vol 103, pp 164-168.

Vermaak, M. K. G., Miller, J. D., and Lee, J., 2007, *Electrochemical interactions of industrially important platinum-containing minerals*, Minerals Engineering, In press.

Vermaak, M. K. G., and Pistorius, P. C., 2005, *Fundamental of the flotation behaviour of balladium bismuth tellurides,* Thesis Submitted in partial fulfilment of the requirement for the degree Philosophiae Doctor (Metallurgical Engineering), In the faculty of Engineering, built Environment and information Technology, University of Pretoria.

Verryn, S., 2006, Personal Communication.

Verryn, S., 2003, *Introduction to x-ray powder diffraction,* presented by the XRD and XRF Laboratory, Department of Earth Sciences, University of Pretoria, November.

Vos, C. F., 2006, *The role of long-chain trithiocarbonates in the optimisation of impala platinum's flotation circuit.* Submitted in partial fulfilment of the requirements for the degree in masters of metallurgical engineering, Faculty of engineering, build environment and information technology, University of Pretoria, South Africa.

Wang, X., and Forssberg A., 1989, *Study of the natural and induced hydrophobicity of some sulphide minerals by collectorless flotation,* Processing of complex ores, Proceedings of international symposium on proceedings of complex ores: Halifax, Canada, 20-24 August.

Wiese, J., Harris, P., and Bradshaw, D., 2005, *Investigation of the role and interactions of a dithiophosphate collector in the flotation of sulphides from the Merensky reef*, Minerals engineering, vol. 18, pp 791-800.

Walker, G. W., Walters, C. P., and Richardson, P. E., 1986, *Hydrophobic effects of sulphur and xanthate on metal and mineral surfaces,* International journal of mineral processing, vol. 18, pp. 119-137.

Wills, B. A., 1997, *Mineral processing technology*, An Introduction To The Practical Aspects of Ore Treatment And Mineral Recovery, 6th Edition, Linacre House, Jordan Hill, Oxford OX28DP 225 Wildwood Avenue, Woburn, MA 01801-2041, A division of Reed Educational and Professional Publishing Ltd, Butterworth- Heinemann.

Wilson, M. J., 1994, *Clay mineralogy: spectroscopic and determinative methods*, 2-6 Boundary Row, London SE1 8HN, UK, Chapman and Hall.

Ulusoy, U., and Yekeler, M., 2004, *Correlation of surface roughness of some industrial minerals with their wettability parameters,* Chemical engineering and processing, vol. 44, pp. 557-565.

Uribe-Salas, A., Martinez-Cavazos, T. E., Nava-Alonso, F. C., Mendez-Nonell, J., and Lara-Valenzuela, C., 2000, *Metallurgical improvement of a lead/copper flotation stage by pulp potential control,* International journal of mineral processing, vol. 59, pp. 69-83.

Yan, D., and Dunne, R., 2002, *The effect of ore type on the selective flotation of chalcopyrite and pyrite,* Minerals engineering conference, 25th September.

Yehia, A., and Al-Wakeel, M. I., 1999, *Technical note talc separation from talc-carbonate ore to be suitable for different industrial applications*, Central Metallurgical R & D Institute, September 9.

Yoon, R. H., Basilio, C. I., Marticorena, M. A., Kerr, A. N., and Crawley, R. S., 1995, *A study of the pyrrhotite depression mechanism by diethyenetriamine,* Minerals engineering, vol. 8 pp. 807-816.

Yoshida, H., Norimoto, U., and Fukui, K., 2006, *Effect of blade rotation on particle classification performance of hydro-cyclones*, Powder technology, vol. 164, pp. 103-110.

Yoshida, H., Takashina, T., Fukui, K., and Iwananga, T., 2004, *Effect of inlet shape and slurry temperature on the classification performance of hydro-cyclones*. Powder technology, vol. 140, pp. 1-9.

Zbik, M., and Smart, R. St. C., 2005, *Influence of dry grinding on talc and kaolinite morphology: Inhibition of nano-bubble formation and improved dispersion*, Minerals engineering, vol. 18, pp.969-976.

Zbik, M., and Smart, R. S. C., 2002, *Dispersion of kaolinite and talc in aqueous solution: nano-morphology and nano- bubble entrapment,* Ian Wark Institute, University of South Australia, Minerals Engineering, vol. 15 , pp. 277-286.

APPENDICES

Type of collector used: 132.5 g/t SiBX

	Time (min)	Samples A	Samples B	Samples C	Average (grams)	Std error (grams)
Head mass(g)		3300.0	3300.0	3300.0	3300	0.00
Head sulphur %		0.6	0.6	0.6	0.6	0.01
Mass of S		21.4	21.4	21.0	21.3	0.25
Wet conc.(g)	2	73.4	77.3	74.7	75.1	1.99
	7	264.1	260.2	258.9	261.1	2.71
	17	495.4	493.7	488.2	492.4	3.76
	32	849.0	843.9	853.2	848.7	4.66
Dry conc. mass (g)	2	23.2	21.5	20.2	21.6	1.50
	7	41.0	41.3	40.3	40.9	0.51
	17	57.5	59.0	55.9	57.5	1.55
	32	217.9	214.9	219.8	217.5	2.47
Cum. mass pull (g)	2	23.2	21.5	20.2	21.6	1.50
	7	64.2	62.8	60.5	62.5	1.87
	17	121.7	121.8	116.4	120.0	3.09
	32	339.6	336.7	336.2	337.5	1.84
Cum. mass pull %	2	0.7	0.7	0.6	0.7	0.05
	7	1.9	1.9	1.8	1.9	0.06
	17	3.7	3.7	3.5	3.6	0.09
	32	10.3	10.2	10.2	10.2	0.06
Cum H_2O rec (g)	2	50.2	55.8	54.5	53.5	2.93
	7	273.3	274.7	273.1	273.7	0.87
	17	711.2	709.4	705.4	708.7	2.97
	32	1342.3	1338.4	1338.8	1339.8	2.15
Total						
H_2O recovery %	2	0.8	0.9	0.8	0.8	0.04
	7	4.2	4.2	4.2	4.2	0.01
	17	10.8	10.8	10.8	10.8	0.05
	32	20.5	20.4	20.4	20.4	0.03
Sulphur %	2	24.4	27.3	25.4	25.7	1.48
	7	13.1	16.1	17.2	15.4	2.14
	17	4.0	4.4	4.0	4.2	0.22
	32	0.6	0.6	0.7	0.7	0.03
Total						
Mass of S (g)	2	5.7	5.9	5.1	5.6	0.38
	7	5.4	6.6	6.9	6.3	0.84
	17	2.3	2.6	2.3	2.4	0.19
	32	1.4	1.4	1.5	1.4	0.07
		14.7				
Cum S grade %	2	24.4	27.3	25.4	25.7	1.48
	7	17.2	19.9	20.0	19.0	1.60
	17	11.0	12.4	12.3	11.9	0.81
	32	4.3	4.9	4.7	4.6	0.29
Cum. S rec. %	2	26.4	27.4	24.5	26.1	1.49
	7	51.5	58.4	57.5	55.8	3.76
	17	62.3	70.5	68.3	67.0	4.26
	32	68.7	77.0	75.4	73.7	4.38
Tails: mass (g)		3002.4	2961.4	2965.9	2976.6	22.49
Tails: sulphur %		0.1	0.2	0.1	0.1	0.01
Tails: mass of S (g)		4.0	4.8	4.3	4.4	0.39

Type of collector used: 265 g/t SiBX

	Time (min)	Samples A	B	C	Average (grams)	Std error (grams)
Head mass(g)		3300	3300	3300	3300	0.00
Head sulphur %		0.6	0.6	0.6	0.6	0.01
Mass of S		20.0	20.4	20.4	20.3	0.21
Wet conc.(g)	2	84.2	83.2	81.2	82.9	1.53
	7	330.0	329.4	328.2	329.2	0.92
	17	574.4	575.4	576.0	575.3	0.81
	32	597.6	603.2	610.9	603.9	6.68
Dry conc. mass (g)	2	20.8	22.8	23.2	22.3	1.29
	7	45.5	45.2	45.6	45.4	0.21
	17	65.2	60.6	59.0	61.6	3.22
	32	238.2	240.3	241.5	240.0	1.67
Cum. mass pull (g)	2	20.8	22.8	23.2	22.3	1.29
	7	66.3	68.0	68.8	67.7	1.28
	17	131.5	128.6	127.8	129.3	1.95
	32	369.7	368.9	369.3	369.3	0.40
Cum. mass pull %	2	0.6	0.7	0.7	0.7	0.04
	7	2.0	2.1	2.1	2.1	0.04
	17	4.0	3.9	3.9	3.9	0.06
	32	11.2	11.2	11.2	11.2	0.01
Cum H_2O rec (g)	2	63.4	60.4	58.0	60.6	2.71
	7	347.9	344.6	340.6	344.4	3.66
	17	857.1	859.4	857.6	858.0	1.21
	32	1216.5	1222.3	1227.0	1221.9	5.26
Total						
H_2O recovery %	2	1.0	0.9	0.9	0.9	0.04
	7	5.3	5.3	5.2	5.2	0.06
	17	13.1	13.1	13.1	13.1	0.02
	32	18.5	18.6	18.7	18.6	0.08
Sulphur %	2	25.1	26.1	25.5	25.6	0.52
	7	14.8	14.7	14.5	14.7	0.17
	17	3.2	2.9	3.5	3.2	0.35
	32	0.5	0.5	0.4	0.5	0.01
Total						
Mass of S (g)	2	5.2	6.0	5.9	5.7	0.41
	7	6.7	6.7	6.6	6.7	0.07
	17	2.1	1.7	2.1	2.0	0.21
	32	1.1	1.1	1.1	1.1	0.01
Cum S grade %	2	25.1	26.1	25.5	25.6	0.52
	7	18.0	18.6	18.2	18.3	0.26
	17	10.7	11.2	11.4	11.1	0.37
	32	4.1	4.2	4.2	4.2	0.07
Cum. S rec. %	2	26.1	29.2	29.1	28.1	1.77
	7	59.7	61.8	61.5	61.0	1.12
	17	70.2	70.2	71.8	70.7	0.90
	32	75.7	75.6	77.1	76.2	0.83
Tails: mass (g)		2928.0	2906.0	2948.5	2927.5	21.25
Tails: sulphur %		0.2	0.1	0.2	0.2	0.01
Tails: mass of S (g)		4.9	4.3	4.9	4.7	0.33

Type of collector used: 530 g/t SiBX

	Time (min)	Samples A	B	C	Average (grams)	Std error (grams)
Head mass(g)		3300.0	3300.0	3300.0	3300	0.00
Head sulphur %		0.6	0.6	0.6	0.6	0.00
Mass of S		20.0	19.9	20.0	20.0	0.09
Wet conc.(g)	2	180.4	179.5	179.1	179.7	0.67
	7	403.7	399.2	405.9	402.9	3.42
	17	678.9	674.6	675.3	676.3	2.31
	32	1169.8	1160.3	1161.3	1163.8	5.22
Dry conc. mass (g)	2	42.4	39.5	42.6	41.5	1.73
	7	44.3	48.2	47.0	46.5	2.00
	17	72.3	73.1	70.7	72.0	1.22
	32	233.9	230.4	235.8	233.4	2.74
Cum. mass pull (g)	2	42.4	39.5	42.6	41.5	1.73
	7	86.7	87.7	89.6	88.0	1.47
	17	159.0	160.8	160.3	160.0	0.93
	32	392.9	391.2	396.1	393.4	2.49
Cum. mass pull %	2	1.3	1.2	1.3	1.3	0.05
	7	2.6	2.7	2.7	2.7	0.04
	17	4.8	4.9	4.9	4.8	0.03
	32	11.9	11.9	12.0	11.9	0.08
Cum H_2O rec (g)	2	138.0	140.0	136.5	138.2	1.76
	7	497.4	491.0	495.4	494.6	3.27
	17	1104.0	1092.5	1100.0	1098.8	5.84
	32	2039.9	2022.4	2025.5	2029.3	9.34
Total						
H_2O recovery %	2	2.1	2.1	2.1	2.1	0.03
	7	7.6	7.5	7.6	7.5	0.05
	17	16.8	16.7	16.8	16.8	0.09
	32	31.1	30.8	30.9	30.9	0.14
Sulphur %	2	23.0	22.1	23.1	22.7	0.57
	7	9.8	9.2	8.2	9.1	0.83
	17	1.9	2.1	0.9	1.6	0.61
	32	0.4	0.5	0.4	0.4	0.04
Total						
Mass of S (g)	2	9.8	8.7	9.8	9.4	0.63
	7	4.4	4.4	3.8	4.2	0.31
	17	1.3	1.5	0.7	1.2	0.46
Rmax	32	1.0	1.1	0.9	1.0	0.09
Cum S grade %	2	23.0	22.1	23.1	22.7	0.57
	7	16.3	15.0	15.3	15.5	0.68
	17	9.7	9.1	9.0	9.3	0.41
	32	4.2	4.0	3.9	4.0	0.16
Cum. S rec. %	2	48.9	43.9	49.1	47.3	2.94
	7	70.7	66.2	68.3	68.4	2.26
	17	77.4	73.8	71.6	74.3	2.95
	32	82.3	79.4	76.2	79.3	3.05
Tails: mass (g)		2904.0	2897.0	2701.2	2834.1	115.12
Tails: sulphur %		0.1	0.1	0.1	0.1	0.00
Tails: mass of S (g)		3.4	3.2	2.9	3.2	0.26

Type of collector used: 530 g/t SiBX in mill

	Time	Samples			Average	Std error
	(min)	A	B	C	(grams)	(grams)
Head mass(g)		3300	3300	3300	3300	0.00
Head sulphur %		0.6	0.6	0.6	0.6	0.01
Mass of S		19.9	19.5	19.8	19.8	0.20
Wet conc.(g)	2	101.4	119.5	110.0	110.3	9.05
	7	301.1	313.2	309.6	308.0	6.21
	17	537.6	560.6	546.6	548.3	11.59
	32	1125.8	1130.3	1120.4	1125.5	4.96
Dry conc. mass (g)	2	23.8	25.0	26.5	25.1	1.35
	7	42.9	49.2	45.2	45.8	3.19
	17	81.2	88.1	71.6	80.3	8.29
	32	267.9	260.0	251.6	259.8	8.15
Cum. mass pull (g)	2	23.8	25.0	26.5	25.1	1.35
	7	66.7	74.2	71.7	70.9	3.82
	17	147.9	162.3	143.3	151.2	9.91
	32	415.8	422.3	394.9	411.0	14.32
Cum. mass pull %	2	0.7	0.8	0.8	0.8	0.04
	7	2.0	2.2	2.2	2.1	0.12
	17	4.5	4.9	4.3	4.6	0.30
	32	12.6	12.8	12.0	12.5	0.43
Cum H_2O rec (g)	2	77.6	94.5	83.5	85.2	8.58
	7	335.8	358.5	347.9	347.4	11.36
	17	792.2	831.0	822.9	815.4	20.47
	32	1650.1	1701.3	1691.7	1681.0	27.22
Total						
H_2O recovery %	2	1.2	1.4	1.3	1.3	0.13
	7	5.1	5.5	5.3	5.3	0.17
	17	12.1	12.7	12.5	12.4	0.31
	32	25.2	25.9	25.8	25.6	0.41
Sulphur %	2	22.8	22.2	23.5	22.8	0.66
	7	12.9	10.0	13.0	12.0	1.71
	17	3.5	3.6	2.7	3.3	0.47
	32	0.8	0.8	0.8	0.8	0.04
Total						
Mass of S (g)	2	5.4	5.5	6.2	5.7	0.43
	7	5.5	4.9	5.9	5.4	0.48
	17	2.8	3.1	2.0	2.7	0.62
	32	2.0	2.0	2.1	2.1	0.03
Cum S grade %	2	22.8	22.2	23.5	22.8	0.66
	7	16.4	14.1	16.9	15.8	1.49
	17	9.3	8.4	9.8	9.2	0.72
	32	3.8	3.7	4.1	3.9	0.20
Cum. S rec. %	2	27.2	28.4	31.4	29.0	2.16
	7	55.0	53.5	60.9	56.5	3.93
	17	69.3	69.6	70.8	69.9	0.79
	32	79.6	80.0	81.4	80.3	0.93
Tails: mass (g)		2695.6	2897.0	2520.0	2704.2	188.65
Tails: sulphur %		0.1	0.1	0.1	0.1	0.02
Tails: mass of S (g)		3.6	3.2	3.7	3.5	0.23

Type of collector used: 100% C4 TTC

	Time (min)	Samples A	Samples B	Samples C	Average (grams)	Std error (grams)
Head mass(g)		3300	3300	3300	3300	0.00
Head sulphur %		0.60	0.60424	0.62	0.6	0.01
Mass of S		19.8	19.9	20.5	20.1	0.34
Wet conc.(g)	2	307.1	315	314.7	312.3	4.48
	7	909.8	911.4	913.7	911.6	1.96
	17	1627.3	1623.3	1618.4	1623.0	4.46
	32	1703.6	1693.4	1706.3	1701.1	6.80
Total						
Dry conc. mass (g)	2	66.3	65.3	67.6	66.4	1.15
	7	117.7	126	123.6	122.4	4.27
	17	206.0	202.4	203.3	203.9	1.87
	32	278.6	270.5	267	272.0	5.95
Total						
Cum. mass pull (g)	2	66.3	65.3	67.6	66.4	1.15
	7	184.0	191.3	191.2	188.8	4.17
	17	390.0	393.7	394.5	392.7	2.38
	32	668.6	664.2	661.5	664.8	3.60
Total						
Cum. mass pull %	2	2.0	2.0	2.0	2.0	0.03
	7	5.6	5.8	5.8	5.7	0.13
	17	11.8	11.9	12.0	11.9	0.07
	32	20.3	20.1	20.0	20.1	0.11
Cum H_2O rec (g)	2	240.8	249.7	247.1	245.9	4.59
	7	1032.9	1035.1	1037.2	1035.1	2.17
	17	2454.2	2456.0	2452.3	2454.2	1.85
	32	3879.2	3878.9	3891.6	3883.2	7.26
Total						
Cum H_2O rec %	2	3.7	3.8	3.8	3.7	0.07
	7	15.7	15.8	15.8	15.8	0.03
	17	37.4	37.4	37.4	37.4	0.03
	32	59.1	59.1	59.3	59.2	0.11
% Sulphur	2	14.51	14.43	14.45	14.5	0.04
	7	4.20	2.95	3.87	3.7	0.65
	17	0.84	0.56	0.58	0.7	0.16
	32	0.25	0.19	0.23	0.2	0.03
Total						
Mass of S (g)	2	9.6	9.4	9.8	9.6	0.17
	7	4.9	3.7	4.8	4.5	0.66
	17	1.7	1.1	1.2	1.3	0.33
	32	0.7	0.5	0.6	0.6	0.10
%S Cum. grade	2	14.5	14.4	14.4	14.5	0.04
	7	7.9	6.9	7.6	7.5	0.54
	17	4.2	3.6	4.0	3.9	0.28
	32	2.5	2.2	2.5	2.4	0.17
%S Cum. rec.	2	48.6	47.3	47.7	47.9	0.67
	7	73.5	65.9	71.1	70.2	3.89
	17	82.3	71.6	76.9	76.9	5.33
	32	85.8	74.1	79.8	79.9	5.83
Tails: mass (g)		2490.2	2559.4	2425.9	2491.8	66.76
Tails: sulphur %		0.11	0.10	0.09	0.1	0.01
Tails: mass of S (g)		2.8	2.6	2.2	2.5	0.34

Type of collector used: 25% C4 TTC

	Time (min)	Samples A	Samples B	Samples C	Average (grams)	Std error (grams)
Head mass(g)		3300.0	3300.0	3300.0	3300	0.00
Head sulphur %		0.6002	0.59404	0.5973	0.6	0.00
Mass of S		19.8	19.6	19.7	19.7	0.10
Wet conc.(g)	2	214.6	216	218	216.2	1.71
	7	561.6	558.6	562.5	560.9	2.04
	17	1270.6	1275.9	1271.4	1272.6	2.86
	32	2117.7	2120.2	2119.9	2119.3	1.37
Total						
Dry conc. mass (g)	2	39.9	44.2	50.4	44.8	5.28
	7	60.2	62.7	65.2	62.7	2.50
	17	157.4	153.5	159.7	156.9	3.13
	32	355.3	361.9	356.8	358.0	3.46
Total						
Cum. mass pull (g)	2	39.9	44.2	50.4	44.8	5.28
	7	100.1	106.9	115.6	107.5	7.77
	17	257.5	260.4	275.3	264.4	9.55
	32	612.8	622.3	632.1	622.4	9.65
Total						
Cum. mass pull %	2	1.2	1.3	1.5	1.4	0.16
	7	3.0	3.2	3.5	3.3	0.24
	17	7.8	7.9	8.3	8.0	0.29
	32	18.6	18.9	19.2	18.9	0.29
Cum H_2O rec (g)	2	174.7	171.8	167.6	171.4	3.57
	7	676.1	667.7	664.9	669.6	5.83
	17	1789.3	1790.1	1776.6	1785.3	7.57
	32	3551.7	3548.4	3539.7	3546.6	6.20
Total						
Cum H_2O rec %	2	2.7	2.6	2.6	2.6	0.05
	7	10.3	10.2	10.1	10.2	0.09
	17	27.3	27.3	27.1	27.2	0.12
	32	54.1	54.1	54.0	54.1	0.09
% Sulphur	2	20.30	19.28	17.09	18.9	1.64
	7	7.39	5.97	5.98	6.4	0.82
	17	1.59	1.11	0.95	1.2	0.33
	32	0.44	0.33	0.40	0.4	0.06
Total						
Mass of S (g)	2	8.1	8.5	8.6	8.4	0.28
	7	4.4	3.7	3.9	4.0	0.37
	17	2.5	1.7	1.5	1.9	0.52
	32	1.6	1.2	1.4	1.4	0.19
%S Cum. grade	2	20.3	19.3	17.1	18.9	1.64
	7	12.5	11.5	10.8	11.6	0.86
	17	5.8	5.4	5.1	5.4	0.38
	32	2.7	2.4	2.4	2.5	0.16
%S Cum. rec.	2	40.9	43.5	43.7	42.7	1.56
	7	63.3	62.6	63.5	63.1	0.50
	17	76.0	71.3	71.2	72.8	2.74
	32	83.9	77.3	78.4	79.9	3.53
Tails: mass (g)		2705.2	2613.6	2536.1	2618.3	84.65
Tails: sulphur %		0.12	0.10	0.10	0.1	0.01
Tails: mass of S (g)		3.2	2.6	2.6	2.8	0.35

Type of collector used: 6.25 % C4 TTC

	Time (min)	Samples A	B	C	Average (grams)	Std error (grams)
Head mass(g)		3300.0	3300.0	3300.0	3300	0.00
Head sulphur %		0.6039	0.6067	0.61	0.6	0.00
Mass of S		19.9	20.0	20.1	20.0	0.07
Wet conc.(g)	2	156.4	160.1	153.4	156.6	3.36
	7	424.5	427.2	430.3	427.3	2.90
	17	1035.9	1046.7	1033.6	1038.7	7.0
	32	1662.6	1658.7	1660.3	1660.5	2.0
Total						
Dry conc. mass (g)	2	39.7	40.2	32.2	37.4	4.48
	7	56.7	65.8	54.3	58.9	6.07
	17	112.4	124.5	115.3	117.4	6.32
	32	276.9	287.8	283.6	282.8	5.50
Total						
Cum. mass pull (g)	2	39.7	40.2	32.2	37.4	4.48
	7	96.4	106.0	86.5	96.3	9.75
	17	208.8	230.5	201.8	213.7	14.96
	32	485.7	518.3	485.4	496.5	18.91
Total						
Cum. mass pull %	2	1.2	1.2	1.0	1.1	0.14
	7	2.9	3.2	2.6	2.9	0.3
	17	6.3	7.0	6.1	6.5	0.45
	32	14.7	15.7	14.7	15.0	0.57
Cum H_2O rec (g)	2	116.7	119.9	121.2	119.3	2.32
	7	484.5	481.3	497.2	487.7	8.41
	17	1408.0	1403.5	1415.5	1409.0	6.1
	32	2793.7	2774.4	2792.2	2786.8	10.7
Total						
Cum H_2O rec %	2	1.8	1.8	1.8	1.8	0.0
	7	7.4	7.3	7.6	7.4	0.1
	17	21.5	21.4	21.6	21.5	0.1
	32	42.6	42.3	42.6	42.5	0.2
% Sulphur	2	21.54	20.54	21.16	21.1	0.51
	7	9.27	7.65	10.16	9.0	1.27
	17	1.31	1.67	2.41	1.8	0.56
	32	0.57	0.47	0.59	0.5	0.07
Total						
Mass of S (g)	2	8.6	8.3	6.8	7.9	0.93
	7	5.3	5.0	5.5	5.3	0.24
	17	1.5	2.1	2.8	2.1	0.65
	32	1.6	1.3	1.7	1.5	0.17
%S Cum. grade	2	21.5	20.5	21.2	21.1	0.51
	7	14.3	12.5	14.3	13.7	1.01
	17	7.3	6.7	7.5	7.2	0.43
	32	3.5	3.2	3.5	3.4	0.14
%S Cum. rec.	2	42.9	41.2	34.0	39.4	4.76
	7	69.3	66.4	61.5	65.7	3.95
	17	76.7	76.8	75.3	76.3	0.83
	32	84.6	83.5	83.6	83.9	0.60
Tails: mass (g)		2788.3	2706.2	2712.4	2735.6	45.72
Tails: sulphur %		0.10713	0.11	0.10	0.1	0.00
Tails: mass of S (g)		3.0	3.0	2.8	2.9	0.09

Type of collector used: 35% C10 TTC

	Time (min)	Samples A	B	C	Average (grams)	Std error (grams)
Head mass(g)		3300	3300	3300	3300	0.00
Head sulphur %		0.59	0.59	0.59	0.6	0.00
Mass of S		19.3	19.5	19.5	19.4	0.10
Wet conc.(g)	2	528.2	506.2	512.7	515.7	11.30
	7	1064.7	1060.5	1077.2	1067.5	8.69
	17	1727.7	1719.1	1721.6	1722.8	4.42
	32	1186.5	1175.9	1164.9	1175.8	10.80
Total						
Dry conc. mass (g)	2	97.8	84.6	93.2	91.9	6.70
	7	117.8	124.6	133.2	125.2	7.72
	17	305.5	310.7	309.4	308.5	2.71
	32	354.4	348.2	340.2	347.6	7.12
Total						
Cum. mass pull (g)	2	97.8	84.6	93.2	91.9	6.70
	7	215.6	209.2	226.4	217.1	8.69
	17	521.1	519.9	535.8	525.6	8.85
	32	875.5	868.1	876.0	873.2	4.42
Total						
Cum. mass pull %	2	3.0	2.6	2.8	2.8	0.20
	7	6.5	6.3	6.9	6.6	0.26
	17	15.8	15.8	16.2	15.9	0.27
	32	26.5	26.3	26.5	26.5	0.13
Cum H_2O rec (g)	2	430.4	421.6	419.5	423.8	5.78
	7	1377.3	1357.5	1363.5	1366.1	10.15
	17	2799.5	2765.9	2775.7	2780.4	17.28
	32	3631.6	3593.6	3600.4	3608.5	20.26
Total						
H_2O recovery %	2	6.6	6.4	6.4	6.5	0.09
	7	21.0	20.7	20.8	20.8	0.15
	17	42.7	42.2	42.3	42.4	0.26
	32	55.4	54.8	54.9	55.0	0.31
Sulphur %	2	6.3	6.0	5.4	5.9	0.46
	7	2.3	2.8	2.6	2.6	0.25
	17	1.8	1.6	1.3	1.6	0.25
	32	0.8	0.7	0.9	0.8	0.09
Total						
Mass of S (g)	2	6.2	5.1	5.0	5.4	0.64
	7	2.7	3.5	3.4	3.2	0.42
	17	5.4	5.1	4.0	4.8	0.75
	32	3.0	2.5	3.1	2.9	0.29
S cum. grade %	2	6.3	6.0	5.4	5.9	0.46
	7	4.1	4.1	3.7	4.0	0.22
	17	2.8	2.6	2.3	2.6	0.22
	32	2.0	1.9	1.8	1.9	0.10
S cum. rec. %	2	32.0	26.2	25.9	28.0	3.43
	7	46.1	44.2	43.4	44.6	1.41
	17	74.2	70.1	63.8	69.4	5.26
	32	89.6	83.1	79.5	84.1	5.09
Tails: mass (g)		2572.4	2565.2	2535.8	2557.8	19.39
Tails: sulphur		0.1	0.1	0.1	0.1	0.01
Tails: mass of S (g)		2.7	2.3	2.4	2.5	0.22

Type of collector used: 25% C10 TTC

	Time	Samples			Average	Std error
	(min)	A	B	C	(grams)	(grams)
Head mass(g)		3300.0	3300.0	3300.0	3300	0.00
Head sulphur %		0.61	0.60	0.60	0.6	0.01
Mass of S		20.1	19.7	19.8	19.9	0.21
Wet conc.(g)	2	290.8	292.4	295.4	292.9	2.34
	7	724.2	732.3	720.8	725.8	5.91
	17	1323.8	1328.7	1317.6	1323.4	5.56
	32	1864.4	1869.3	1873.9	1869.2	4.75
Total						
Dry conc. mass (g)	2	69.3	71.7	72.0	71.0	1.48
	7	144.0	151.0	153.9	149.6	5.09
	17	199.9	209.0	201.6	203.5	4.84
	32	280.3	284.2	278.3	280.9	3.00
Total		693.5	715.9	705.8		
Cum. mass pull (g)	2	69.3	71.7	72.0	71.0	1.48
	7	213.3	222.7	225.9	220.6	6.55
	17	413.2	431.7	427.5	424.1	9.70
	32	693.5	715.9	705.8	705.1	11.22
Total		1389.3	1442.0	1431.2		
Cum. mass pull %	2	2.1	2.2	2.2	2.2	0.04
	7	6.5	6.7	6.8	6.7	0.20
	17	12.5	13.1	13.0	12.9	0.29
	32	21.0	21.7	21.4	21.4	0.34
Cum H_2O rec (g)	2	221.5	220.7	223.4	221.9	1.39
	7	801.7	802.0	790.3	798.0	6.67
	17	1925.6	1921.7	1906.3	1917.9	10.21
	32	3509.7	3506.8	3501.9	3506.1	3.94
Total						
H_2O recovery %	2	3.4	3.4	3.4	3.4	0.02
	7	12.2	12.2	12.0	12.2	0.10
	17	29.4	29.3	29.1	29.2	0.16
	32	53.5	53.5	53.4	53.4	0.06
Sulphur %	2	9.35	9.41	9.00	9.3	0.22
	7	3.66	3.74	2.83	3.4	0.50
	17	1.04	0.76	1.00	0.9	0.15
	32	0.58	0.57	0.61	0.6	0.02
Total						
Mass of S (g)	2	6.5	6.7	6.5	6.6	0.15
	7	5.3	5.6	4.4	5.1	0.66
	17	2.1	1.6	2.0	1.9	0.27
	32	1.6	1.6	1.7	1.7	0.05
S cum. grade %	2	9.3	9.4	9.0	9.3	0.22
	7	5.5	5.6	4.8	5.3	0.43
	17	3.3	3.2	3.0	3.2	0.18
	32	2.2	2.2	2.1	2.2	0.09
S cum. rec. %	2	32.2	34.2	32.7	33.0	1.06
	7	58.5	62.9	54.6	58.7	4.15
	17	68.8	71.0	64.7	68.2	3.17
	32	76.9	79.2	73.3	76.5	2.97
Tails: mass (g)		2437.1	2444.2	2396	2425.8	26.02
Tails: sulphur		0.08	0.11	0.08	0.1	0.02
Tails: mass of S (g)		1.9	2.7	1.8	2.2	0.45

Type of collector used: 6.25% C10 TTC

	Time (min)	Samples A	Samples B	Samples C	Average (grams)	Std error (grams)
Head mass(g)		3300.0	3300.0	3300.0	3300	0.00
Head sulphur %		0.60	0.61	0.62	0.6	0.01
Mass of S		19.9	20.1	20.4	20.1	0.23
Wet conc.(g)	2	214	200.6	220	211.5	9.93
	7	652.0	659.7	670.6	660.8	9.35
	17	890.7	900.4	911.0	900.7	10.2
	32	1668.1	1675.9	1656.4	1666.8	9.8
Total						
Dry conc. mass (g)	2	46.3	52.3	47.1	48.6	3.26
	7	102.2	91.1	89.5	94.3	6.92
	17	157.4	151.5	155.5	154.8	3.01
	32	221.0	212.9	213.3	215.7	4.57
Total						
Cum. mass pull (g)		46.3	52.3	47.1	48.6	3.26
		148.5	143.4	136.6	142.8	5.97
		305.9	294.9	292.1	297.6	7.29
		526.9	507.8	505.4	513.4	11.78
Total						
Cum. mass pull %		1.4	1.6	1.4	1.5	0.10
		4.5	4.3	4.1	4.3	0.2
		9.3	8.9	8.9	9.0	0.22
		16.0	15.4	15.3	15.6	0.36
Cum H_2O rec (g)	2	167.7	148.3	172.9	163.0	12.97
	7	717.5	716.9	754.0	729.5	21.25
	17	1450.8	1465.8	1509.5	1475.4	30.5
	32	2897.9	2928.8	2952.6	2926.4	27.4
Total						
H_2O recovery %	2	2.6	2.3	2.6	2.5	0.2
	7	10.9	10.9	11.5	11.1	0.3
	17	22.1	22.3	23.0	22.5	0.5
	32	44.2	44.6	45.0	44.6	0.4
Sulphur %	2	16.70	16.24	17.47	16.8	0.62
	7	4.98	4.24	5.85	5.0	0.80
	17	1.21	1.26	1.85	1.4	0.36
	32	0.53	0.49	0.68	0.6	0.10
Total						
Mass of S (g)	2	7.7	8.5	8.2	8.2	0.39
	7	5.1	3.9	5.2	4.7	0.75
	17	1.9	1.9	2.9	2.2	0.56
	32	1.2	1.0	1.5	1.2	0.21
S cum. grade %	2	16.7	16.2	17.5	16.8	0.62
	7	8.6	8.6	9.9	9.0	0.71
	17	4.8	4.8	5.6	5.1	0.44
	32	3.0	3.0	3.5		0.29
S cum. rec. %	2	38.8	42.4	40.4	40.5	1.75
	7	64.4	61.6	66.1	64.0	2.26
	17	74.0	71.1	80.2	75.1	4.65
	32	79.8	76.3	87.4	81.2	5.66
Tails: mass (g)		2654.3	2617.0	2646.0	2639.1	19.58
Tails: sulphur		0.12	0.11	0.10	0.1	0.01
Tails: mass of S (g)		3.1	2.8	2.7	2.9	0.22

Type of collector used: 100% C12 TTC

	Time (min)	Samples A	Samples B	Samples C	Average (grams)	Std error (grams)
Head mass(g)		3300	3300	3300	3300	0.00
Head sulphur %		0.60	0.60	0.60	0.6	0.00
Mass of S		19.9	19.8	19.9	19.9	0.05
Wet conc.(g)	2	339.3	327.8	326.6	331.2	7.01
	7	546.3	551.9	556.9	551.7	5.30
	17	724.4	712.3	706.7	714.5	9.05
	32	1122.2	1137.6	1132.5	1130.8	7.84
Dry conc. mass (g)	2	107.3	91.6	96.3	98.4	8.06
	7	151.2	164.8	157.1	157.7	6.82
	17	198.8	209.2	204.8	204.3	5.22
	32	239.0	248.8	239.8	242.5	5.44
Cum. mass pull (g)	2	107.3	91.6	96.3	98.4	8.06
	7	258.5	256.4	253.4	256.1	2.56
	17	457.3	465.6	458.2	460.4	4.55
	32	696.3	714.4	698.0	702.9	10.00
Cum. mass pull %	2	3.3	2.8	2.9	3.0	0.24
	7	7.8	7.8	7.7	7.8	0.08
	17	13.9	14.1	13.9	14.0	0.14
	32	21.1	21.6	21.2	21.3	0.30
Cum H_2O rec (g)	2	232.0	236.2	230.3	232.8	3.04
	7	627.1	623.3	630.1	626.8	3.41
	17	1152.7	1126.4	1132.0	1137.0	13.85
	32	2035.9	2015.2	2024.7	2025.3	10.36
Total						
H_2O recovery %	2	3.5	3.6	3.5	3.5	0.05
	7	9.6	9.5	9.6	9.6	0.05
	17	17.6	17.2	17.3	17.3	0.21
	32	31.0	30.7	30.9	30.9	0.16
Sulphur %	2	4.87	7.14	7.91	6.6	1.58
	7	2.86	2.67	3.09	2.9	0.21
	17	1.38	1.11	1.16	1.2	0.14
	32	0.89	1.01	0.88	0.9	0.07
Total						
Mass of S (g)	2	5.2	6.5	7.6	6.5	1.20
	7	4.3	4.4	4.8	4.5	0.28
	17	2.7	2.3	2.4	2.5	0.23
	32	2.1	2.5	2.1	2.2	0.22
Cum S grade %	2	4.9	7.1	7.9	6.6	1.58
	7	3.7	4.3	4.9	4.3	0.61
	17	2.7	2.8	3.2	2.9	0.28
	32	2.1	2.2	2.4	2.2	0.18
Cum. S rec. %	2	26.3	32.9	38.2	32.5	5.98
	7	48.0	55.1	62.5	55.2	7.25
	17	61.8	66.9	74.4	67.7	6.35
	32	72.5	79.5	85.0	79.0	6.24
Tails: mass (g)		2166.7	2585	2354.9	2368.9	209.50
Tails: sulphur %		0.20	0.19	0.20	0.2	0.01
Tails: mass of S (g)		4.3	4.9	4.8	4.7	0.33

Type of collector used: 25% C12 TTC

	Time (min)	Samples A	Samples B	Samples C	Average (grams)	Std error (grams)
Head mass(g)		3300.0	3300.0	3300.0	3300.0	0.00
Head sulphur %		0.6	0.6	0.6	0.6	0.00
Mass of S		20.0	19.9	19.9	19.9	0.03
Wet conc.(g)	2	405.6	400.9	392.2	399.6	6.80
	7	895.1	892.7	880.7	889.5	7.72
	17	1250.9	1247.3	1261.6	1253.3	7.44
	32	1371.4	1364.6	1355.8	1363.9	7.82
Dry conc. mass (g)	2	106.0	94.4	89.1	96.5	8.64
	7	126.2	130.4	147.2	134.6	11.11
	17	210.4	183.9	187.8	194.0	14.31
	32	162.0	142.4	155.7	153.4	10.01
Cum. mass pull (g)	2	106.0	94.4	89.1	96.5	8.64
	7	232.2	224.8	236.3	231.1	5.83
	17	442.6	408.7	424.1	425.1	16.97
	32	604.6	551.1	579.8	578.5	26.77
Cum. mass pull %	2	3.2	2.9	2.7	2.9	0.26
	7	7.0	6.8	7.2	7.0	0.18
	17	13.4	12.4	12.9	12.9	0.51
	32	18.3	16.7	17.6	17.5	0.81
Cum H_2O rec (g)	2	299.6	306.5	303.1	303.1	3.45
	7	1068.5	1068.8	1036.6	1058.0	18.51
	17	2109.0	2132.2	2110.4	2117.2	13.03
	32	3318.4	3354.4	3310.5	3327.8	23.42
Total						
H_2O recovery %	2	4.6	4.7	4.6	4.6	0.05
	7	16.3	16.3	15.8	16.1	0.28
	17	32.1	32.5	32.2	32.3	0.20
	32	50.6	51.1	50.5	50.7	0.36
Sulphur %	2	10.0	12.2	12.4	11.6	1.36
	7	1.8	2.0	1.9	1.9	0.10
	17	0.9	1.0	0.9	0.9	0.06
	32	0.6	0.6	0.6	0.6	0.03
Total						
Mass of S (g)	2	10.6	11.6	11.1	11.1	0.48
	7	2.3	2.6	2.8	2.5	0.25
	17	1.8	1.8	1.8	1.8	0.04
	32	0.9	0.9	1.0	0.9	0.06
Cum S grade %	2	10.0	12.2	12.4	11.6	1.36
	7	5.5	6.3	5.9	5.9	0.38
	17	3.3	3.9	3.7	3.6	0.30
	32	2.6	3.1	2.9	2.8	0.24
Cum. S rec. %	2	53.1	58.0	55.7	55.6	2.44
	7	64.4	70.9	69.5	68.3	3.43
	17	73.6	80.1	78.3	77.3	3.36
	32	78.3	84.5	83.4	82.0	3.31
Tails: mass (g)		2574.9	2656.2	2660.6	2630.6	48.26
Tails: sulphur %		0.1	0.1	0.1	0.1	0.01
Tails: mass of S (g)		2.1	2.0	2.4	2.2	0.21

Type of collector used: 6.25% C12 TTC

	Time (min)	Samples A	Samples B	Samples C	Average (grams)	Std error (grams)
Head mass(g)		3300.0	3300.0	3300.0	3300	0.00
Head sulphur %		0.61	0.60	0.62	0.6	0.01
Mass of S		20.3	19.9	20.3	20.2	0.25
Wet conc.(g)	2	155.4	164.8	140.9	153.7	12.04
	7	460.8	452.2	435.2	449.4	13.03
	17	851.7	829.7	857.8	846.4	14.8
	32	1137.4	1132	1143.8	1137.7	5.9
Dry conc. mass (g)	2	46.9	49.6	46.2	47.6	1.80
	7	83.3	85.3	88.3	85.6	2.52
	17	121.5	123.8	135	126.8	7.22
	32	177.1	165.7	176.1	173.0	6.31
Cum. mass pull (g)	2	46.9	49.6	46.2	47.6	1.80
	7	130.2	134.9	134.5	133.2	2.61
	17	251.7	258.7	269.5	260.0	8.97
	32	428.8	424.4	445.6	432.9	11.19
Cum. mass pull %	2	1.4	1.5	1.4	1.4	0.05
	7	3.9	4.1	4.1	4.0	0.08
	17	7.6	7.8	8.2	7.9	0.27
	32	13.0	12.9	13.5	13.1	0.34
Cum H_2O rec (g)	2	108.5	115.2	94.7	106.1	10.45
	7	486.0	482.1	441.6	469.9	24.59
	17	1216.2	1188.0	1164.4	1189.5	25.9
	32	2176.5	2154.3	2132.1	2154.3	22.2
Total						
H_2O recovery %	2	1.7	1.8	1.4	1.6	0.2
	7	7.4	7.3	6.7	7.2	0.4
	17	18.5	18.1	17.8	18.1	0.4
	32	33.2	32.8	32.5	32.8	0.3
Sulphur %	2	20.28	17.74	17.77	18.6	1.46
	7	5.84	5.73	5.91	5.8	0.09
	17	1.29	1.55	1.78	1.5	0.25
	32	0.55	0.62	0.63	0.6	0.04
Total						
Mass of S (g)	2	9.5	8.8	8.2	8.8	0.65
	7	4.9	4.9	5.2	5.0	0.20
	17	1.6	1.9	2.4	2.0	0.42
	32	1.0	1.0	1.1	1.0	0.07
Cum S grade %	2	20.3	17.7	17.8	18.6	1.46
	7	11.0	10.1	10.0	10.4	0.57
	17	6.3	6.0	5.9	6.1	0.23
	32	3.9	3.9	3.8	3.9	0.08
Cum. S rec. %	2	46.9	44.3	40.4	43.9	3.24
	7	70.8	68.9	66.1	68.6	2.36
	17	78.5	78.6	78.0	78.4	0.32
	32	83.3	83.7	83.5	83.5	0.20
Tails: mass (g)		2787.2	2784.4	2718.8	2763.5	38.71
Tails: sulphur %		0.08	0.09	0.09	0.1	0.01
Tails: mass of S (g)		2.2	2.6	2.5	2.5	0.22

Type of collector used: DTP (2.27 mol/t)

	Time (min)	Samples A	Samples B	Samples C	Average (grams)	Std error (grams)
Head mass(g)		3300	3300	3300	3300	0.00
Head sulphur %		0.60	0.61	0.61	0.6	0.00
Mass of S		19.8	20.1	20.1	20.0	0.16
Wet conc.(g)	2	305.0	319.8	290.4	305.1	14.70
	7	849.2	862.3	838.1	849.9	12.11
	17	1762.5	1739.7	1747.1	1749.8	11.63
	32	1746.5	1727.5	1733.3	1735.8	9.74
Dry conc. mass (g)	2	70.9	79	66.3	72.1	6.43
	7	160.4	152.6	150.1	154.4	5.37
	17	335.7	336.2	331.4	334.4	2.64
	32	375.5	371.6	377.3	374.8	2.91
Cum. mass pull (g)	2	70.9	72.3	66.3	69.8	3.14
	7	231.3	224.9	216.4	224.2	7.47
	17	567.0	561.1	547.8	558.6	9.83
	32	942.5	932.7	925.1	933.4	8.72
Cum. mass pull %	2	2.1	2.2	2.0	2.1	0.10
	7	7.0	6.8	6.6	6.8	0.23
	17	17.2	17.0	16.6	16.9	0.30
	32	28.6	28.3	28.0	28.3	0.26
Cum H_2O rec (g)	2	234.1	240.8	224.1	233.0	8.40
	7	922.9	950.5	912.1	928.5	19.80
	17	2349.7	2354.0	2327.8	2343.8	14.05
	32	3720.7	3709.9	3683.8	3704.8	18.97
Total						
H_2O recovery %	2	3.6	3.7	3.4	3.6	0.13
	7	14.1	14.5	13.9	14.2	0.30
	17	35.8	35.9	35.5	35.7	0.21
	32	56.7	56.6	56.2	56.5	0.29
Sulphur %	2	15.76	15.14	15.77	15.5	0.45
	7	2.69	2.50	3.63	3.1	0.80
	17	0.23	0.28	0.38	0.3	0.07
	32	0.08	0.11	0.12	0.1	0.00
Total						
Mass of S (g)	2	11.2	12.0	10.5	11.2	0.75
	7	4.3	3.8	5.4	4.5	0.83
	17	0.8	1.0	1.3	1.0	0.26
	32	0.3	0.4	0.4	0.4	0.08
Cum S grade %	2	15.8	15.1	15.8	15.6	0.36
	7	6.7	6.8	7.3	7.0	0.35
	17	2.9	2.9	3.1	3.0	0.14
	32	1.8	1.8	1.9	1.8	0.07
Cum. S rec. %	2	56.4	59.5	52.1	56.0	3.68
	7	78.2	78.4	79.3	78.6	0.56
	17	82.1	83.2	85.6	83.6	1.82
	32	83.5	85.3	87.8	85.5	2.15
Tails: mass (g)		1949.8	2324.9	2327.3	2200.7	217.26
Tails: sulphur %		0.04	0.04	0.04	0.04	0.00
Tails: mass of S (g)		0.7	0.9	0.9	0.8	0.10

Type of collector used: DTP (1.28 mol/t)

	Time (min)	Samples A	B	C	Average (grams)	Std error (grams)
Head mass(g)		3300.0	3300.0	3300.0	3300	0.00
Head sulphur %		0.61	0.57	0.58	0.6	0.02
Mass of S		20.1	19.0	19.3	19.4	0.58
Wet conc.(g)	2	375	361	362.4	366.1	7.71
	7	751.2	769.2	763.3	761.2	9.18
	17	1356.5	1338.8	1342.8	1346.0	9.28
	32	1608.2	1624.5	1614.3	1615.7	8.24
Dry conc. mass (g)	2	76	80.9	67.9	74.9	6.57
	7	86.5	85.1	86	85.9	0.71
	17	118.7	127.5	130.5	125.6	6.13
	32	315.7	300.5	320.1	312.1	10.28
		596.9	594.0	604.5		
Cum. mass pull (g)	2	76.0	80.9	67.9	74.9	6.57
	7	162.5	166.0	153.9	160.8	6.23
	17	281.2	293.5	284.4	286.4	6.38
	32	596.9	594.0	604.5	598.5	5.42
Cum. mass pull %	2	2.3	2.5	2.1	2.3	0.20
	7	4.9	5.0	4.7	4.9	0.19
	17	8.5	8.9	8.6	8.7	0.19
	32	18.1	18.0	18.3	18.1	0.16
Cum H_2O rec (g)	2	299.0	280.1	294.5	291.2	9.87
	7	963.7	964.2	971.8	966.6	4.54
	17	2201.5	2175.5	2184.1	2187.0	13.25
	32	3494.0	3499.5	3478.3	3490.6	11.00
Total						
H_2O recovery %	2	4.6	4.3	4.5	4.4	0.15
	7	14.7	14.7	14.8	14.7	0.07
	17	33.6	33.2	33.3	33.3	0.20
	32	53.3	53.3	53.0	53.2	0.17
Sulphur %	2	17.77	16.88	19.13	17.9	1.13
	7	4.30	4.05	5.12	4.5	0.56
	17	0.65	0.54	0.57	0.6	0.06
	32	0.17	0.15	0.13	0.1	0.02
Total						
Mass of S (g)	2	13.5	13.7	13.0	13.4	0.35
	7	3.7	3.4	4.4	3.9	0.49
	17	0.8	0.7	0.7	0.7	0.04
	32	0.5	0.4	0.4	0.5	0.05
Cum S grade %	2	17.8	16.9	19.1	17.9	1.13
	7	10.6	10.3	11.3	10.7	0.51
	17	6.4	6.1	6.4	6.3	0.19
	32	3.1	3.1	3.1	3.1	0.02
Cum. S rec. %	2	67.3	72.0	67.4	68.9	2.69
	7	85.8	90.2	90.3	88.8	2.59
	17	89.6	93.8	94.2	92.5	2.56
	32	92.2	96.1	96.4	94.9	2.35
Tails: mass (g)		2726.7	2589.7	2645.0	2653.8	68.92
Tails: sulphur %		0.05	0.05	0.04	0.05	0.00
Tails: mass of S (g)		1.2	1.3	1.2	1.2	0.06

Type of collector used: DTP (0.64 mol/t)

	Time (min)	Samples A	Samples B	Samples C	Average (grams)	Std error (grams)
Head mass(g)		3300.0	3300.0	3300.0	3300	0.00
Head sulphur %		0.6	0.6	0.6	0.6	0.00
Mass of S		19.7	19.7	19.9	19.8	0.09
Wet conc.(g)	2	250.4	265.3	245.1	253.6	10.47
	7	755.2	742.4	737.8	745.1	9.02
	17	1219.3	1215.9	1228.2	1221.1	6.4
	32	1663.2	1675.7	1672.8	1670.6	6.5
Dry conc. mass (g)	2	63.9	73.4	59.2	65.5	7.23
	7	80.6	73.8	86.8	80.4	6.50
	17	110.3	101.3	118.9	110.2	8.80
	32	301.3	311	315	309.1	7.04
Cum. mass pull (g)		63.9	73.4	59.2	65.5	7.23
		144.5	147.2	146.0	145.9	1.35
		254.8	248.5	264.9	256.1	8.27
		556.1	559.5	579.9	565.2	12.87
Cum. mass pull %		1.9	2.2	1.8	2.0	0.22
		4.4	4.5	4.4	4.4	0.0
		7.7	7.5	8.0	7.8	0.25
		16.9	17.0	17.6	17.1	0.39
Cum H_2O rec (g)	2	186.5	191.9	185.9	188.1	3.30
	7	861.1	860.5	836.9	852.8	13.80
	17	1970.1	1975.1	1946.2	1963.8	15.4
	32	3332.0	3339.8	3304.0	3325.3	18.8
Total						
H_2O recovery %	2	2.8	2.9	2.8	2.9	0.1
	7	13.1	13.1	12.8	13.0	0.2
	17	30.0	30.1	29.7	29.9	0.2
	32	50.8	50.9	50.4	50.7	0.3
Sulphur %	2	19.5	18.7	20.7	19.6	1.04
	7	5.6	4.1	6.0	5.2	0.99
	17	0.8	0.7	0.7	0.7	0.06
	32	0.2	0.2	0.2	0.2	0.01
Total						
Mass of S (g)	2	12.4	13.7	12.3	12.8	0.78
	7	4.5	3.0	5.2	4.2	1.11
	17	0.9	0.7	0.8	0.8	0.06
	32	0.5	0.5	0.5	0.5	0.02
Cum S grade %	2	19.5	18.7	20.7	19.6	1.04
	7	11.7	11.4	12.0	11.7	0.30
	17	7.0	7.0	6.9	7.0	0.07
	32	3.3	3.2	3.2	3.2	0.04
Cum. S rec. %	2	63.1	69.5	61.8	64.8	4.13
	7	85.9	84.8	87.9	86.2	1.56
	17	90.2	88.5	91.9	90.2	1.69
	32	92.9	91.3	94.5	92.9	1.60
Tails: mass (g)		2683.8	2675.1	2597.9	2652.3	47.28
Tails: sulphur %		0.1	0.1	0.1	0.1	0.00
Tails: mass of S (g)		1.9	2.0	1.7	1.9	0.15

De-sliming cyclone: 36.9 mm
Concentration of depressant used: 500 g/t

	Time (Min)	Sample #		Mean	STDV
		A	B		
Head Mass(g)		3300	3300	3300	0.00
Head Sulphur %		0.6	0.6	0.6	0.00
Mass of S		19.8	19.8	19.8	0.00
Wet conc.(g)	2	257.8	284.4	271.1	18.81
	10	857.2	1052.1	954.65	137.8
Total					
Dry conc. mass (g)	2	74.2	78.4	76.3	2.97
	10	101.0	114.8	107.9	9.76
Total					
Cum. Mass pull (g)	2	74.2	78.4	76.3	2.97
	10	175.2	193.2	184.2	12.73
% Mass pull	2	2.2	2.4	2.3	0.09
	10	5.3	5.9	5.6	0.39
Water Recovery (g)	2	183.6	206.0	194.8	15.84
	10	756.2	937.3	846.8	128.1
Total					
% Water Recovery	2	2.7	3.0	2.9	0.23
	10	11.1	13.7	12.4	1.88
% Sulphur	2	17.5	17.9	17.7	0.31
	10	4.0	3.4	3.7	0.40
Total					
Mass of S (g)	2	13.0	14.1	13.5	0.76
	10	4.0	3.9	4.0	0.07
%S Cum. Grade	2	17.5	17.9	17.7	0.31
	10	12.3	11.1	11.7	0.86
		29.8	29.0	29.4	0.55
%S Cum. Rec.	2	65.6	71.1	68.3	3.84
	10	86.0	90.9	88.5	3.47
Tails: Mass (g)		2636.7	2985.2	2811.0	246.43
Tails % Sulphur		0.091819	0.0756	0.1	0.01
Tails Mass of S (g)		2.4	2.3	2.3	0.12

De-sliming cyclone: 36.9 mm
Concentration of depressant used: 400 g/t

	Time (Min)	Sample #		Mean	STDV
		A	B		
Head Mass(g)		3300	3300	3300	0.00
Head Sulphur %		0.6	0.6	0.6	0.00
Mass of S		19.8	19.8	19.8	0.00
Wet conc.(g)	2	300.4	326.9	313.7	18.74
	10	1133.5	1175.4	1154.5	29.63
Total					
Dry conc. mass (g)	2	84.2	87.1	85.7	2.05
	10	119.3	115.6	117.5	2.62
Total					
Cum. Mass pull (g)	2	84.2	87.1	85.7	2.05
	10	203.5	202.7	203.1	0.57
Total					
% Mass pull	2	2.6	2.6	2.6	0.06
	10	6.2	6.1	6.2	0.02
Water Recovery (g)	2	216.2	239.8	228.0	16.69
	10	1014.2	1059.8	1037.0	32.24
Total					
% Water Recovery	2	3.2	3.5	3.3	0.24
	10	14.9	15.5	15.2	0.47
% Sulphur	2	17.9	16.8	17.4	0.73
	10	3.2	3.2	3.2	0.04
Total					
Mass of S (g)	2	15.0	14.7	14.9	0.27
	10	3.8	3.6	3.7	0.13
%S Cum. Grade	2	17.9	16.8	17.4	0.73
	10	10.4	9.9	10.1	0.35
		28.2	26.7	27.5	1.08
%S Cum. Rec.	2	76.0	74.0	75.0	1.37
	10	95.3	92.4	93.9	2.02
Tails: Mass (g)		3078.6	3172.7	3125.7	66.54
Tails % Sulphur		0.07	0.08	0.1	0.00
Tails Mass of S (g)		2.3	2.5	2.4	0.16

De-sliming cyclone: 36.9 mm
Concentration of depressant used: 300 g/t

	Time (Min)	Sample # A	Sample # B	Mean	STDV
Head Mass(g)		3300	3300	3300	0.00
Head Sulphur %		0.6	0.6	0.6	0.00
Mass of S		19.8	19.8	19.8	0.00
Wet conc.(g)	2	347.2	310.1	328.7	26.23
	10	1148.6	1112.5	1130.6	25.53
Total					
Dry conc. mass (g)	2	95.3	86.0	90.7	6.58
	10	116.1	114.3	115.2	1.27
Total					
Cum. Mass pull (g)	2	95.3	86.0	90.7	6.58
	10	211.4	200.3	205.9	7.85
Total					
% Mass pull	2	2.9	2.6	2.7	0.20
	10	6.4	6.1	6.2	0.24
Water Recovery (g)	2	251.9	224.1	238.0	19.66
	10	1032.5	998.2	1015.4	24.25
Total					
% Water Recovery	2	3.7	3.3	3.5	0.29
	10	15.1	14.6	14.9	0.36
% Sulphur	2	16.5	17.5	17.0	0.71
	10	2.6	3.0	2.8	0.27
Total					
Mass of S (g)	2	15.7	15.0	15.4	0.47
	10	3.1	3.5	3.3	0.28
%S Cum. Grade	2	16.5	17.5	17.0	0.71
	10	9.0	10.2	9.6	0.84
%S Cum. Rec.	2	79.3	75.9	77.6	2.40
	10	94.8	93.4	94.1	0.98
Tails: Mass (g)		3177.6	3054.4	3116.0	87.12
Tails % Sulphur		0.1	0.1	0.1	0.01
Tails Mass of S (g)		2.8	2.3	2.6	0.30

De-sliming cyclone: 76 mm
Concentration of depressant used: 500 g/t

	Time (Min)	Sample # A	Sample # B	Mean	STDV
Head Mass(g)		3300	3300	3300	0.00
Head Sulphur %		0.6	0.6	0.6	0.00
Mass of S		19.8	19.8	19.8	0.00
Wet conc.(g)	2	284.1	321.0	302.6	26.09
	10	795.9	903.6	849.8	76.16
Total					
Dry conc. mass (g)	2	84.6	89.6	87.1	3.54
	10	72.6	75.3	74.0	1.91
Total					
Cum. Mass pull (g)	2	84.6	89.6	87.1	3.54
	10	157.2	164.9	161.1	5.44
Total					
% Mass pull	2	2.6	2.7	2.6	0.11
	10	4.8	5.0	4.9	0.16
Water Recovery (g)	2	199.5	231.4	215.5	22.56
	10	723.3	828.3	775.8	74.25
Total					
% Water Recovery	2	2.9	3.4	3.2	0.33
	10	10.6	12.1	11.4	1.09
% Sulphur	2	17.6	17.2	17.4	0.28
	10	4.4	3.4	3.9	0.70
Total					
Mass of S (g)	2	14.9	15.5	15.2	0.37
	10	3.2	2.6	2.9	0.45
%S Cum. Grade	2	17.6	17.2	17.4	0.28
	10	14.0	12.5	13.3	1.06
Total		31.7	29.8	30.7	1.34
%S Cum. Rec.	2	75.4	78.0	76.7	1.89
	10	91.6	91.1	91.4	0.37
Tails: Mass (g)		3258.3	3162.6	3210	68
Tails % Sulphur		0.044647	0.0679	0.1	0.02
Tails Mass of S (g)		1.5	2.1	1.8	0.49

De-sliming cyclone: 76 mm
Concentration of depressant used: 400 g/t

	Time (Min)	Sample #		Mean	STDV
		A	B		
Head Mass(g)		3300	3300	3300	0.00
Head Sulphur %		0.6	0.6	0.6	0.00
Mass of S		19.8	19.8	19.8	0.00
Wet conc.(g)	2	298.1	316.5	307.3	13.01
	10	1004.7	954.8	979.8	35.28
Total					
Dry conc. mass (g)	2	83.6	85.3	84.45	1.20
	10	94.8	89.1	92.0	4.03
Total					
Cum. Mass pull (g)	2	83.6	85.3	84.5	1.20
	10	178.4	174.4	176.4	2.83
Total					
% Mass pull	2	2.5	2.6	2.6	0.04
	10	5.4	5.3	5.3	0.09
Water Recovery (g)	2	214.5	231.2	222.9	11.81
	10	909.9	865.7	887.8	31.25
Total					
% Water Recovery	2	3.1	3.4	3.3	0.17
	10	13.3	12.7	13.0	0.46
% Sulphur	2	17.6	17.3	17.4	0.23
	10	3.8	3.6	3.7	0.13
Total					
Mass of S (g)	2	14.7	14.7	14.7	0.02
	10	3.6	3.2	3.4	0.27
%S Cum. Grade	2	17.6	17.3	17.4	0.23
	10	12.0	12.0	12.0	0.01
%S Cum. Rec.	2	74.3	74.4	74.3	0.08
	10	92.5	90.7	91.6	1.27
Tails: Mass (g)		3085.8	3166.1	3126.0	56.78
Tails % Sulphur		0.1	0.1	0.1	0.01
Tails Mass of S (g)		2.4	2.0	2.2	0.27

De-sliming cyclone: 76 mm
Concentration of depressant used: 300 g/t

	Time (Min)	Sample # A	Sample # B	Mean	STDV
Head Mass(g)		3300	3300	3300	0.00
Head Sulphur %		0.6	0.6	0.6	0.00
Mass of S		19.8	19.8	19.8	0.00
Wet conc.(g)	2	316.4	345.9	331.2	20.86
	10	965.6	946.4	956.0	13.58
Total					
Dry conc. mass (g)	2	94	92.9	93.5	0.78
	10	89.1	81.8	85.5	5.16
Total					
Cum. Mass pull (g)	2	94.0	92.9	93.5	0.78
	10	183.1	174.7	178.9	5.94
Total					
% Mass pull	2	2.8	2.8	2.8	0.02
	10	5.5	5.3	5.4	0.18
Water Recovery (g)	2	222.4	253.0	237.7	21.64
	10	876.5	864.6	870.6	8.41
Total					
% Water Recovery	2	3.3	3.7	3.5	0.32
	7	12.8	12.7	12.8	0.12
% Sulphur	2	16.6	16.0	16.3	0.38
	7	3.5	3.5	3.5	0.02
Total					
Mass of S (g)	2	15.6	14.9	15.2	0.48
	7	3.1	2.9	3.0	0.17
%S Cum. Grade	2	16.6	16.0	16.3	0.38
	7	11.0	11.2	11.1	0.17
		27.6	27.2	27.4	0.21
%S Cum. Rec.	2	78.7	75.3	77.0	2.43
	7	94.5	89.8	92.2	3.27
Tails: Mass (g)		3210.0	3242.2	3226	23
Tails % Sulphur		0.0	0.1	0.1	0.02
Tails Mass of S (g)		1.4	2.3	1.8	0.64

APPENDIX C, COLLECTORS AND MIXTURE DOSAGES

Sodium iso-Butyl Xanthate			
%	Mass(g)/ton	Mass in g per 3.3 kg solids	Moles/ton
100	530.0	1.749	2.545
93.75	496.9	1.640	2.386
75	397.5	1.312	1.909
0	0.0	0.000	0.000

Potasium n-Butyl tri-thiocarbonate				Combined collectors	
%	Mass(g/ton)	Mass in g per 3.3 kg solids	Moles/ton	Total mass (g/t)	Total mole (mol/t)
0	0.0	0.0	0.000	530.0	2.545
6.25	35.4	0.1	0.159	532.3	2.545
25	141.5	0.5	0.636	539.0	2.545
100	566.1	1.9	2.545	566.1	2.545

Potasium n-Decyl tri-thiocarbonate				Combined collectors	
%	Mass(g/ton)	Mass in g per 3.3 kg solids	Moles/ton	Total mass (g/t)	Total mole (mol/t)
0	0.0	0.000	0.000	530.0	2.545
6.25	48.8	0.161	0.159	545.6	2.545
25	195.1	0.644	0.636	592.6	2.545
100	780.3	2.575	2.545	780.3	2.545

Potasium n-Dodecyl tri-thiocarbonate				Combined collectors	
%	Mass(g/ton)	Mass in g per 3.3 kg solids	Moles/ton	Total mass (g/t)	Total mole (mol/t)
0	0.0	0.000	0.000	530.0	2.545
6.25	53.2	0.176	0.159	550.1	2.545
25	212.9	0.703	0.636	610.4	2.545
100	851.7	2.811	2.545	851.7	2.545

APPENDIX C, COLLECTORS AND MIXTURE DOSAGES

Sodium iso-butyl xanthate (SIBX)	**wt %**	**Mass(g)/ton**	**Moles/ton**	**Molar % of total mix**
	50	265	1.273	56.1
	50	150	0.720	56.1
	50	75	0.360	56.1
Sodium di-n-butyl dithiophosphate (DTP)	**wt %**	**Mass(g/ton)**	**Moles/ton**	**Molar % of total mix**
	50	265	0.996	43.9
	50	150	0.564	43.9
	50	75	0.282	43.9
Combined DTP and SIBX collectors	**Acronys for the cobined collectors**	**Total mass (g/ton)**	**Total mole (mol/t)**	**-**
	2.27 mol/t (SIBX+DTP)	530.0	2.27	-
	1.28 mol/t (SIBX+DTP)	300.0	1.28	-
	0.64 mol/t (SIBX+DTP)	150.0	0.64	-

APPENDIX D, MASS AND CHEMICAL BALANCE OF THE CYCLONES

36.9mm cyclone

Time (sec)	UF slurry mass (kg)	UF slurry rate (t/h)	U.F. solids (kg)	UF solids rec. rate (t/h)	% solids UF (kg)	UF H_2O recovery (kg)	UF H_2O rec (t/h)	α_{water}	Sulphur grade (%)	Sulphur Mass (kg/h)	% sulphur	3PGM + Au (g/t)
5.03	1.60	1.14	0.71	0.51	86.8	0.88	0.63	19.32	0.58	2.96	86.2	4.06
5.11	1.50	1.05	0.67	0.47	84.3	0.82	0.58	16.93	0.58	2.74	83.6	4.06
4.71	1.48	1.13	0.69	0.53	86.1	0.79	0.60	18.12	0.58	3.05	85.5	4.06
5.23	1.47	1.01	0.70	0.48	85.8	0.77	0.53	16.83	0.58	2.80	85.2	4.06
								17.80				

Time (sec)	OF slurry mass (kg)	OF slurry rate (t/h)	O.F. solids (kg)	OF solids rec. rate (t/h)	% solids OF (kg)	OF H_2O recovery (kg)	OF H_2O rec (t/h)	O.F. H_2O (%)	Sulphur grade (%)	Sulphur Mass (kg/h)	% sulphur	3PGM + Au (g/t)
5.03	3.79	2.71	0.11	0.078	13.2	3.68	2.63	80.7	0.61	0.47	13.8	4.07
5.11	4.17	2.94	0.13	0.088	15.7	4.05	2.85	83.1	0.61	0.54	16.4	4.07
4.71	3.67	2.81	0.11	0.085	13.9	3.56	2.72	81.9	0.61	0.52	14.5	4.07
5.23	3.92	2.70	0.12	0.080	14.2	3.80	2.62	83.2	0.61	0.49	14.8	4.07

Time (sec)	Total H_2O rec. rate (t/h)	Total H_2O rec. kg	Total solids (kg)	Total solids rec. rate (t/h)	Feed Sulphur Mass (kg/h)
5.03	3.27	4.56	0.82	0.588	3.44
5.11	3.43	4.87	0.80	0.560	3.28
4.71	3.32	4.35	0.80	0.610	3.57
5.23	3.15	4.57	0.82	0.562	3.28

Chemical and mass balance

	Feed	Underflow	Overflow
Solids (t/h)	0.58	0.50	0.08
Sulphur (kg/h)	3.39	2.89	0.50
(PGM+ Au) (g/h)	2.29	2.02	0.27
Talc (t/h)	0.05	0.03	0.02

Recoveries

Consituent	Recovery to UF	Recovery to OF
Solids (wt%)	85.772	14.2
Water recovery (wt%)	17.8	82.2
Sulphur (wt%)	85.1	14.9
(PGM+ Au) (wt%)	88.0	12.0
Talc (wt%)	64.4	35.6

APPENDIX D, MASS AND CHEMICAL BALANCE OF THE CYCLONES

76.0 mm cyclone

Time (sec)	UF slurry mass (kg)	UF slurry rate (t/h)	U.F. solids (kg)	UF solids rec. rate (t/h)	% solids UF (kg)	UF H_2O recovery (kg)	UF H_2O rec (t/h)	α_{water}	Sulphur grade (%)	Sulphur Mass (kg/h)	% sulphur	3PGM + Au (g/t)
1.56	1.5	3.46	0.9	2.05	79.7	0.6	1.41	15.00	0.55	11.23	76.9	4.07
1.97	1.5	2.74	0.9	1.67	82.0	0.6	1.07	15.94	0.55	9.14	79.4	4.07
1.61	1.1	2.46	0.8	1.69	81.9	0.3	0.77	11.51	0.55	9.29	79.3	4.07
1.26	1.0	2.86	0.7	1.89	79.8	0.3	0.97	11.02	0.55	10.37	77.0	4.07
6.25	4.1	2.36	2.7	1.54	79.2	1.4	0.83	11.17	0.55	8.42	76.3	4.07
2.42	1.9	2.83	1.2	1.84	79.9	0.7	0.99	11.96	0.55	10.08	77.1	4.07
								12.77				

Time (sec)	OF slurry mass (kg)	OF slurry rate (t/h)	O.F. solids (kg)	OF solids rec. rate (t/h)	% solids OF (kg)	OF H_2O recovery (kg)	OF H_2O rec (t/h)	O.F. H_2O (%)	Sulphur grade (%)	Sulphur Mass (kg/h)	% sulphur	3PGM + Au (g/t)
1.56	3.7	8.54	0.2	0.52	20.3	3.5	8.02	85.0	0.65	3.38	23.1	3.99
1.97	3.3	6.03	0.2	0.37	18.0	3.1	5.66	84.1	0.65	2.37	20.6	3.99
1.61	2.8	6.26	0.2	0.37	18.1	2.6	5.89	88.5	0.65	2.42	20.7	3.99
1.26	2.9	8.29	0.2	0.48	20.2	2.7	7.81	89.0	0.65	3.09	23.0	3.99
6.25	12.1	6.97	0.7	0.40	20.8	11.4	6.57	88.8	0.65	2.61	23.7	3.99
2.42	5.2	7.74	0.3	0.46	20.1	4.9	7.27	88.0	0.65	2.99	22.9	3.99

Time (sec)	Total H_2O rec. rate (t/h)	Total H_2O rec. kg	Total solids (kg)	Total solids rec. rate (t/h)	Feed Sulphur Mass (kg/h)
1.56	9.43	4.1	1.1	2.57	14.6
1.97	6.74	3.7	1.1	2.03	11.5
1.61	6.65	3.0	0.9	2.07	11.7
1.26	8.77	3.1	0.8	2.37	13.5
6.25	7.39	12.8	3.4	1.94	11.0
2.42	8.26	5.6	1.5	2.30	13.1

Chemical and mass balance

	Feed	Underflow	Overflow
Solids (t/h)	2.21	1.8	0.4
Sulphur (kg/h)	12.57	9.8	2.8
(PGM+ Au) (g/h)	6.49	5.0	1.5
Talc (t/h)	0.21	0.1	0.1

Recoveries

Consituent	Recovery to UF	Recovery to OF
Solids (wt%)	80.4	19.6
Water recovery (wt%)	12.8	87.2
Sulphur (wt%)	77.6	22.4
(PGM+ Au) (wt%)	77.2	22.8
Talc (wt%)	54.4	45.6